Spring 2021

A secreted signal from the gut inhibits axon regeneration in C. elegans

Alexander Tianma Lin-Moore
Yale University Graduate School of Arts and Sciences, alexander.lin.moore@gmail.com

Abstract

A Secreted Signal From the Gut Inhibits Axon Regeneration in *C. elegans*

Alexander Tianma Lin-Moore

2021

The nervous system responds to injury through axon regeneration, a process in which damaged axons regrow to restore nervous system connection and function. Axon regeneration is a complex cellular process controlled by diverse pathways that both positively and negatively regulate regeneration success, and these supportive or inhibitory signals can come from the injured axon itself as well as from the extracellular environment. Identification of pathways affecting regeneration is a major topic of study, and novel regulatory pathways are frequently identified. The Rabs, a large family of GTPases, has recently been shown to contain several members that regulate axon regeneration success. Within this group, RAB-27 plays an important role as an inhibitor of axon regeneration. We have shown for the first time that RAB-27 contributes to the inhibition of axon regeneration *in vivo* using the model nematode *C. elegans*. Initial results pointed towards a neuronal role for RAB-27 in regeneration inhibition, with its role in regeneration independent of its function in the tethering of synaptic vesicles at the axon terminal and not shared with the closely related RAB-3. Further investigation showed that RAB-27 primarily inhibits regeneration from the intestine, where it is involved in a vesicle fusion pathway regulating secretion of the neuropeptide NLP-40. Loss of several components in this vesicle secretory pathway, including regulators of neuropeptide processing, dense core

vesicle maturation and vesicle exocytosis, as well as *nlp-40* itself, also enhance regeneration. Therefore, RAB-27 participates in a pathway of extrinsic inhibition of axon regeneration that originates in the intestine, the first such inhibitor to be identified in this tissue, and the first long-distance extrinsic regulator of axon regeneration identified in *C. elegans*.

A Secreted Signal From the Gut Inhibits Axon Regeneration in *C. elegans*

A Dissertation

Presented to the Faculty of the Graduate School

Of

Yale University

In Candidacy for the Degree of

Doctor of Philosophy

by

Alexander Tianma Lin-Moore

Dissertation Director: Marc Hammarlund, PhD

June 2021

Table of Contents

Regulation of axon regeneration in *C. elegans*

Introduction

The ability to regenerate is an essential function of the nervous system. Unlike other tissues, where damage can be repaired through cell replacement, restoring nervous system function relies on axon regeneration and the reestablishment of synaptic connections. In order to successfully regenerate, neurons must be able to detect injury, initiate regrowth through formation of a growth cone, re-extend towards their targets, and reform synaptic connections. The intrinsic and extrinsic pathways regulating axon regeneration are diverse both in origin and effect, but are remarkably conserved across species, making model systems an attractive resource for the discovery and characterization of genes regulating axon regeneration. The nematode *Caenorhabditis elegans* has emerged as an excellent model for the study of axon regeneration, and many fundamental pathways governing both positive and negative regulation of regeneration have been identified in this system.

C. elegans as a model system for axon regeneration

Regeneration of the nervous system is widespread among animals, and as an established model system for nearly half a century, *C. elegans* provides exceptional accessibility for molecular and genetic analysis required for the study of regeneration. Its genome, the first to be sequenced of any animal, is well conserved with other species, with most major signaling pathways represented

and close to half the total genome conserved with humans (Shaye & Greenwald, 2011). The *C. elegans* genome is also highly accessible to transgenic manipulation, with diverse tools and techniques available for both classical and modern genetic and genomic analyses (Nance & Frøkjær-Jensen, 2019). Its nervous system is the most completely characterized of any animal, and as one of the only available animal models with an invariant cell lineage, it is the only system in which the complete developmental lineage (Sulston & Horvitz, 1977) and connectome (White et al., 1986) are mapped. Additionally, its transparent body permits the visualization and manipulation of neurons *in situ*, allowing for studies of axon regeneration in living animals at single-cell resolution.

The nervous system of the *C. elegans* hermaphrodite is invariably comprised of 302 neurons categorized into 118 distinct classes based on morphology, neurotransmitter expression, and connectivity (White et al., 1986). Several of these neuron classes have been extensively studied in the context of axon regeneration, including the glutamatergic mechanosensory neurons PLM, ALM and AVM (Gabel et al., 2008; Chen et al., 2011), and the inhibitory GABAergic DD and VD neurons, the system in which axon regeneration was first demonstrated in *C. elegans* (Yanik et al., 2004, Hammarlund et al., 2009). The invariance of the nervous system means that individual neurons or neuron types can be studied across large groups of animals, not only facilitating study of regeneration in single cells, but also for high-resolution analysis of regeneration variability between different neuron types or ages. Studies of regeneration in *C. elegans* have not only identified key regulatory pathways and genes that govern

fundamental regeneration success (Hammarlund et al., 2009; Yan et al., 2009) but also additional, external factors that lead to conditional decline in regeneration capacity, most notably aging (Byrne et al., 2014; Kaletsky et al., 2016). Regeneration success at different life stages is variable between neuron types (Wu et al., 2007; (Gabel et al., 2008; Byrne et al., 2014), suggesting that more can yet be learned about fundamental aspects of axon regeneration biology through the study of *C. elegans*.

Several experimental strategies for studying axon regeneration have been developed in *C. elegans*, the most widespread of which is the severing of individual axons using a pulsed laser (Yanik et al., 2004; Byrne et al., 2011; Chen et al., 2011). Using a femtosecond or pulsed UV laser (Yanik et al., 2004; Williams et al., 2011), this strategy allows for targeted damage to individual neuronal processes, with the ability to control both the specific timing and location of injury, without damaging other neurons or tissues in the subject animal. Although the single-neuron nature of laser axotomy does limit its utility in screening approaches, its efficiency, as well as the invariant nature of the *C. elegans* nervous system, permits the study of large numbers of mutant or transgenic animals, and strategies have been implemented to support higher-throughput screening and live imaging of recovery using laser axotomy (Cornaglia et al., 2017). Beyond targeted axotomy, conditioning mutants has also been used to screen for regulators of regeneration. Loss of β-spectrin/*unc-70* leads to axonal breakage in mature animals, leading to a condition of constant axon regeneration throughout the body in adult worms (Hammarlund et al., 2007)

(Fig. 1A). Screening in this mutant background has identified key conserved positive regulators of axon regeneration (Hammarlund et al., 2009). Discovery of novel regulatory pathways and signals in *C. elegans* is ongoing, reinforcing both the diverse nature of regulation and the importance of *C. elegans* as a model system for studying regeneration.

Positive regulation of axon regeneration

Regeneration is supported by a complex network of regulatory pathways responsible for mediating different aspects of the regeneration program (Fig. 2). While loss or disruption of many of these pathways leads to severe impairment of regenerative capability, no single pathway yet identified is wholly responsible for controlling the entire regeneration program across the nervous system. Instead, diverse signals appear to play contributing roles to overall regeneration success, with only a few key signaling cascades governing initiation of the broader regeneration program. Positive regeneration regulators are active at all stages of regeneration, and these signals originate both from the injured neuron itself and the neuron's cellular environment.

Signal transduction of the initial axonal injury is mediated by an influx of intracellular Ca^{2+}, not only by entry through the site of injury, but also through active transport via the voltage-gated Ca^{2+} channel EGL-19 (Ghosh-Roy et al., 2010), and supplemented by release of Ca^{2+} from the endoplasmic reticulum of the axon itself, facilitated by ryanodine receptor *unc-68* (Pinan-Lucarre et al., 2012; Sun et al., 2014). Cytosolic Ca^{2+} influx in turn activates the MAP kinase

kinase kinase DLK-1 (Yan & Jin, 2012). DLK-1 is essential for regeneration in the DD/VD neurons (Hammarlund et al., 2009) (Fig. 1B) and PLM (Ghosh-Roy et al., 2010; Yan & Jin, 2012). Loss of *dlk-1* in these neurons almost completely eliminates regeneration after injury, while DLK-1 upregulation enhances regeneration beyond wild-type levels, including significant enhancement of regeneration in aged animals that normally show significant regeneration deficits (Hammarlund et al., 2009). DLK-1's role in regeneration is variable across neuron types: in ALM, ASJ and ASH, its importance to regeneration is reduced, and some *dlk-1* mutant animals are still able to initiate regeneration (Pinan-Lucarre et al., 2012; Chung et al., 2016). Another MAPKKK, MLK-1 plays a similar role in promoting axon regeneration (Nix et al., 2011; Pastuhov et al., 2012), and differing reliance of these partially independent cascades may explain the variable importance of DLK-1 in regeneration across neuron types. In intact axons, the DLK-1 pathway regulates synapse formation (Yan et al. 2009), but despite its critical role in axon regeneration, DLK-1 is not required for developmental axon outgrowth, as *dlk-1* mutants do not display structural nervous system defects (Hammarlund et al., 2009); DLK-1's role in axon outgrowth appears to be specific to post-injury regeneration. The DLK-1 pathway's role in axon regeneration is conserved, as disruption of *Drosophila* homolog Wallenda (Xiong et al., 2010; Karney-Grobe et al., 2018) or mammalian homolog ZPK/DLK (Itoh et al., 2009) also lead to significant regeneration defects.

DLK-1 regulates axon regeneration through the initiation of a MAP kinase signaling cascade, with downstream MAPK pathway members such as MKK-4

and PMK-3 playing similarly important roles in regeneration success (Hammarlund et al., 2009). The DLK-1 MAPK cascade in turn leads to the activation of multiple intracellular, pro-regenerative pathways including JNK pathway activation (C. Li et al., 2012; C. Li et al., 2015) and reorganization of microtubule dynamics (Ghosh-Roy et al., 2012). As part of the early response to axon injury, the DLK-1 pathway acts upstream of many cellular programs that modulate regeneration, and many regeneration factors that act at later stages of the regeneration response rely either directly or indirectly on DLK-1 activation. Loss of *dlk-1* is sufficient to eliminate high regeneration phenotypes seen in Notch/*lin-12* mutants (El Bejjani & Hammarlund, 2012) and in disruption of O-GlcNAc signaling (Taub et al., 2018). Conversely high regeneration caused by DLK-1 overexpression can be suppressed by disruption of downstream positive regeneration pathways, such as poly(ADP-ribosylation) inhibition (Byrne et al., 2014).

Not all regeneration programs act downstream of DLK-1. Cytoskeletal organization is essential for growth cone formation and axonal outgrowth, and disruption of microtubule organization leads to regeneration failure (Ertürk et al., 2007). While aspects of microtubule stabilization are regulated in part by the DLK-1 pathway (Ghosh-Roy et al., 2012), other aspects of microtubule-dependent axon regeneration appear to be DLK-1-independent. The microtubule minus-end-binding protein Patronin/PTRN-1 limits axonal microtubule dynamics, and loss of *ptrn-1* significantly impairs regeneration (Chuang et al., 2014). Loss of both *ptrn-1* in conjunction with *dlk-1* further impairs PLM regeneration, while

PTRN-1 overexpression is able to partially rescue PLM regeneration and leads to enhanced neurite sprouting in the absence of *dlk-1*, suggesting that PTRN-1-dependent control of regeneration is partially independent of DLK-1.

A striking example of DLK-1-independent regeneration regulation comes from the caspase CED-3, which is required cell-autonomously for initiation of regeneration in ALM (Pinan-Lucarre et al., 2012). CED-3, its activator CED-4, and the ER Ca^{2+} chaperone CRT-1 genetically interact to initiate regeneration, independent of CED-3's role in activation of apoptosis and likely upstream of DLK-1 (Pinan-Lucarre et al., 2012). The existence of this CED-3-dependent pathway of regeneration initiation not only presents an explanation for how certain neuron types are able to initiate regeneration independent of DLK-1, but also highlights the diversity in origin of pathways regulating axon regeneration.

Another unexpected source of a pro-regenerative signal comes from the *xbp-1* mRNA. *xbp-1* pre-mRNA is cleaved by IRE-1 and ligated by RtcB/RTCB-1 prior to translation as an essential step of the unfolded protein response (Kosmaczewski et al., 2014), but prior to ligation by RtcB, the spliced *xbp-1* 3' RNA fragment strongly promotes axon regeneration. Loss of *rtcb-1* leads to significant regeneration enhancement, which occurs cell-autonomously and is independent of its role in tRNA ligation (Kosmaczewski et al., 2015). Instead, loss of *rtcb-1* improves regeneration via accumulation of the unligated *xbp-1* 3' mRNA fragment, which contains a single loop in the *xbp-1* 3' UTR, is dispensable for XBP-1 protein function but wholly responsible for the ncRNA's effect on regeneration (Liu et al., 2020). Structural disruption of the loop by single base

pairing changes is sufficient to prevent the pro-regenerative effects of the *xbp-1* 3' fragment, and this RNA loop is only found in the spliced *xbp-1* 3' fragment, as uncleavable *xbp-1* mRNA is unable to recapitulate high regeneration and indeed leads to regeneration impairment. The identification of this unusual pathway highlights the diversity of strategies employed to regulate axon regeneration, as well as the usefulness of screening approaches to identifying novel regeneration regulators (Nix et al., 2014).

Inhibition of axon regeneration

Despite an abundance of diverse pro-regenerative pathways, regeneration does not always occur successfully. This failure of regeneration often seen in *C. elegans* and other systems is not solely caused by incomplete activation of pro-regeneration pathways; similarly diverse signals are also present that actively inhibit or impair axon regeneration. While in mammalian regeneration models inhibitory signals are dominated by powerful myelin-associated signals (Cafferty et al., 2010), the absence of myelin-producing glia in *C. elegans* has facilitated the identification of a wide array of inhibitory factors. Loss of these inhibitory signals leads to enhancement of regeneration beyond wild type levels, and as with factors that promote regeneration, inhibitory pathways can affect different phases of regeneration, including initiation, outgrowth efficiency, and age-dependent regeneration declines.

Several identified regeneration inhibitors act through direct downregulation of pro-regenerative pathways. The E3 ubiquitin ligase RPM-1 inhibits regeneration

by directly targeting DLK-1 and MLK-1 for degradation (Nix et al., 2011; Baker et al., 2015). Loss of *rpm-1* increases available DLK-1 and leads to significant improvement in regeneration success, dependent on both the MLK-1 and DLK-1 MAPKKK signaling cascades (Nakata et al., 2005; Nix et al., 2011), while overexpression of RPM-1 significantly reduces regeneration below control levels (Hammarlund et al., 2009) (Fig. 3A). The DLK-1 and MLK-1 signaling cascades are further negatively regulated by the MAP kinase phosphatase VHP-1, which inactivates PMK-3 and KGB-1 (Fig. 3B,C). Loss of *vhp-1* partially rescues the reduced regeneration seen in *pmk-3* or *kgb-1* mutants, MAP kinases that act downstream of DLK-1 and MLK-1, though *vhp-1* loss is unable to restore regeneration when both MAPKs are lost (Nix et al., 2011).Given the importance of DLK-1 and MLK-1 signaling to regeneration, the identification of antagonists of these pathways as regeneration inhibitors is unsurprising, and other regeneration inhibitors also function as direct antagonists of pro-regenerative pathways.

The guanine nucleotide exchange factor (GEF) EFA-6 acts as an intrinsic regeneration inhibitor, as does the GTPase ARF-6, a target of EFA-6's GEF activity (Chen et al., 2011). Surprisingly, EFA-6's mechanism of regeneration is independent of ARF-6. Instead, EFA-6 inhibits axon regeneration through disruption of microtubule dynamics. EFA-6 is rapidly recruited to the axon in response to axotomy, and strongly interacts with microtubule-associated proteins TAC-1 and ZYG-8. TAC-1 and ZYG-8 are required for normal axon regeneration, and function downstream of EFA-6, suggesting that EFA-6 may inhibit regeneration through sequestration of these microtubule-associated proteins.

EFA-6 axonal relocalization and interaction with TAC-1 and ZYG-8 are both dependent on an EFA-6 N-terminal domain, but are independent of its GEF activity (Chen et al., 2015). EFA-6 may additionally inhibit axon regeneration through its role in ARF-6 activation, but the relationship between these two factors in regeneration inhibition has not yet been characterized.

Beyond direct antagonism of pro-regenerative factors, regeneration inhibition can be found in many well-characterized signaling pathways. The Notch receptor LIN-12 is a potent inhibitor of regeneration in adult *C. elegans*, with loss of *lin-12* enhancing growth cone formation and functional recovery, and LIN-12 gain of function mutants reducing regeneration below control levels (El Bejjani & Hammarlund, 2012). Loss of either ADAM/*sup-17* or presenilin/*sel-12*, the enzymes responsible for Notch cleavage and activation, phenocopies *lin-12* loss of function, and does not further enhance regeneration when combined with *lin-12* loss, while overexpression of Notch intracellular domain (NICD) significantly reduces regeneration. Notch functions in the mature *C. elegans* nervous system to regulate, among other processes, synaptic activity (Sorkaç et al., 2018), sleep (Huang et al., 2017), chemosensation (Singh et al., 2011) and dauer entrance and recovery (Ouellet et al., 2008), and Notch signaling at or shortly after the time of injury is required to inhibit regeneration: conditional inhibition of LIN-12 cleavage by a temperature-sensitive *sup-17* was sufficient to enhance regeneration, while at the *sup-17*-permissive temperature regeneration was indistinguishable from wild type axons. Notch-dependent regeneration inhibition appears to be conserved, as gamma-secretase inhibition is sufficient to enhance

regeneration in vertebrates (Sobrido-Cameán et al., 2020), though the downstream mechanism of inhibition is not known. Developmental Notch signaling is involved in axon guidance in *Drosophila*, regulating the defasciculation of the ISNb motor neuron via local suppression of the Abl tyrosine kinase (Crowner et al., 2003; Kannan et al., 2018). However, since developmental Notch plays a supportive role in axon outgrowth and guidance, its relationship to regeneration inhibition in adult animals remains incompletely understood.

Regeneration is also inhibited by the amyloid precursor ortholog APL-1 (Zeng et al., 2018). Although amyloid precursor family members are known to play important roles in development, the *C. elegans* APL-1 is not essential for the gross architecture and development of the nervous system. APL-1 presence at the plasma membrane is mediated by the Rab GTPase RAB-6.2, which regulates trafficking of endosomes to the trans-Golgi network to recycle transmembrane proteins. Loss of *rab-6.2* leads to reductions in neuronal APL-1 expression and a high regeneration phenotype epistatic to *apl-1* mutants. APL-1 expression in GABA neurons potently inhibits regeneration via its extracellular E2 domain, which is exposed to the hypodermis. Expression of the secreted APL-1 E2 domain in the hypodermis is sufficient to impair regeneration, pointing to an inhibitory role for the APL-1 E2 domain in the extracellular space.

Extrinsic regulation of axon regeneration

While a neuron's intrinsic regeneration programs are important for determining successful recovery after injury, the extracellular environment of the injured axon also plays an extremely important role in determining regeneration success. Identified extracellular mechanisms of regeneration primarily focus on pathways of axon guidance and stabilization, and are reminiscent of similar pathways active during initial development of the nervous system. However, while developmental axon outgrowth is tightly regulated by a host of extracellular cues that attract or repel extending growth cones (Chisholm et al., 2016), roles for extracellular guidance cues are different during adult axon regeneration. Unlike in development, regenerating axons must navigate a much larger area, with a much less directed landscape of attractive or repellant guidance cues. Some developmental guidance cues play more significant roles in adult regeneration compared to development, while other signals critical for developmental outgrowth are absent or even inhibit regenerative outgrowth.

The heparin sulfate proteoglycan Syndecan/SDN-1 acts cell-autonomously during development to regulate axon outgrowth and neural migration (Rhiner et al., 2005; Saied-Santiago et al., 2017), but functions extrinsically in the hypodermis to support axon regeneration via growth cone stabilization (Edwards & Hammarlund, 2014). UNC-34 and CED-10, intracellular signals acting downstream of the Netrin and SLT-1 receptors UNC-40 and SAX-3, are dispensable for developmental outgrowth of the AVM axon, but are individually required for successful AVM regeneration in young adult animals (Gabel et al., 2008). SLT-1/Slit itself promotes multiple aspects of axon guidance via axon

repellence and regulates PLM cell body positioning during development (Hao et al., 2001; H. Li et al., 2008), but potently inhibits axon regeneration in adults (Gabel et al., 2008; Chen et al., 2011).

Loss of F-spondin/*spon-1* or Peroxidasin/*pxn-2* both lead to significant enhancement of PLM regeneration (Chen et al., 2011; Gotenstein et al., 2010). Both PXN-2 and SPON-1 are required for formation of the basement membrane, and contribute to the formation of the extracellular matrix (Woo et al., 2008; Josephson et al., 2016) and are involved in developmental neuronal migration and axon guidance. Weak alleles of *spon-1* show significant defasciculation in the ventral nerve cord, as well as defects in left-right and dorsoventral guidance of commissural axons, pointing to an important role for SPON-1 in maintenance of developmental axon guidance. SPON-1 appears to also be somewhat involved in developmental axon outgrowth, as *spon-1* mutants significantly enhance outgrowth defects seen in mutants of *unc-71*, an important outgrowth regulator (Woo et al., 2008). Loss of *pxn-2* during development leads to defects in left-right guidance of commissural axons, though it does not specifically affect axon outgrowth capability. In contrast, axon regeneration of adult animals is significantly affected by *pxn-2* loss, with significant enhancements in both growth cone formation and regenerative extension in adult *pxn-2* mutants (Gotenstein et al., 2010). Thus PXN-2 appears to play divergent roles in regulation of axon growth in adult regeneration compared to developmental patterning. Taken together, extrinsic factors play important roles in adult axon regeneration, and

individual signals may play highly different roles in developmental and adult axonal outgrowth.

Extrinsic inhibitory mechanisms of regeneration in *C. elegans*, though unrelated to the well-characterized myelin-associated extrinsic inhibitors nonetheless appear to be partially conserved in mammalian regeneration models (Burstyn-Cohen et al., 1998). Additionally, while extrinsic inhibition of axon regeneration in *C. elegans* is primarily known from basement membrane components, other extrinsic sources of regeneration regulation may also exist. Communication between neurons and other tissues via secreted signals is an important mechanism in mammalian models of post-injury regeneration (Pan et al., 2007), but a role for long-range signals in *C. elegans* has not been demonstrated.

A common theme among extrinsic regeneration regulators, particularly regeneration inhibitors, is pleiotropy. Many inhibitors have well-characterized roles in nervous system development or homeostasis, but their roles in regeneration are not clearly related to these canonical functions. The relationship of extrinsic inhibitory pathways to one another as an inhibitory network is unclear. While intrinsic regeneration regulators generally function in a few key regenerative pathways, such as the DLK-1 pathway, extrinsic regeneration inhibitors do not appear to genetically interact in such an interconnected way, instead operating largely independent of one another or converging only on broad pathways of outgrowth regulation. So many disparate pathways all

contributing to impairment of adult axon regeneration suggests that regeneration could be inhibited as a byproduct of other signaling pathways linking neurons to other tissues. Alternatively, outgrowth inhibition in adult animals may indeed be an evolutionarily acquired strategy to prevent aberrant or ectopic outgrowth and connections in the developed nervous system of adult animals. Further characterization of the landscape of axon regeneration in C. elegans may rely not only on the description of novel inhibitory mechanisms, but also on further description of the relationship between the mature nervous system and the rest of the body.

References

Baker, S. T., Turgeon, S. M., Tulgren, E. D., Wigant, J., Rahimi, O., Opperman, K. J., & Grill, B. (2015). Neuronal Development in Caenorhabditis elegans Is Regulated by Inhibition of an MLK MAP Kinase Pathway. *Genetics*, *199*(1), 151–156. https://doi.org/10.1534/genetics.114.170589

Burstyn-Cohen, T., Frumkin, A., Xu, Y.-T., Scherer, S. S., & Klar, A. (1998). Accumulation of F-Spondin in Injured Peripheral Nerve Promotes the Outgrowth of Sensory Axons. *Journal of Neuroscience*, *18*(21), 8875–8885. https://doi.org/10.1523/JNEUROSCI.18-21-08875.1998

Byrne, A. B., Edwards, T. J., & Hammarlund, M. (2011). In vivo Laser Axotomy in C. elegans. *JoVE (Journal of Visualized Experiments)*, *51*, e2707. https://doi.org/10.3791/2707

Byrne, A. B., & Hammarlund, M. (2017). Axon Regeneration in C. elegans: Worming our way to mechanisms of axon regeneration. *Experimental Neurology*, *287*(Pt 3), 300–309. https://doi.org/10.1016/j.expneurol.2016.08.015

Byrne, A. B., Walradt, T., Gardner, K. E., Hubbert, A., Reinke, V., & Hammarlund, M. (2014). Insulin/IGF1 Signaling Inhibits Age-Dependent Axon Regeneration. *Neuron*, *81*(3), 561–573. https://doi.org/10.1016/j.neuron.2013.11.019

Cafferty, W. B. J., Duffy, P., Huebner, E., & Strittmatter, S. M. (2010). MAG and OMgp Synergize with Nogo-A to Restrict Axonal Growth and Neurological Recovery after Spinal Cord Trauma. *Journal of Neuroscience*, *30*(20), 6825–6837. https://doi.org/10.1523/JNEUROSCI.6239-09.2010

Chen, L., Chuang, M., Koorman, T., Boxem, M., Jin, Y., & Chisholm, A. D. (2015). Axon injury triggers EFA-6 mediated destabilization of axonal microtubules via TACC and doublecortin like kinase. *ELife*, *4*, e08695. https://doi.org/10.7554/eLife.08695

Chen, L., Wang, Z., Ghosh-Roy, A., Hubert, T., Yan, D., O'Rourke, S., Bowerman, B., Wu, Z., Jin, Y., & Chisholm, A. D. (2011). Axon Regeneration Pathways Identified by Systematic Genetic Screening in C. elegans. *Neuron*, *71*(6), 1043–1057. https://doi.org/10.1016/j.neuron.2011.07.009

Chisholm, A. D., Hutter, H., Jin, Y., & Wadsworth, W. G. (2016). The Genetics of Axon Guidance and Axon Regeneration in Caenorhabditis elegans. *Genetics*, *204*(3), 849–882. https://doi.org/10.1534/genetics.115.186262

Chuang, M., Goncharov, A., Wang, S., Oegema, K., Jin, Y., & Chisholm, A. D. (2014). The Microtubule Minus-End-Binding Protein Patronin/PTRN-1 Is Required for Axon Regeneration in C. elegans. *Cell Reports*, *9*(3), 874–883. https://doi.org/10.1016/j.celrep.2014.09.054

Chung, S. H., Awal, M. R., Shay, J., McLoed, M. M., Mazur, E., & Gabel, C. V. (2016). Novel DLK-independent neuronal regeneration in Caenorhabditis elegans shares links with activity-dependent ectopic outgrowth. *Proceedings of the National Academy of Sciences*, *113*(20), E2852–E2860. https://doi.org/10.1073/pnas.1600564113

Cornaglia, M., Lehnert, T., & Gijs, M. A. M. (2017). Microfluidic systems for high-throughput and high-content screening using the nematode Caenorhabditis elegans. *Lab on a Chip*, *17*(22), 3736–3759. https://doi.org/10.1039/c7lc00509a

Crowner, D., Le Gall, M., Gates, M. A., & Giniger, E. (2003). Notch Steers Drosophila ISNb Motor Axons by Regulating the Abl Signaling Pathway. *Current Biology*, *13*(11), 967–972. https://doi.org/10.1016/S0960-9822(03)00325-7

Edwards, T. J., & Hammarlund, M. (2014). Syndecan Promotes Axon Regeneration by Stabilizing Growth Cone Migration. *Cell Reports*, *8*(1), 272–283. https://doi.org/10.1016/j.celrep.2014.06.008

El Bejjani, R., & Hammarlund, M. (2012). Notch Signaling Inhibits Axon Regeneration. *Neuron*, *73*(2), 268–278. https://doi.org/10.1016/j.neuron.2011.11.017

Ertürk, A., Hellal, F., Enes, J., & Bradke, F. (2007). Disorganized Microtubules Underlie the Formation of Retraction Bulbs and the Failure of Axonal Regeneration. *Journal of Neuroscience*, *27*(34), 9169–9180. https://doi.org/10.1523/JNEUROSCI.0612-07.2007

Gabel, C. V., Antoine, F., Chuang, C.-F., Samuel, A. D. T., & Chang, C. (2008). Distinct cellular and molecular mechanisms mediate initial axon development and adult-stage axon regeneration in C. elegans. *Development*, *135*(21), 3623–3623. https://doi.org/10.1242/dev.030817

Gabel, Christopher V., Antoine, F., Chuang, C.-F., Samuel, A. D. T., & Chang, C. (2008a). Distinct cellular and molecular mechanisms mediate initial axon development and adult-stage axon regeneration in C. elegans. *Development*, *135*(6), 1129–1136. https://doi.org/10.1242/dev.013995

Gabel, Christopher V., Antoine, F., Chuang, C.-F., Samuel, A. D. T., & Chang, C. (2008b). Distinct cellular and molecular mechanisms mediate initial axon development and adult-stage axon regeneration in C. elegans. *Development*, *135*(6), 1129–1136. https://doi.org/10.1242/dev.013995

Ghosh-Roy, A., Goncharov, A., Jin, Y., & Chisholm, A. D. (2012). Kinesin-13 and Tubulin Posttranslational Modifications Regulate Microtubule Growth in Axon Regeneration. *Developmental Cell*, *23*(4), 716–728. https://doi.org/10.1016/j.devcel.2012.08.010

Ghosh-Roy, A., Wu, Z., Goncharov, A., Jin, Y., & Chisholm, A. D. (2010). Calcium and Cyclic AMP Promote Axonal Regeneration in Caenorhabditis elegans and Require DLK-1 Kinase. *Journal of Neuroscience*, *30*(9), 3175–3183. https://doi.org/10.1523/JNEUROSCI.5464-09.2010

Gotenstein, J. R., Swale, R. E., Fukuda, T., Wu, Z., Giurumescu, C. A., Goncharov, A., Jin, Y., & Chisholm, A. D. (2010). The C. elegans peroxidasin PXN-2 is essential for embryonic morphogenesis and inhibits adult axon regeneration. *Development*, *137*(21), 3603–3613. https://doi.org/10.1242/dev.049189

Hammarlund, M., Jorgensen, E. M., & Bastiani, M. J. (2007). Axons break in animals lacking β-spectrin. *The Journal of Cell Biology*, *176*(3), 269–275. https://doi.org/10.1083/jcb.200611117

Hammarlund, M., Nix, P., Hauth, L., Jorgensen, E. M., & Bastiani, M. (2009). Axon Regeneration Requires A Conserved MAP Kinase Pathway. *Science (New York, N.Y.)*, *323*(5915), 802–806. https://doi.org/10.1126/science.1165527

Hao, J. C., Yu, T. W., Fujisawa, K., Culotti, J. G., Gengyo-Ando, K., Mitani, S., Moulder, G., Barstead, R., Tessier-Lavigne, M., & Bargmann, C. I. (2001). C. elegans Slit Acts in Midline, Dorsal-Ventral, and Anterior-Posterior Guidance via the SAX-3/Robo Receptor. *Neuron*, *32*(1), 25–38. https://doi.org/10.1016/S0896-6273(01)00448-2

Huang, H., Zhu, C.-T., Skuja, L. L., Hayden, D. J., & Hart, A. C. (2017). Genome-Wide Screen for Genes Involved in Caenorhabditis elegans Developmentally Timed Sleep. *G3: Genes|Genomes|Genetics*, *7*(9), 2907–2917. https://doi.org/10.1534/g3.117.300071

Itoh, A., Horiuchi, M., Bannerman, P., Pleasure, D., & Itoh, T. (2009). Impaired regenerative response of primary sensory neurons in ZPK/DLK gene-trap mice. *Biochemical and Biophysical Research Communications*, *383*(2), 258–262. https://doi.org/10.1016/j.bbrc.2009.04.009

Josephson, M. P., Miltner, A. M., & Lundquist, E. A. (2016). Nonautonomous Roles of MAB-5/Hox and the Secreted Basement Membrane Molecule SPON-1/F-Spondin in Caenorhabditis elegans Neuronal Migration. *Genetics*, *203*(4), 1747–1762. https://doi.org/10.1534/genetics.116.188367

Kaletsky, R., Lakhina, V., Arey, R., Williams, A., Landis, J., Ashraf, J., & Murphy, C. T. (2016). The C. elegans adult neuronal IIS/FOXO transcriptome reveals adult phenotype regulators. *Nature*, *529*(7584), 92–96. https://doi.org/10.1038/nature16483

Kannan, R., Cox, E., Wang, L., Kuzina, I., Gu, Q., & Giniger, E. (2018). Tyrosine phosphorylation and proteolytic cleavage of Notch are required for non-canonical Notch/Abl signaling in Drosophila axon guidance. *Development (Cambridge, England)*, *145*(2). https://doi.org/10.1242/dev.151548

Karney-Grobe, S., Russo, A., Frey, E., Milbrandt, J., & DiAntonio, A. (2018). HSP90 is a chaperone for DLK and is required for axon injury signaling. *Proceedings of the National Academy of Sciences*, *115*(42), E9899–E9908. https://doi.org/10.1073/pnas.1805351115

Kosmaczewski, S. G., Edwards, T. J., Han, S. M., Eckwahl, M. J., Meyer, B. I., Peach, S., Hesselberth, J. R., Wolin, S. L., & Hammarlund, M. (2014). The RtcB RNA ligase is an essential component of the metazoan unfolded protein response. *EMBO Reports*, *15*(12), 1278–1285. https://doi.org/10.15252/embr.201439531

Kosmaczewski, S. G., Han, S. M., Han, B., Irving Meyer, B., Baig, H. S., Athar, W., Lin-Moore, A. T., Koelle, M. R., & Hammarlund, M. (2015). RNA ligation in neurons by RtcB inhibits axon regeneration. *Proceedings of the National Academy of Sciences of the United States of America*, *112*(27), 8451–8456. https://doi.org/10.1073/pnas.1502948112

Li, C., Hisamoto, N., & Matsumoto, K. (2015). Axon Regeneration Is Regulated by Ets–C/EBP Transcription Complexes Generated by Activation of the cAMP/Ca2+

Signaling Pathways. *PLOS Genetics*, *11*(10), e1005603. https://doi.org/10.1371/journal.pgen.1005603

Li, C., Hisamoto, N., Nix, P., Kanao, S., Mizuno, T., Bastiani, M., & Matsumoto, K. (2012). The growth factor SVH-1 regulates axon regeneration in C. elegans via the JNK MAPK cascade. *Nature Neuroscience*, *15*(4), 551–557. https://doi.org/10.1038/nn.3052

Li, H., Kulkarni, G., & Wadsworth, W. G. (2008). RPM-1, a Caenorhabditis elegans Protein That Functions in Presynaptic Differentiation, Negatively Regulates Axon Outgrowth by Controlling SAX-3/robo and UNC-5/UNC5 Activity. *Journal of Neuroscience*, *28*(14), 3595–3603. https://doi.org/10.1523/JNEUROSCI.5536-07.2008

Liu, X., Beaudoin, J.-D., Davison, C. A., Kosmaczewski, S. G., Meyer, B. I., Giraldez, A. J., & Hammarlund, M. (2020). A Functional Non-coding RNA Is Produced from xbp-1 mRNA. *Neuron*, *107*(5), 854-863.e6. https://doi.org/10.1016/j.neuron.2020.06.015

Nakata, K., Abrams, B., Grill, B., Goncharov, A., Huang, X., Chisholm, A. D., & Jin, Y. (2005). Regulation of a DLK-1 and p38 MAP Kinase Pathway by the Ubiquitin Ligase RPM-1 Is Required for Presynaptic Development. *Cell*, *120*(3), 407–420. https://doi.org/10.1016/j.cell.2004.12.017

Nance, J., & Frøkjær-Jensen, C. (2019). The *Caenorhabditis elegans* Transgenic Toolbox. *Genetics*, *212*(4), 959–990. https://doi.org/10.1534/genetics.119.301506

Nix, P., Hammarlund, M., Hauth, L., Lachnit, M., Jorgensen, E. M., & Bastiani, M. (2014). Axon Regeneration Genes Identified by RNAi Screening in C. elegans. *Journal of Neuroscience*, *34*(2), 629–645. https://doi.org/10.1523/JNEUROSCI.3859-13.2014

Nix, P., Hisamoto, N., Matsumoto, K., & Bastiani, M. (2011). Axon regeneration requires coordinate activation of p38 and JNK MAPK pathways. *Proceedings of the National Academy of Sciences*, *108*(26), 10738–10743. https://doi.org/10.1073/pnas.1104830108

Ouellet, J., Li, S., & Roy, R. (2008). Notch signalling is required for both dauer maintenance and recovery in C. elegans. *Development*, *135*(15), 2583–2592. https://doi.org/10.1242/dev.012435

Pan, H.-C., Cheng, F.-C., Chen, C.-J., Lai, S.-Z., Lee, C.-W., Yang, D.-Y., Chang, M.-H., & Ho, S.-P. (2007). Post-injury regeneration in rat sciatic nerve facilitated by neurotrophic factors secreted by amniotic fluid mesenchymal stem cells. *Journal of Clinical Neuroscience*, *14*(11), 1089–1098. https://doi.org/10.1016/j.jocn.2006.08.008

Pastuhov, S. Iv., Fujiki, K., Nix, P., Kanao, S., Bastiani, M., Matsumoto, K., & Hisamoto, N. (2012). Endocannabinoid-Goα signalling inhibits axon regeneration in Caenorhabditis elegans by antagonizing Gqα-PKC-JNK signalling. *Nature Communications*, *3*, 1136. https://doi.org/10.1038/ncomms2136

Pinan-Lucarre, B., Gabel, C. V., Reina, C. P., Hulme, S. E., Shevkoplyas, S. S., Slone, R. D., Xue, J., Qiao, Y., Weisberg, S., Roodhouse, K., Sun, L., Whitesides, G. M., Samuel, A., & Driscoll, M. (2012). The Core Apoptotic Executioner Proteins CED-3 and

CED-4 Promote Initiation of Neuronal Regeneration in Caenorhabditis elegans. *PLOS Biology*, *10*(5), e1001331. https://doi.org/10.1371/journal.pbio.1001331

Rhiner, C., Gysi, S., Fröhli, E., Hengartner, M. O., & Hajnal, A. (2005). Syndecan regulates cell migration and axon guidance in C. elegans. *Development*, *132*(20), 4621–4633. https://doi.org/10.1242/dev.02042

Saied-Santiago, K., Townley, R. A., Attonito, J. D., Cunha, D. S. da, Díaz-Balzac, C. A., Tecle, E., & Bülow, H. E. (2017). Coordination of Heparan Sulfate Proteoglycans with Wnt Signaling To Control Cellular Migrations and Positioning in Caenorhabditis elegans. *Genetics*, *206*(4), 1951–1967. https://doi.org/10.1534/genetics.116.198739

Shaye, D. D., & Greenwald, I. (2011). OrthoList: A Compendium of C. elegans Genes with Human Orthologs. *PLOS ONE*, *6*(5), e20085. https://doi.org/10.1371/journal.pone.0020085

Singh, K., Chao, M. Y., Somers, G. A., Komatsu, H., Corkins, M. E., Larkins-Ford, J., Tucey, T., Dionne, H. M., Walsh, M. B., Beaumont, E. K., Hart, D. P., Lockery, S., & Hart, A. C. (2011). C. elegans Notch signaling regulates adult chemosensory response and larval molting quiescence. *Current Biology : CB*, *21*(10), 825–834. https://doi.org/10.1016/j.cub.2011.04.010

Sobrido-Cameán, D., Robledo, D., Romaus-Sanjurjo, D., Pérez-Cedrón, V., Sánchez, L., Rodicio, M. C., & Barreiro-Iglesias, A. (2020). Inhibition of Gamma-Secretase Promotes Axon Regeneration After a Complete Spinal Cord Injury. *Frontiers in Cell and Developmental Biology*, *8*, 173. https://doi.org/10.3389/fcell.2020.00173

Sorkaç, A., DiIorio, M. A., O'Hern, P. J., Baskoylu, S. N., Graham, H. K., & Hart, A. C. (2018). LIN-12/Notch Regulates GABA Signaling at the Caenorhabditis elegans Neuromuscular Junction. *G3: Genes|Genomes|Genetics*, *8*(8), 2825–2832. https://doi.org/10.1534/g3.118.200202

Sulston, J. E., & Horvitz, H. R. (1977). Post-embryonic cell lineages of the nematode, Caenorhabditis elegans. *Developmental Biology*, *56*(1), 110–156. https://doi.org/10.1016/0012-1606(77)90158-0

Sun, L., Shay, J., McLoed, M., Roodhouse, K., Chung, S. H., Clark, C. M., Pirri, J. K., Alkema, M. J., & Gabel, C. V. (2014). Neuronal Regeneration in C. elegans Requires Subcellular Calcium Release by Ryanodine Receptor Channels and Can Be Enhanced by Optogenetic Stimulation. *Journal of Neuroscience*, *34*(48), 15947–15956. https://doi.org/10.1523/JNEUROSCI.4238-13.2014

Taub, D. G., Awal, M. R., & Gabel, C. V. (2018). O-GlcNAc Signaling Orchestrates the Regenerative Response to Neuronal Injury in Caenorhabditis elegans. *Cell Reports*, *24*(8), 1931-1938.e3. https://doi.org/10.1016/j.celrep.2018.07.078

White, J. G., Southgate, E., Thomson, J. N., & Brenner, S. (1986). The structure of the nervous system of the nematode Caenorhabditis elegans. *Philosophical Transactions of the Royal Society of London. B, Biological Sciences*, *314*(1165), 1–340. https://doi.org/10.1098/rstb.1986.0056

Williams, W., Nix, P., & Bastiani, M. (2011). Constructing a low-budget laser axotomy system to study axon regeneration in C. elegans. *Journal of Visualized Experiments: JoVE*, *57*. https://doi.org/10.3791/3331

Woo, W.-M., Berry, E. C., Hudson, M. L., Swale, R. E., Goncharov, A., & Chisholm, A. D. (2008). The C. elegans F-spondin family protein SPON-1 maintains cell adhesion in neural and non-neural tissues. *Development*, *135*(16), 2747–2756. https://doi.org/10.1242/dev.015289

Wu, Z., Ghosh-Roy, A., Yanik, M. F., Zhang, J. Z., Jin, Y., & Chisholm, A. D. (2007). Caenorhabditis elegans neuronal regeneration is influenced by life stage, ephrin signaling, and synaptic branching. *Proceedings of the National Academy of Sciences*, *104*(38), 15132–15137. https://doi.org/10.1073/pnas.0707001104

Xiong, X., Wang, X., Ewanek, R., Bhat, P., DiAntonio, A., & Collins, C. A. (2010). Protein turnover of the Wallenda/DLK kinase regulates a retrograde response to axonal injury. *Journal of Cell Biology*, *191*(1), 211–223. https://doi.org/10.1083/jcb.201006039

Yan, D., & Jin, Y. (2012). Regulation of DLK-1 Kinase Activity by Calcium-Mediated Dissociation from an Inhibitory Isoform. *Neuron*, *76*(3), 534–548. https://doi.org/10.1016/j.neuron.2012.08.043

Yan, D., Wu, Z., Chisholm, A. D., & Jin, Y. (2009). The DLK-1 Kinase Promotes mRNA Stability and Local Translation in C. elegans Synapses and Axon Regeneration. *Cell*, *138*(5), 1005–1018. https://doi.org/10.1016/j.cell.2009.06.023

Yanik, M. F., Cinar, H., Cinar, H. N., Chisholm, A. D., Jin, Y., & Ben-Yakar, A. (2004). Functional regeneration after laser axotomy. *Nature*, *432*(7019), 822–822. https://doi.org/10.1038/432822a

Zeng, L., Bejjani, R. E., & Hammarlund, M. (2018). The Amyloid Precursor-like Protein APL-1 Regulates Axon Regeneration. *BioRxiv*, 305284. https://doi.org/10.1101/305284

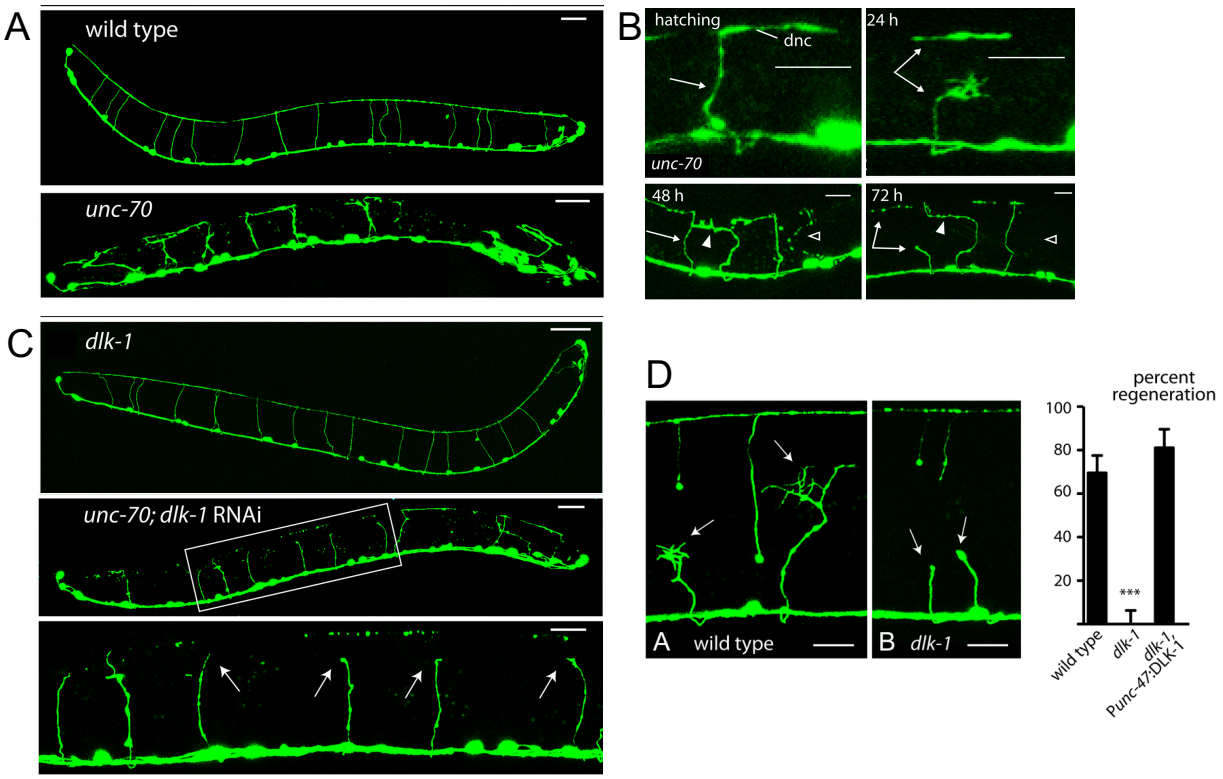

Figure 1. Axons break in *unc-70* mutant animals. A) Animals lacking β-spectrin/UNC-70 show severe nervous system damage, exemplified in the GABA neurons of *unc-70* mutants. B) This damage is caused by accumulation of axon breakages, which begin after hatching and continue to occur throughout the lifespan of the worm, even in axons actively undergoing regeneration. Regeneration of broken axons in *unc-70* mutants is blocked in *dlk-1* animals. The GABAergic nervous system of *dlk-1* mutants develops normally, but is unable to regenerate successfully following C) breakage in an *unc-70* model or D) targeted laser axotomy. Adapted from Hammarlund et al. 2007 and Hammarlund et al. 2009.

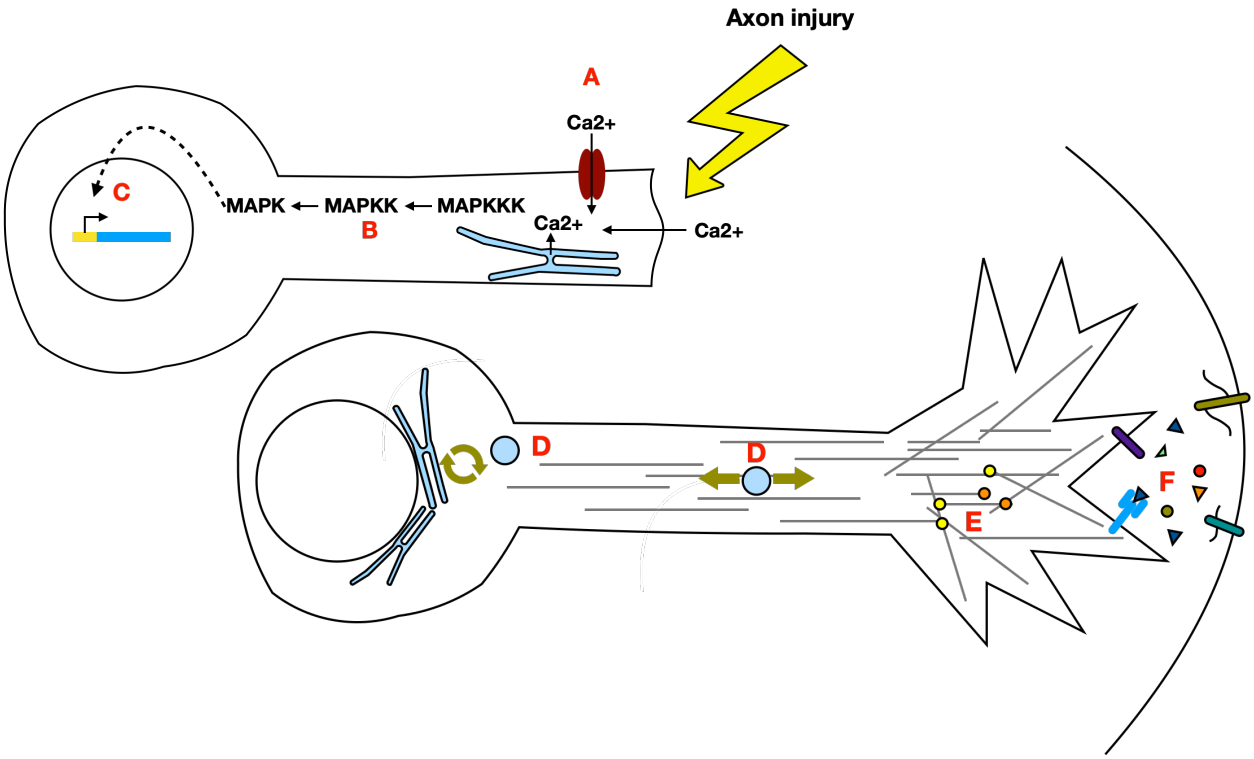

Figure 2. Intracellular and extrinsic mechanisms of axon regeneration regulation. Axon injury is initially detected by an influx of axonal Ca^{2+} (A), which is mediated in part by active internalization by the voltage-gated Ca^{2+} channel EGL-19 (Ghosh-Roy et al. 2010) and release of intracellular Ca^{2+} from ER stores by the ryanodine receptor UNC-68 (Sun et al. 2014). Ca^{2+} influx activates several pro-regenerative MAPKKK signaling cascades (B), including DLK-1 and MLK-1, which are required for regeneration in many neuron types. Activation of these cascades leads to upregulation of genes regulating downstream regenerative programs (C). In later stages of regeneration, trafficking of signals to and from the cell body (D), cytoskeletal remodeling (E) and interaction with the regenerating axon's extracellular environment (F) are all critical regulators of regeneration success, and are sources of both positive and inhibitory regeneration signals. Adapted from Byrne & Hammarlund, 2017.

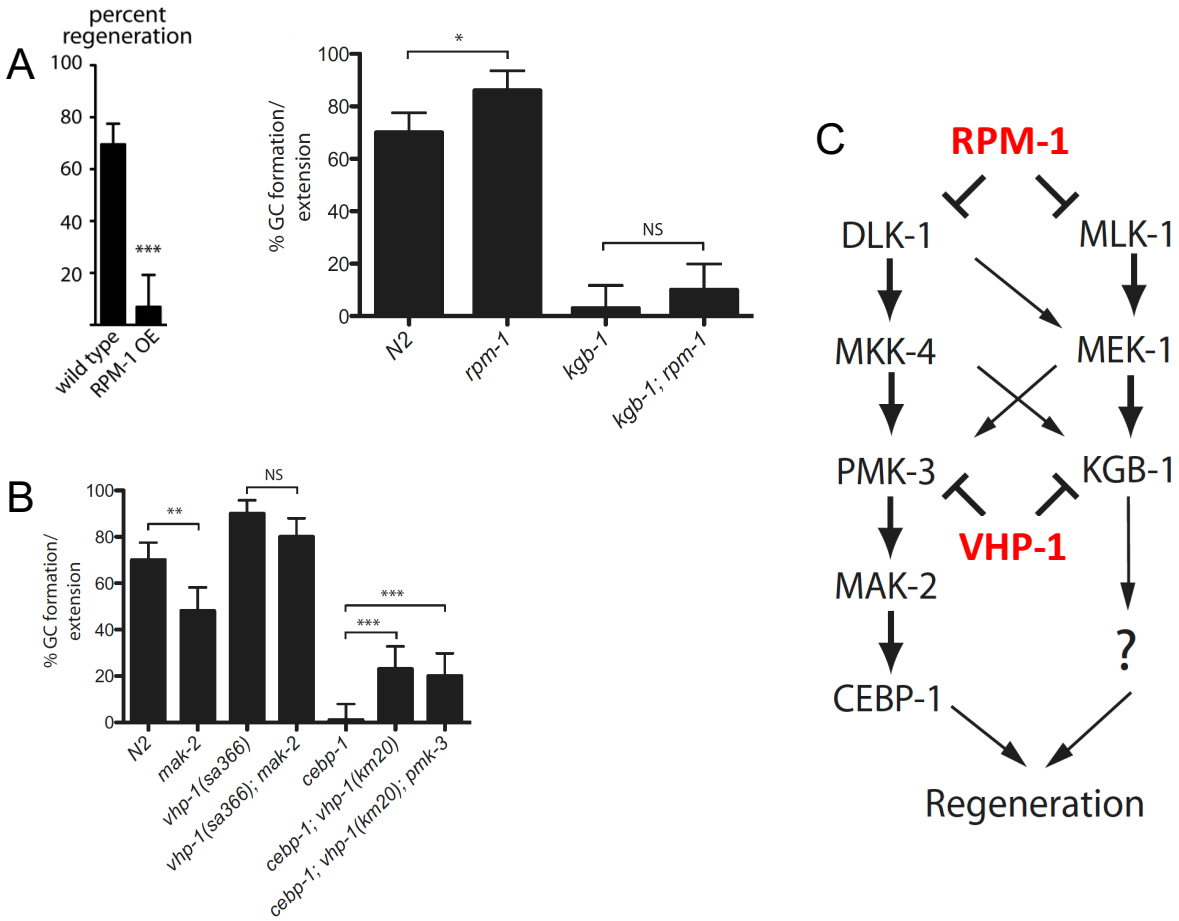

Figure 3. Negative regulation of axon regeneration by MAPKKK cascade inhibition**.** A) The E3 ubiquitin ligase RPM-1 inhibits axon regeneration by downregulating both DLK-1 and MLK-1. Overexpression of RPM-1 significantly reduces regeneration, while loss leads to regeneration improvement, dependent on downstream members of the pro-regenerative MLK-1 cascade. B) The MAP kinase phosphatase VHP-1 targets downstream components of both DLK-1 and MLK-1 signaling cascades. Loss of *vhp-1* improves axon regeneration, and is able to partially compensate for loss of *mak-2* or *cebp-1*, downstream components of the DLK-1 cascade, likely due to the loss of KGB-1 downregulation. C) Visualization of the interacting DLK-1 and MLK-1 MAPKKK cascades, which are required for regeneration. Multiple steps of these cascades are targeted for degradation or dephosphorylation to limit axon regeneration. Adapted from Nix et al. 2011.

Rab biology and *C. elegans* RAB-27

Preface

My dissertation research was motivated by the identification of the Rab GTPases as a family enriched in uncharacterized inhibitors of axon regeneration, as described below in Sekine et al. 2018. As key regulators of intracellular membrane identity and trafficking, the study of Rabs offers a window into trafficking pathways that may be involved in diverse cellular processes. Similarly, the manipulation of Rabs through changes in expression and activity presents a powerful toolkit to identify signals and processes regulating cellular programs. While the link between Rabs and axon regeneration, a process fundamentally requiring rearrangement of many intracellular membrane compartments, seems clear, Rabs had only sparingly been implicated in regulation of regeneration, and had never been targeted as a method to identify pathways regulating axon regeneration. This section describes fundamental aspects of Rab biology, including their conservation, activation, and mechanisms of subcellular localization, with a specific focus on Rab3 and Rab27, two Rab subfamilies regulating vesicle exocytosis.

Introduction

One of the defining features of eukaryotic cells is the variety of membrane-bound organelles and vesicles that populate the cytoplasm. These compartments rely on a host of factors to demarcate and traffic them within the cell. Within this

host of factors, the Rab GTPases play a crucial role in defining intracellular membrane identity and regulating the steps of trafficking and membrane fusion. Like other members of the Ras superfamily of GTPases, Rabs act as molecular switches though GTP binding and hydrolysis. Rabs are inserted into their target membrane, where, following activation, they mediate recruitment of downstream effectors that transduce a myriad of processes related to membrane trafficking, tethering and fusion. Loss of gain of Rab function, or dysregulation of activation via disruption of GTP binding or hydrolysis can lead to significant intracellular disruption, and is implicated in several diseases and pathogenic phenotypes.

Structural conservation and diversity in Rab GTPases

Like all members of the Ras superfamily of GTPases, Rabs contain a GTP-binding pocket, a highly conserved domain found in Rabs across metazoans (Pereira-Leal & Seabra 2001; Yun et al. 2019). As molecular switches, binding of GTP in this domain leads to activation of the Rab through changes in conformation. The reorganization of the switch I and II regions is particularly important, as these two regions physically interact with the GTP *γ* phosphate and reorganize into highly ordered structures to activate the Rab (Lee et al. 2009). Unsurprisingly, disruption of nucleotides in the highly conserved GTP-binding pocket can lead to major changes in the ability of a Rab to bind GTP, remain activate, or to hydrolyze GTP to GDP to inactivate (Gallegos et al. 2012).

In addition to the GTP-binding pocket, the Rab C-terminal region contains a CAAX-box C-terminal motif, which serves as the site of post-translational addition

of geranylgeranyl moieties that anchor the Rab into its target membrane. Within the Ras GTPase superfamily, Rabs can further be clustered by the presence of Rab family-specific sequences (RabF1-RabF5), a series of conserved stretches of sequence unique to and characteristic of the Rab family (Pereira-Leal & Seabra 2000) that cluster around the switch I and II domains (Hutagalung & Novick 2011; Müller & Goody 2018), whose conformational changes following GTP binding contribute to Rab activation. Detection of these five conserved stretches is sufficient to identify candidate Rab sequence, and has been successfully used as a discovery tool for novel Rabs (Pereira-Leal & Seabra 2000; Gallegos et al. 2012).

As small proteins with multiple highly conserved regions required for their essential function (Fig. 1) the diversity of functions between Rabs is determined by only a few key regions where non-deleterious sequence variability is possible. Upstream of the c-terminal CAAX box motif is a hypervariable sequence of 30-40 amino acids, which is thought to regulate targeting of Rabs to their specific membranes (Chavrier et al. 1991; Aivazian et al. 2006). Manipulation of these domains is sufficient to alter Rab effector recruitment and target membrane localization, as chimeric Rabs were able to recruit effectors specific to both donor Rabs, and addition of the c-terminal hypervariable region of Rab9 onto either Rab5 or Rab1 is sufficient to mislocalize chimeric Rab1 and Rab5 to the Rab9-specific membrane compartment (Li et al. 2014).

Beyond the c-terminal hypervariable region, recruitment of Rab-specific interactors is also regulated by sequence variability in and adjacent to the switch

I and II regions, which interact with specific guanine nucleotide exchange factors (GEFs) leading to Rab activation (Dong et al. 2007), and in part by a series of four semi-conserved, Rab subfamily-specific regions flanking the RabF1-F5 domains (Pereira-Leal & Seabra 2000). Rab subfamily-specific sequences (RabSF1-SF4) are shared between closely related Rabs, and are thought to partially define effector compatibility within Rab subfamilies (Ostermeier & Brunger 1999; Hutagalung & Novick 2011).

Rab localization and membrane attachment

As important regulators of intracellular membrane identity, trafficking, and fusion, active Rabs localize to the membrane periphery of their target compartment. Lacking native hydrophobic domains that would facilitate membrane anchoring, Rabs are tethered to intracellular membrane by one or two geranylgeranyl groups, which are post-translationally attached to the CAAX box domain at the Rab c-terminus (Desnoyers et al. 1996; Müller & Goody 2018). While this prenylation motif is essential for Rab function, it is surprisingly not highly conserved beyond maintenance of cysteine residues in one of several combinations, and constitutes part of the greater c-terminal hypervariable domain (Pylypenko et al. 2018). Post-translational modification of all Rabs is regulated by a pair of highly conserved, essential cofactors, the Rab escort protein (REP) and the Rab geranylgeranyltransferase (RabGGT) (Anant et al. 1998). RabGGT binding of geranylgeranyl pyrophosphate promotes the formation of a RabGGT-

REP complex, which then binds and prenylates translated, GDP-bound Rabs (Baron & Seabra 2008).

After the geranylgeranyl groups are added to the c-terminus, GDP-bound, inactive Rabs are retained in the cytosol through interaction with Rab GDP dissociation inhibitor (RabGDI). RabGDI is structurally similar to REP, and similarly is recruited to GDP-bound Rabs, but unlike REP, RabGDI specifically binds to Rab prenyl groups, but has low affinity for unmodified Rabs themselves (Wu et al. 2007). RabGDI both masks the newly-added lipid anchor and exposes the c-terminal hypervariable domain of the Rab (Rak et al. 2003), allowing for highly specific insertion of Rabs only when presented to their target membranes (Pfeffer & Aivazian 2004). RabGDI recruitment to GDP-bound Rabs is facilitated by recognition of the Rab switch I and II domains, and the high sequence conservation within these regions between Rabs means that only a few RabGDI isoforms are sufficient to bind all known Rabs (Pfeffer & Aivazian 2004).

Rab release from GDI and insertion into their target membrane is facilitated by a class of GDI dissociation factors (GDFs), though the specific identities and roles of Rab-specific GDFs remain incompletely understood, and novel Rab GDFs are still being identified (Collins et al. 2003; Pfeffer & Aivazian 2004; Qi et al. 2019). In addition to their role as chaperones for Rabs prior to membrane insertion, RabGDI can also be recruited to and excise GDP-bound, inactive Rabs tethered to their target membrane, returning them to the cytosolic Rab pool (Ullrich et al. 1993; Collins 2003). Together, the RabGGT-REP complex, as well

as GDI play essential roles in controlling accurate modification, activation and target membrane insertion of all Rabs (Fig. 2).

Regulation of Rab activation by GTP

After being anchored in their target membrane, Rabs must be activated through GTP binding to regulate membrane trafficking. GTP binding to Rabs is regulated by guanine nucleotide exchange factors (GEFs), which stimulate release of GDP by altering the conformation of the Rab GTP binding pocket, allowing binding of a new GTP molecule (Bos et al. 2007; Müller & Goody 2018). GEF recruitment is required for Rab activation, and recruitment of specific GEFs is determined by sequence variation in the Rab switch I and II domains (Langemeyer et al. 2014).

GEFs are highly diverse in origin, do not share significant sequence motifs or structural similarities, and show highly variable conservation across species (Bos et al. 2007), making the identification of GEFs and their relationships to specific Rabs particularly challenging. Specific Rabs can be targeted by multiple GEFs (Ho et al. 2012), and individual GEFs are also able to activate multiple related Rabs (Iwasaki & Tonoyaga 2000; Mahoney et al. 2006). GEFs have been found in multimeric tethering complexes that are themselves recruited to Rabs, including the HOPS tethering complex, which regulates endosome-lysosome fusion and contains a GEF of the yeast Rab7 ortholog Ypt7 (Wurmser et al. 2000), and in the yeast exocyst complex, where phosphorylated Sec2, a GEF, associates with the effector Sec15 to facilitate activity of the Rab Sec4 (Medkova

et al. 2006). Colocalization of GEFs with downstream Rab effectors stabilizes local Rab activation via a positive feedback loop of multimer recruitment and Rab activation (Grosshans et al. 2006). As important regulators of Rab activity, and therefore membrane trafficking and fusion, GEFs are themselves regulatory targets, and multiple pathways have been identified that mediate GEF expression (Ho et al. 2012), post-translational modification (Kulsekaran et al. 2015), and protein-protein interaction (Iwasaki & Tonoyaga 2000), either to promote or repress GEF activity.

Contrasting GEF activity are GTPase activating proteins (GAPs), which bind the target Rab and catalyze GTP hydrolysis, leading to rapid inactivation of the Rab. Despite being part of the GTPase superfamily, Rab GTP hydrolysis is slow and inefficient, making GAP activity a common strategy for efficient and regulatable regulation of Rab activity (Simon et al. 1996; Bos et al. 2007). Unlike the diverse Rab GEFs, almost all Rab GAPs contain a conserved TBC domain, which is required for their activity (Pan et al. 2006), but Rab GAPs are nonetheless both numerous (Frasa et al. 2012), and undiscriminating, with individual GAPs targeting multiple different Rabs (Frasa et al. 2012). This overlap does mean that despite containing diagnostic, conserved sequence, identification of a specific Rab's GAP or GAPs remains challenging, and the GAPs of many Rabs remain unidentified (Müller & Goody 2018).

Rab effectors

GTP-bound, active Rabs are able to recruit a series of effector proteins (Fig. 2), which in turn facilitate a diverse set of Rab-dependent functions including vesicle tethering prior to fusion (Mahoney et al. 2006), membrane coupling to motor proteins to facilitate transport (Hanafusa et al. 2019), and intracellular cargo sorting (Ailion et al. 2014). Each specific pathway relies on the recruitment of specific effectors to its target Rab or Rabs, and individual Rabs can recruit multiple different effectors, which can coordinate different membrane interactions or reinforce a single process.

Similar to GEFs, Rab effector recruitment is largely mediated by the small regions of variable sequence surrounding the switch I and II domains, and the c-terminal hypervariable domain. The Rab subfamily-specific domains that flank the switch domains are particularly important, as the conformation changes that occur in the switch domains following GTP binding are generally a prerequisite for effector recruitment (Fig. 3). Structural analysis of Rab3 complexed with its effector Rabphilin showed that effector binding was determined by three complementarity-determining regions (CDRs) corresponding to three Rab subfamily-specific domains (Ostermeier & Brunger 1999), and structural comparison of activated Rabs showed that the greatest regions of conformational variability occurred in the RabSF2 and SF3 domains, which include the switch I domain (Merithew et al. 2001). The conservation of sequence in RabSF domains between closely related Rabs also means that related Rabs frequently share effectors, and thus similar functions. However, even small sequence changes in switch domains are sufficient to confer significant differences in effector binding

specificity. The effector Rabenosyn-5, which normally targets the endosomally-localized Rab5 and Rab22, is unable to interact with endosomal Rab21 due to a single substitution, where the normally invariant glycine 55 in the switch I domain is replaced by glutamine. A corresponding G55Q substitution in Rab5 effectively eliminates binding affinity for this Rab-effector pair (Eathiraj et al. 2005).

As a large group of proteins with independent origins, Rab effectors show a high diversity in structure, function and Rab affinity, and exceptions to the typical rules of GTPase activation exist. Several effectors have been identified that are preferentially recruited to their target Rabs in their GDP-bound, inactive form. The effector protrudin, which regulates neurite outgrowth through positive regulation of anterograde vesicular traffic, interacts with GDP-bound, but not GTP-bound Rab11, and expression of a GTP-locked, constitutively active Rab11 phenocopied protrudin loss of function and inhibited neurite growth (Shirane & Nakayama 2006). Rab27a regulates multiple steps of vesicle exocytosis and subsequent endocytosis through interaction with canonical effectors, which interact with its active, GTP-bound form, and the effector coronin3, which specifically interacts with GDP-Rab27a to regulate membrane endocytosis (Kimura et al. 2008). Intracellular glucose, which triggers exocytosis of GTP-Rab27a-primed vesicles, also precipitates GTP-Rab27a hydrolysis, transitioning Rab27a into its coronin3-sensitive conformation and promoting endocytosis (Fig. 4). These interactions between effectors and GDP-bound, inactive Rabs not only highlights the diversity of Rab-effector relationships, but also the modularity of the canonical Rab cycle: while GDP-bound, inactive Rabs are canonically

extracted from their target membrane by GDIs, the phase between GTP hydrolysis and extraction still provides opportunities for important, Rab-dependent interactions affecting membrane trafficking.

Rabs in *C. elegans*

The model nematode *C. elegans* provides a uniquely accessible opportunity to study the roles of Rab-dependent pathways *in vivo*. While in mammalian systems over 60 Rab GTPases have been described (Hutagalung & Novick 2011), the *C. elegans* genome contains approximately half that number (Fig. 5) (Gallegos et al. 2012). Despite this reduction, nearly every Rab-dependent function is conserved between worms and mammals. Instead, this decreased number is largely attributable to reductions in redundant and partially redundant isoforms. For example, the Rab3 group, which is represented by four closely related isoforms in mice, Rab3A,B,C,D (Schlüter et al. 2004), is solely represented by *rab-3* in worms. In spite of a significant decrease in redundancy in the worm genome, relatively few *C. elegans* Rabs are essential, permitting *in vivo* study of whole-animal loss of function mutants and high-throughput screening approaches to mutant *rab* phenotypes. Functional redundancy does occur in worms, but this is more likely due to convergent function of related Rabs, rather than phenotypic coverage by multiple isoforms of a single Rab species (Mahoney et al. 2006). In spite of this loss of redundancy, Rabs as a family have not been functionally replaced in *C. elegans*, as many cellular phenotypes remain conserved between worm and mammal orthologs (Schlüter et al. 2004; Sekine et

al. 2018), and loss of general Rab family cofactors such as *rggt-1* and *rep-1* causes lethality and adult sterility, respectively (Tanaka et al. 2008). Taken together, *C. elegans* provides an *in vivo* opportunity to study individual Rabs without the challenges of either multiple isoform knockouts or knockout lethality.

Rab3 and Rab27 in humans and *C. elegans*

As with most intracellular membrane trafficking processes, the movement, tethering and fusion of secretory vesicles is regulated by Rab GTPases. The secretory vesicle Rabs cluster phylogenetically and are conserved among animals (Fukuda 2008), suggesting a shared evolutionary history. This group of Rabs can be defined by their exclusive localization to mature vesicles bound for secretion from the plasma membrane, and their direct involvement in secretion of these vesicles. Through a combination of fluorescent tagging of Rabs and proteomic analysis of secretory vesicles, Rab3A,B,C,D, Rab26, Rab27A,B, and Rab37 have been identified as secretory Rabs in mammalian cell culture systems (Takamori et al. 2006; Tsuboi et al. 2006; Brunner et al. 2007; Casey et al. 2007; Rindler et al. 2007). Of these, the Rab3 and Rab27 groups are the most ubiquitously represented across secretory vesicle types, and most research on Rab-dependent regulation of vesicle secretion has focused on these two Rab groups.

Rab3 and Rab27 subfamily members can be found on secretory vesicles in multiple cell types (Takai et al. 1996; Gomi et al. 2007; Mahoney et al. 2008; Fukuda et al. 2012), but are especially enriched in neurons, where they localize

to synapses and regulate tethering of synaptic vesicles at the axon terminal prior to activation-dependent fusion (Fischer von Mollard et al. 1990; Nonet et al. 1997; Mahoney et al. 2006). Rab27 and Rab3 subfamily members act highly redundantly, and normal synaptic transmission is possible even when multiple Rabs are lost. In mice, knockout of all four Rab3 proteins (Rab3A,B,C,D), despite leading to postnatal lethality, produces negligible defects in synaptic transmission, and only leads to declines in vesicular release probability and recruitment of Rab effectors to the synapse, pointing to a role for the Rab3 family as regulators of normal Ca^{2+}-triggered vesicle exocytosis, but not fundamental components of synaptic vesicle release (Schlüter et al. 2004).

Outside the nervous system, Rab3 has been implicated in secretory vesicle regulation upstream of exocytosis, including regulation of secretory granule size and insulin granule availability (Riedel et al. 2002; Yaekura et al. 2003), but is not known to be directly involved in tethering vesicles to the plasma membrane as it does for synaptic vesicles in neurons. By contrast, the Rab27 subfamily members have well-defined roles in granule trafficking and tethering outside the nervous system. A function for Rab27a was initially identified in melanocytes and T-lymphocytes, where it is required for anterograde transport of melanosomes and release of lytic granules, respectively (Bahadoran et al. 2001; Haddad et al. 2001). Loss of RAB27A in humans results in Griscelli syndrome, characterized by pigment trafficking deficiencies and T-lymphocyte activation defects (Ménasché et al. 2000); the first Rab to be directly implicated in a human disease.

In *C. elegans*, *rab-3* and *rab-27* are the sole representatives of the secretory Rab family with confirmed roles in vesicle secretion (Fig. 6) (Mahoney et al. 2006; Mahoney et al. 2008; Feng et al. 2012; Gallegos et al. 2012; Johnson et al. 2013). As in mammalian systems, *rab-3* and *rab-27* play functionally redundant roles in synaptic vesicle tethering and synaptic transmission. Loss of either *rab-27* or *rab-3* leads to only minor defects in synaptic transmission, while loss of both Rabs produces a significant transmission defect, it does not completely eliminate transmission (Mahoney et al. 2006), suggesting, as with Rab3A,B,C,D in mammals, that these secretory Rabs are not fundamentally required for vesicle fusion, but rather are essential for the regulation of normal vesicle exocytosis and availability in neurons. Neuronal *rab-27* and *rab-3* are further linked by their shared GEF, AEX-3, which is similarly partially required for synaptic transmission, and whose loss phenocopies dual loss of *rab-3* and *rab-27* (Mahoney et al. 2006). Active RAB-27 recruits the effector RBF-1, a relative of the mammalian effectors rabphilin, to mediate synaptic vesicle tethering (Mahoney et al. 2006). While mammalian Rabphilin is an effector of both Rab27 and Rab3 members, *C. elegans rbf-1* only interacts with *rab-27* (Barclay et al. 2012; Feng et al. 2012), suggesting that *rbf-1* may be more similar to the mammalian granuphilin/Slp4, a Rab27 effector not known to interact with Rab3 (Yi et al. 2002).

As in mammalian systems, *rab-27* also plays an important role in vesicle secretion outside the nervous system (Mahoney et al. 2008; Feng et al. 2012). While *rab-3* is not known to be expressed outside neurons (Stefanakis et al.

2015), *rab-27* is also expressed in the posterior and anterior cells of the intestine (Mahoney et al. 2006), where it is required for dense core vesicle fusion and neuropeptide release into the pseudocoelom, also mediated through the effector RBF-1 (Feng et al. 2012). *rab-27* is a member of the *aex* genes, a genetic pathway that regulates the maturation, release and reception of the neuropeptide NLP-40 from the intestine to the nervous system (Mahoney et al. 2008; Wang et al. 2013). This pathway includes the RAB-27 and RAB-3 GEF *aex-3*, but interestingly does not include the effector RBF-1, though it is involved in RAB-27-dependent dense core vesicle secretion in the intestine. Instead, RAB-27's effector in the *aex* pathway is believed to be AEX-1, an ortholog of Munc13, which links RAB-27 to the SNAP25 ortholog AEX-4 to mediate vesicle fusion (Doi & Iwasaki 2002).

The Rab family of GTPases are essential regulators of intracellular membrane sorting, trafficking, maturation and fusion. Manipulation of Rabs and the pathways that regulate their modification, activation and interactions provide a window into diverse intracellular pathways that regulate development (Bhat & Hutter 2016), regeneration (Sekine et al. 2018) and disease (Ménasché et al. 2000). Understanding how Rabs control these pathways, and how they themselves are controlled may go far to unlocking both central principles of cell biology and potential treatments or therapies for injuries and diseases.

References

Ailion M, Hannemann M, Dalton S, Pappas A, Watanabe S, Hegermann J, Liu Q, Han H, Gu M, Goulding MQ, Sasidharan N, Schuske K, Hullett P, Eimer S, Jorgensen EM. 2014. Two Rab2 interactors regulate dense-core vesicle maturation. *Neuron* 82:167-180.

Aivazian D., Serrano RL, Pfeffer S. 2006. TPI47 is a key effector for Rab9 localization. *J Cell Biol* 173:917-926.

Anant JS, Desnoyers L, Machius M, Demeler B, Hansen JC, Westover KD, Deisenhofer J, Seabra MC. 1998. Mechanism of Rab geranylgeranylation: formation of the catalytic ternary complex. *Biochemistry* 37:12559-12568.

Bahadoran P et al. 2001. Rab27a: a key to melanosome transport in human melanocytes. *J Cell Biol* 152:843-850.

Barclay JW, Morgan A, Burgoyne RD. 2012. Neurotransmitter release mechanisms studied in *Caenorhabditis elegans*. *Cell Calcium* 52:289-295.

Baron RA, Seabra MC. 2008. Rab geranylgeranylation occurs preferentially via the pre-formed REP-RGGT complex and is regulated by geranylgeranyl pyrophosphate. *Biochem J* 415:67-75.

Bhat JM, Hutter H. 2016. Pioneer axon navigation is controlled by AEX-3, a guanine nucleotide exchange factor for RAB-3 in *Caenorhabditis elegans*. *Genetics* 204:1235-1247.

Bos JL, Rehmann H, Wittinghofer A. 2007. GEFs and GAPs: critical elements in the control of small G proteins. *Cell* 129:865-877.

Brunner Y, Couté Y, Iezzi M, Foti M, Fukuda M, Hochstrasser DF, Wollheim CB, Sanchez J. 2007. Proteomics analysis of insulin secretory granules. *Mol Cell Proteomics* 6:1007-1017.

Casey TM, Meade JL, Hewitt EW. 2007. Organelle proteomics: identification of the exocytic machinery associated with the natural killer cell secretory lysosome. *Mol Cell Proteomics* 6:767-780.

Chavrier P, Gorvel J, Stelzer E, Simons K, Gruenberg J, Zerial M. 1991. Hypervariable C-terminal domain of rab proteins acts as a targeting signal. *Nature* 353:769-772.

Collins RN. 2003. “Getting it on” – GDI displacement and small GTPase membrane recruitment. *Mol Cell* 5:1064-1066.

Desnoyers L, Anant JS, Seabra MC. 1996. Geranylgeranylation of Rab proteins. *Biochem Soc Trans*24:699-703.

Doi M, Iwasaki K. 2002. Regulation of retrograde signaling at neuromuscular junctions by the novel C2 domain protein AEX-1. *Neuron* 33:249-259.

Dong G, Medkova M, Novick P, Reinisch KM. 2007. A catalytic coiled coil: structural insights into the activation of the Rab GTPase Sec4p by Sec2p. *Mol Cell* 25:455-462.

Feng W, Liang T, Yu J, Zhou W, Zhang Y, Wu Z, Xu T. 2012. Rab-27 and its effector RBF-1 regulate the tethering and docking steps of DCV exocytosis in *C. elegans*. *Sci China Life Sci* 55:228-235.

Fischer von Mollard G, Mignery GA, Baumert M, Perin MS, Hanson TJ Burger PM, Jahn R, Südhof TC. 1990. Rab3 is a small GTP-binding protein exclusively localized to synaptic vesicles. *PNAS* 87:1988-1992.

Frasa MAM, Koessmeier KT, Ahmadian MR, Braga VMM. 2012. Illuminating the functional and structural repertoire of human TBC/RABGAPs. *Nat Rev* 13:67-73.

Fukuda M. 2008. Regulation of secretory vesicle traffic by Rab small GTPases. *Cell Mol Life Sci* 65:2801-2813.

Gallegos ME et al. (2012) The C. elegans Rab family: identification, classification and toolkit construction. *PLoS One*: 7:e49387.

Gomi G, Mori K, Itohara S, Izumi T. 2007. Rab27b is expressed in a wide range of exocytic cells and involved in the delivery of secretory granules near the plasma membrane. *Mol Biol Cell* 18:4377-4386.

Grosshans BL, Ortiz D, Novick P. 2006. Rabs and their effectors: achieving specificity in membrane traffic. *PNAS* 103:11821-11827.

Haddad EK, Wu X, Hammer 3rd JA, Henkart PA. 2001. Defective granule exocytosis in Rab27a-deficient lymphocytes from Ashen mice. *J Cell Biol* 152:835-842.

Hanafusa H, Yagi T, Ikeda H, Hisamoto N, Nishioka T, Kaibuchi K, Shirakabe K, Matsumoto K. 2019. LRRK1 phosphorylation of Rab7 at S72 links trafficking of EGFR-containing endosomes to its effector RILP. *J Cell Sci* 132:jcs228809.

Ho JL, Chapeaublanc E, Kirkwood L, Nicolle R, Benhamou S, Lebret T, Allory Y, Southgate J, Radvanyi F, Goud B. 2012. Deregulation of Rab and Rab effector genes in bladder cancer. *PLoS One* 7:e39469.

Hutagalung AH, Novick PJ. 2011. Role of Rab GTPases in membrane traffic and cell physiology. *Physiol Rev* 91:119-149.

Iwasaki K, Tonoyaga R. 2000. The Rab3 GDP/GTP exchange factor homolog AEX-3 has a dual function in synaptic transmission. *EMBO J* 19:4806-4816.

Johnson JR, Kashyap S, Rankin K, Barclay JW. 2013. Rab-3 and unc-18 interactions in alcohol sensitivity are distinct from synaptic transmission. *PLoS One* 8:e81117.

Kimura T, Kaneko Y, Yamada S, Ishihara H, Senda T, Iwamatsu A, Niki I. 2008. The GDP-dependent Rab27a effector coronin3 controls endocytosis of secretory membrane in insulin-secreting cell lines. *J Cell Sci* 121:3092-3098.

Kulasekaran G, Nossova N, Marat AL, Lund I, Cremer C, Ioannou MS, McPherson PS. 2015. Phosphorylation-dependent regulation of Connecdenn/DENND1 guanine nucleotide exchange factors. *J Biol Chem* 290:17999-18008.

Langemeyer L, Nunes Bastos R, Cai Y, Itzen A, Reinisch KM, Barr FA. 2014. Diversity and plasticity in Rab GTPase nucleotide release mechanisms has consequences for Rab activation and inactivation. *eLife* 3:e01623.

Lee MG, Mishra A, Lambright DG. 2009. Structural mechanisms for regulation of membrane traffic by Rab GTPases. *Traffic* 10:1377-1389.

Li F, Yi L, Zhao L, Itzen A, Goody RS, Wu Y. 2014. The role of the hypervariable C-terminal domain in Rab GTPases membrane targeting. *PNAS* 111:2572-2577.

Mahoney TR, Liu Q, Itoh T, Luo S, Hadwiger G, Vincent R, Wang Z, Fukuda M, Nonet ML. 2006. Regulation of synaptic transmission by RAB-3 and RAB-27 in *Caenorhabditis elegans*. *PNAS* 17:2617-2625.

Mahoney TR, Luo S, Round EK, Brauner M, Gottschalk A, Thomas JH, Nonet ML. 2008. Intestinal signaling to GABAergic neurons regulates a rhythmic pattern in *Caenorhabditis elegans*. *PNAS* 105:16350-16355.

Medkova M, France YE, Coleman J, Novick P. 2006. The rab exchange factor Sec2p reversibly associates with the exocyst. *Mol Cell Biol* 17:2757-2769.

Ménasché G et al. 2000. Mutations in RAB27A cause Griscelli syndrome associated with haemophagocytic syndrome. *Nat Genet* 25:173-176.

Merithew E, Hatherly S, Dumas JJ, Lawe DC, Heller-Harrison R, Lambright DG. 2001. Structural plasticity of an invariant hydrophobic triad in the switch regions of Rab GTPases is a determinant of effector recognition. *J Biol Chem* 276:13982-13988.

Müller MP, Goody RS. 2018. Molecular control of Rab activity by GEFs, GAPs and GDI. *Small GTPases* 9:5-21.

Nonet ML, Staunton JE, Kilgard MP, Fergestad T, Hartwieg E, Horvitz HR, Jorgensen EM, Meyer BJ. 1997. *Caenorhabditis elegans rab-3* mutant synapses exhibit impaired function and are partially depleted of vesicles. *J Neurosci* 17:8061-8073.

Ostermeier C, Brunger AT. 1999. Structural basis of Rab effector specificity: crystal structure of the small G protein sA complexed with the effector domain of Rabphilin-3A. *Cell* 96:363-374.

Pan X, Eathiraj S, Munson M, Lambright DG. 2006. TBC-domain GAPs for Rab GTPases accelerate GTP hydrolysis by a dual-finger mechanism. *Nature* 442:303-306.

Pereira-Leal JB, Seabra MC. 2000. The mammalian Rab family of small GTPases: definition of family and subfamily sequence motifs suggests a mechanism for functional specificity in the Ras superfamily. *J Mol Biol* 301:1077-1087.

Pereira-Leal JB, Seabra MC. 2001. Evolution of the Rab family of small GTP-binding proteins. *JMB* 313: 889-901.

Pfeffer S, Aivazian D. 2004. Targeting Rab GTPases to distinct membrane compartments. *Nat Rev* 5:886-896.

Pylypenko O, Hammich H, Yu I, Houdusse A. 2018. Rab GTPases and their interacting protein partners: structural insights into Rab functional diversity. *Small GTPases* 9:22-48.

Qi S, Su L, Li J, Zhao P, Zhang Q, Niu X, Liu J, Jia G, Wei X, Tavernier J, Jiang J, Chen Z, Zhang S. 2019. YIPF2 is a novel Rab-GDF that enhances HCC malignant phenotypes by facilitating CD147 endocytic cycle. *Cell Death & Disease* 10: https://doi.org/10.1038/s41419-019-1709-8

Rak A, Pylypenko O, Durek T, Watzke A, Kushnir S, Brunsveld L, Waldmann H, Goody RS, Alexandrov K. 2003. Structure of a Rab GDP-dissociation inhibitor in complex with prenylated YPT1 GTPase. *Science* 302:646-650.

Riedel D et al. 2002. Rab3D is not required for exocrine exocytosis but for maintenance of normally sized secretory granules. *Mol Biol Cell* 22:6487-6497.

Rindler MJ, Xu C, Gumper I, Smith NN, Neubert TA. 2007. Proteomic analysis of pancreatic zymogen granules: identification of new granule proteins. *J Proteome Res* 5:2987-2992.

Schlüter OM, Schmitz F, Jahn R, Rosenmund C, Südhof TC. 2004. A complete genetic analysis of neuronal Rab3 function. *J Neurosci* 24:6629-6637.

Sekine Y, Lin-Moore A, Chenette DM, Wang X, Jiang Z, Cafferty WB, Hammarlund M, Strittmatter SM. 2018. Functional genome-wide screen identifies pathways restricting central nervous system axonal regeneration. *Cell Rep* 23:415-428.

Shirane M, Nakayama KI. 2006. Protrudin induces neurite formation by directional membrane trafficking. *Science* 314:818-821.

Simon I, Zerial M, Goody RS. 1996. Kinetics of interaction of Rab5 and Rab7 with nucleotides and magnesium ions. *J Biol Chem* 271:20470-20478.

Stefanakis N, Carrera I, Hobert O. 2015. Regulatory logic of pen-neuronal gene expression in *C. elegans*. *Neuron* 87:733-750.

Takai Y, Sasaki T, Shirataki H, Nakanishi H. 1996. Rab3A small TP-binding protein in Ca(2+)-dependent exocytosis. *Genes Cells* 1:615-632.

Takamori S et al. 2006. Molecular anatomy of a trafficking organelle. *Cell* 127:831-846.

Tanaka D, Kameyama K, Okamoto H, Doi M. 2008. *Caenorhabditis elegans* Rab escort protein (REP-1) differently regulates each Rab protein function and localization in a tissue-dependent manner. *Genes Cells* 13:1141-1157.

Tsuboi T, Fukuda M. 2006. Rab3A and Rab27A cooperatively regulate the docking step of dense-core vesicle exocytosis in PC12 cells. *J Cell Sci* 119:2196-2203.

Ullrich O, Stenmark H, Alexandrov K, Huber LA, Kaibuchi K, Sasaki T, Takai Y, Zerial M. 1993. Rab GDP dissociation inhibitor as a general regulator for the membrane association of Rab proteins. *J Biol Chem* 268:18143-18150.

Wang H, Girskis K, Janssen T, Chan JP, Dasgupta K, Knowles JA, Schoofs L, Sieburth D. 2013. Neuropeptide secreted from a pacemaker activates neurons to control a rhythmic behavior. *Curr Biol* 23:746-754.

Wu Y, Tan K, Waldmann H, Goody RS, Alexandrov K. 2007. Interaction analysis of prenylated Rab GTPase with Rab escort protein and GDP dissociation inhibitor explains the need for both regulators. *PNAS* 104:12294-12299.

Wurmser AE, Sato TK, Emr SD. 2000. New component of the vacuolar class C-Vps complex couples nucleotide exchange on the Ypt7 GTPase to SNARE-dependent docking and fusion. *J Biol Chem* 151:551-562.

Yaekura K et al. 2003. Insulin secretory deficiency and glucose intolerance in Rab3A null mice. *J Biol Chem* 278:9715-9721.

Yi Z, Yokota H, Torii S, Aoki T, Hosaka M, hao S, Takata K, Takeuchi T, Izumi T. 2002. The Rab27a/granuphilin complex regulates the exocytosis of insulin-containing dense-core granules. *Mol Cell Biol* 22:1858-1867.

Yun JS, Ha SC, Kim S, Kim YG, Kim H, Chang JH. 2019. Crystal structure of *Arabidopsis thaliana* RabA1a. *J Integr Plant Biol* 61:93-109.

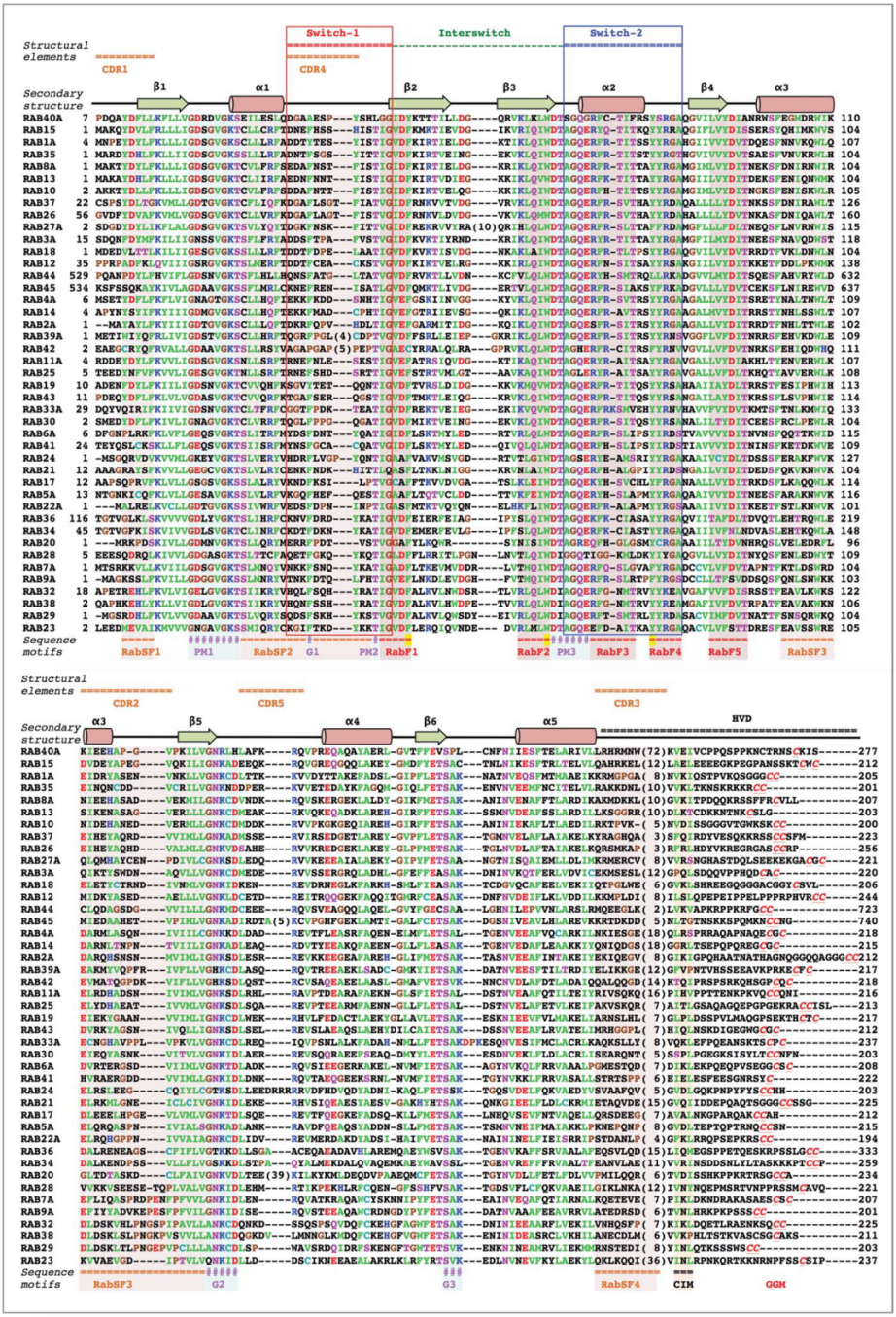

Figure 1. Sequence alignment of human Rab sequences. Rab family domains (RabF1-5) and Rab subfamily-specific (RabSF1-5) domains are highlighted. C-terminal cysteines, highlighted in red, are found at the end of the c-terminal hypervariable domain (HVD). Switch I and II are identified. Secondary structure, as well as complementarity-defining regions (CDRs) that interact with effectors are defined, based on the crystal structure of GTP-Rab3 bound to Rabphilin. Rabs are presented in phylogenetic order of human Rabs. Conserved residues are color coded: red = negatively charged, blue = positively charged, magenta = polar, green = hydrophobic, brown = Pro/Gly. Adapted from Pylypenko et al. 2018.

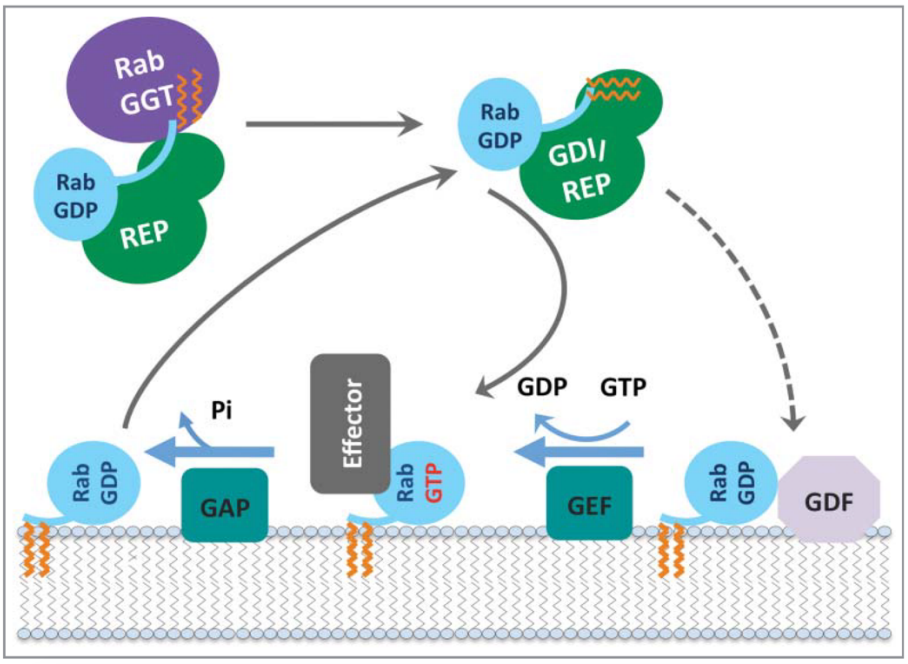

Figure 2. The Rab cycle. Newly-translated Rabs are recognized by Rab escort protein (REP). The Rab-REP complex is recognized by Rab geranylgeranyltransferase (RabGGT), which adds geranylgeranyl groups to the Rab c-terminal cysteines, allowing the Rab to be anchored into its target membrane. Following geranylgeranylation, GDP-bound Rab can be bound by a Rab GDP dissociation inhibitor (GDI), or retained in REP. The GDI protects the Rab's hydrophobic geranylgeranyl tail, and exposes its GEF-specific residues, allowing the complex to be recruited to the Rab's target membrane through interaction with a membrane-localized guanine nucleotide exchange factor (GEF), or in some cases by a specific GDI dissociation factor (GDF). The Rab GEF stimulates the Rab to release its GDP and bind GTP, leading to a conformational change and Rab activation. Activated, membrane-inserted Rabs are able to recruit specific effectors to transduce diverse processes regulating membrane traffic, sorting, and fusion. GTPase activating proteins (GAPs) accelerate the Rab's GTPase activity leading to inactivation and dissociation of most effectors. Inactive, GDP-bound Rabs can be excised from their target membrane by GDI, and returned to a soluble pool of inactive cytosolic Rabs. Adapted from Pylypenko et al. 2018.

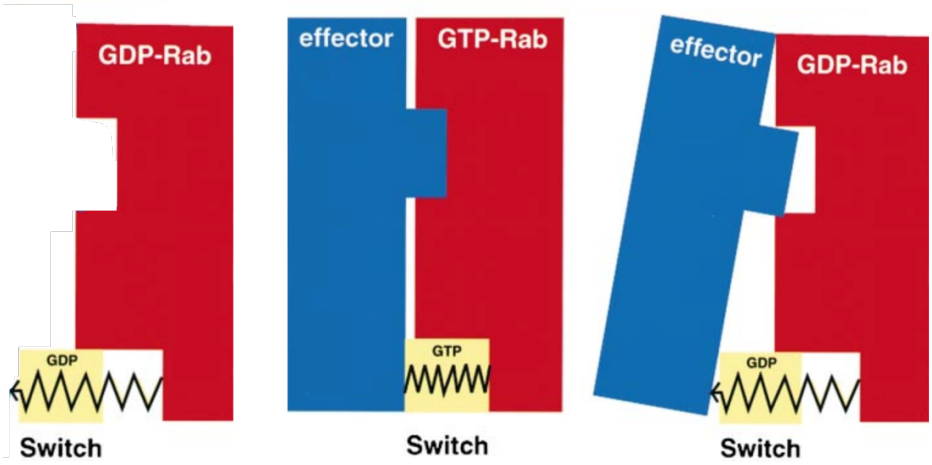

Figure 3. Binding of GTP induces conformational changes that permit stable effector recruitment. GTP-Rab conformation permits effector recruitment, though stable binding is still determined by a secondary binding site c-terminal to the GTP-binding domain. GTP hydrolysis leads to effector dissociation by causing a loss of the ordered conformation in the switch I and II domains that permit effector recruitment. Adapted from Ostermeier & Brunger 1999.

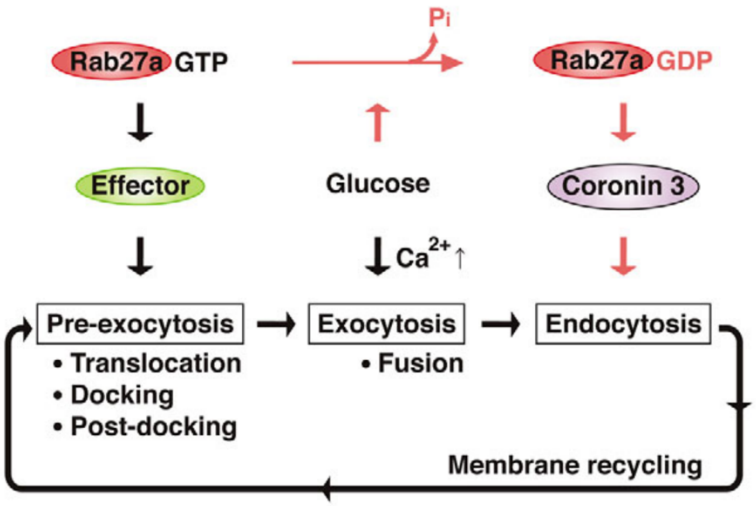

Figure 4. Regulation of membrane cycling by Rab27a in its GTP- and GDP-bound forms. GTP-Rab27a regulates docking of exocytic vesicles through recruitment of its GTP-dependent effectors. An increase in intracellular glucose triggers vesicle exocytosis via an increase in cytosolic Ca^{2+}, and this increase in intracellular glucose also leads to a conversion of GTP-Rab27a to GDP-Rab27a, likely through activation of one or more Rab27a GAPs. GDP-Rab27a is able to recruit coronin3, an unusual effector that preferentially binds its target Rab in its GDP-bound, "inactive" state. Coronin regulates membrane endocytosis, leading to recovery of membrane donated during prior vesicle secretion. Adapted from Kimura et al. 2008.

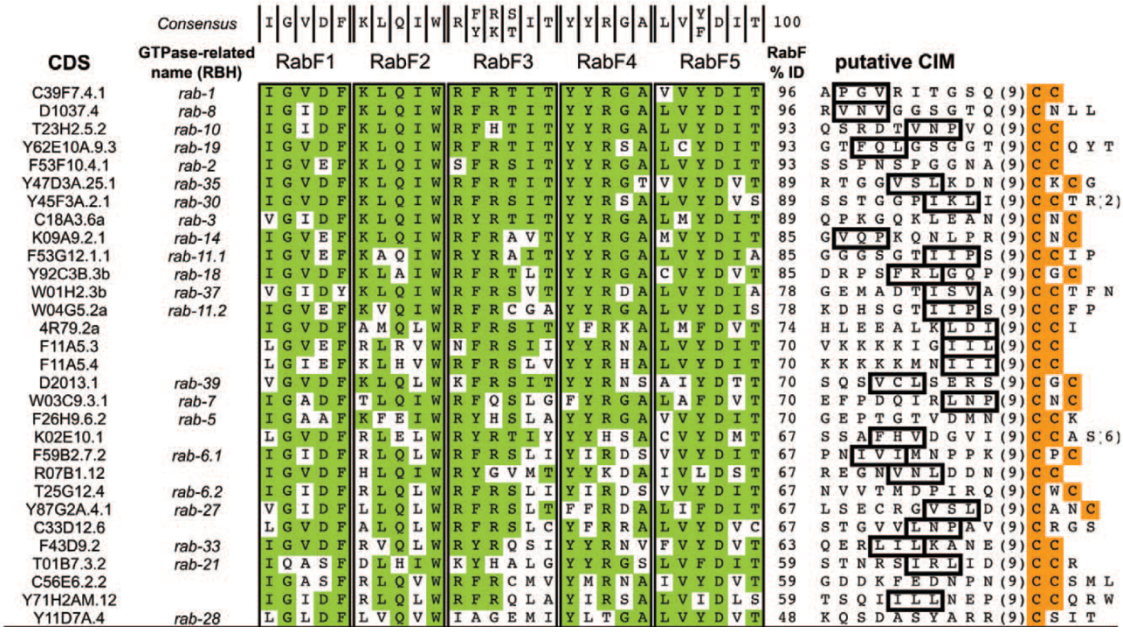

Figure 5. Sequence alignment of known and candidate Rabs in *C. elegans*. Genes are listed in descending order of percent identity to RabF domain sequence, and the proportion of each alignment to the each RabF1-5 sequence is listed as RabF% ID. The hypervariable c-terminal domain for each sequence is shown on the right, with c-terminal cysteines highlighted in orange. Putative c-terminal binding region interacting motifs (CIM) are boxed where detected. Adapted from Gallegos et al. 2012.

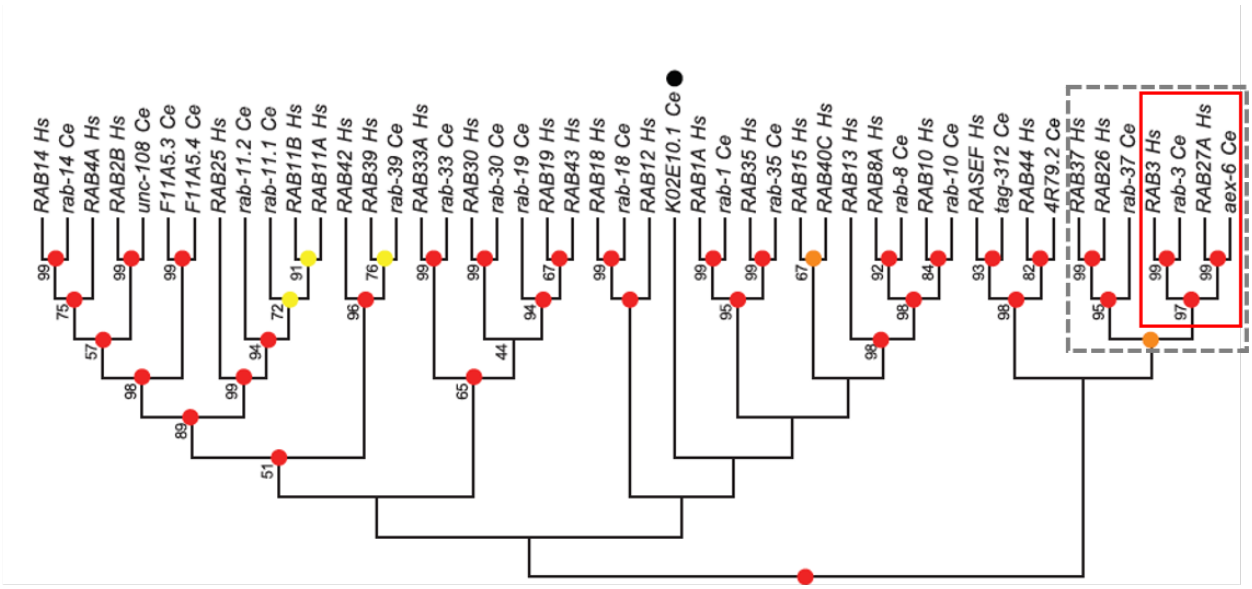

Figure 6. Partial cladogram of Rab family members in *C. elegans* and humans. *C. elegans rab-27* and *rab-3* cluster in the "secretory Rab" clade, which also includes human RAB37 and RAB26, which do not have close orthologs in *C. elegans*. Within each species, RAB3/*rab-3* and RAB27A/*rab-27* are each others closest relatives, but each *C. elegans* Rab is most closely related to its human ortholog, suggesting a high degree of functional similarity. Canonical secretory Rabs cluster together in the dashed box, while the Rab27/Rab3 subfamily is highlighted in the red box. Per the authors: The evolutionary history was inferred using the Neighbor-Joining phylogenetic reconstruction method…The optimal tree is shown with the percentage of replicate trees (>40) in which the associated genes cluster together in the bootstrap test (500 replicates) provided next to each branch…Clades marked with red, orange or yellow circles indicate their degree of stability under a variety of phylogenetic reconstruction parameters. Red =14/14, orange =13/14, yellow = 12/14 trees. Adapted from Gallegos et al. 2012.

Preface to: Functional Genome-wide Screen Identifies Pathways Restricting Central Nervous System Axonal Regeneration

The research summarized in this publication includes essential and foundational parts of my dissertation work, and provides both the intellectual basis for my thesis research on axon regeneration, as well as the crucial initial findings regarding RAB-27 and the Rab family of GTPases as novel regulators of axon regeneration.

The establishment of a high-throughput model for axon regeneration *in vitro* opened the door for screening approaches to identify novel regeneration inhibitors, a functional class of genes previously difficult to identify through forward screening methods. This project was conceived and initiated by Dr. Yuichi Sekine and Dr. Stephen Strittmatter, who carried out the genome-wide *in vitro* axon regeneration screen, validated *in vitro* regeneration phenotypes for over two hundred genes identified by the initial screen, identified the Rab family of GTPases as a gene family enriched in previously unidentified axon regeneration regulators, and confirmed a conserved *in vivo* phenotype of regeneration inhibition in *Rab27b*$^{-/-}$ mice.

My own contribution to this project focused on the initial characterization of *rab-27* as a regeneration inhibitor using *C. elegans*, presented in Figure 6 of the paper. My work outlined the initial validation of *C. elegans rab-27* as a potent inhibitor of regeneration in living animals prior to additional validation in mice. My work in this project also outlines our initial finding that re-expression of RAB-27 in

the GABA neurons of mutant animals was sufficient to restore normal regeneration success, though this result was later partially contradicted by additional discoveries of a *rab-27*-dependent mechanism of regeneration inhibition in worms derived extrinsically from the intestine.

Functional Genome-wide Screen Identifies Pathways Restricting Central Nervous System Axonal Regeneration

Yuichi Sekine[1,2] Alexander Lin-Moore[1,3] Devon M. Chenette[1,2] Xingxing Wang[1,2] Zhaoxin Jiang[1,2] William B. Cafferty[2] Marc Hammarlund[1,3,4] and Stephen M. Strittmatter[1,2,4,5,*]

[1]Program in Cellular Neuroscience, Neurodegeneration & Repair, Yale University School of Medicine, New Haven, CT 06536, USA
[2]Department of Neurology, Yale University, New Haven, CT 06536, USA
[3]Department of Genetics, Yale University, New Haven, CT 06536, USA
[4]Department of Neuroscience, Yale University, New Haven, CT 06536, USA
[5]Lead Contact
*Correspondence: stephen.strittmatter@yale.edu
https://doi.org/10.1016/j.celrep.2018.03.058

ABSTRACT

Axonal regrowth is crucial for recovery from CNS injury but is severely restricted in adult mammals. We used a genome-wide loss-of-function screen for factors limiting axonal regeneration from cerebral cortical neurons in vitro. Knockdown of 16,007 individual genes identified 580 significant phenotypes. These molecules share no significant overlap with those suggested by previous expression profiles. There is enrichment for genes in pathways related to transport, receptor binding, and cytokine signaling, including Socs4 and Ship2. Among transport-regulating proteins, Rab GTPases are prominent. In vivo assessment with C. elegans validates a cell-autonomous restriction of regeneration by Rab27. Mice lacking Rab27b show enhanced retinal ganglion cell axon regeneration after optic nerve crush and greater motor function and raphespinal sprouting after spinal cord trauma. Thus, a comprehensive functional screen reveals multiple pathways restricting axonal regeneration and neurological recovery after injury.

INTRODUCTION

Devastating and persistent functional deficits occur after spinal cord injury (SCI), despite survival of nearly all neurons. Because the primary cause of disability is disconnection of networks by axon transection, axon regrowth has the potential to provide recovery by restoring connectivity, without requiring “new” cells. It is clear that both cell-autonomous and environmental factors contribute to axon growth failure.

There have been genetic attempts to identify axon regeneration factors, but the field has not benefited from unbiased genome-wide functional approaches. Most efforts have started with expression surveys rather than functional studies. No functional screen has focused on endogenous genes in adult mammalian CNS at a level approaching the entire genome (Blackmore et al., 2010; Moore et al., 2009; Park et al., 2008), and existing efforts frequently use gain of function, initial outgrowth, and/or cell lines (Blackmore et al., 2010; Buchser et al., 2010; Loh et al., 2008; Moore et al., 2009; Sepp et al., 2008). Non-mammalian regeneration has been analyzed extensively in C. elegans by loss of function (LOF) with both small interfering RNA (siRNA) and mutant alleles, confirming regeneration mechanisms conserved between mammals and C. elegans (El Bejjani and Hammarlund, 2012). DLK-1, PTEN, and cAMP are important regulators of regeneration in mammals and have similar functions in worms (El Bejjani and Hammarlund, 2012; Hammarlund et al., 2009; Wang and Jin, 2011; Yan et al., 2009). Yet few C. elegans regeneration genes have been validated in mammals.

Moreover, even in this model organism, using both mutant alleles and siRNA screening, less than 25% of the genome has been tested for axon regeneration. In summary, a loss of function screen for mammalian CNS regeneration has not been completed on a scale approaching the entire genome.

Here, we sought an unbiased genome-wide assessment of mammalian genes whose loss of function allows axonal sprouting and regeneration after CNS trauma. Critically, our approach was unbiased at the genome-wide level in mammalian species, focused on axonal regeneration and using cerebral cortical projection neurons. With single clones spanning a lentiviral short hairpin RNA (shRNA) library, we assessed the role of each gene to limit axonal regeneration. Our pilot screen restricted to 219 phosphatases had uncovered a role for Inpp5f in limiting axonal regrowth and neurological recovery from trauma (Zou et al., 2015). Here, a comprehensive genome-wide screen reveals about 500 genes with a regeneration phenotype, and the vast majority were not previously identified by expression surveys or previous limited functional studies. We validate these hits and show that protein transport function is the most highly enriched group limiting axon regeneration. The studies uncover multiple pathways with a role in limiting regeneration, and highlight Rab-dependent membrane trafficking as a key factor for enhancing neurological recovery.

RESULTS

Functional Genomic Screen of Mouse CNS Axon Regeneration

We conducted a loss of function genome-wide in vitro axon regeneration screen in primary mouse cortical neurons (Huebner et al., 2011; Zou et al., 2015). We reasoned that this in vitro model, although lacking features of the in vivo CNS such as environmental contributions from glia and matrix, would capture cell-intrinsic functions of CNS neurons that limit regeneration. In these cultures more than 80% of cells are NeuN-positive cells at day in vitro (DIV) 10 (Figures S1A and S1E). There are low percentages of astrocytic and oligodendrocytic lineage cells with about 10% of cells being detected with O4, anti-PDGFRα, and anti-GFAP antibodies, but there are essentially no detectable microglial cells detected with Iba1 antibodies (Figures S1B–S1E). At DIV 3, clones from a lentiviral mouse shRNA library were added to cortical neurons in 96-well microtiter plates at a titer of 104 to 105. Approximately 83,000 separate clones were tested, with about 20 no-virus controls per plate and each plate tested in two replicates. The resulting screen targeted more than 16,000 protein-coding genes with three to five shRNA species per gene, representing about 70% of the predicted protein-coding genes in the mouse genome. On DIV 8, by which time axon extension had ceased and neurons were quiescent, we initiated axon injury and potential regeneration in each well by using a 96-pin tool to generate a reproducible scrape lesion. After injury, neurons were allowed 2 days for axon regeneration. Then neurons were fixed and stained with anti-βIII tubulin antibody to visualize axons, rhodamine-conjugated phalloidin for growth cones, and DAPI for nuclei (Huebner et al., 2011). The regenerated zone contains axons but essentially no cell soma or dendrites. Stained plates were imaged using an ImageXpress fluorescent

microscopy system with autofocus and motorized stage, and images were processed using scripts written in MATLAB (The MathWorks) to detect the injury zone and measure axonal regeneration with a Z′ of 0.18 (Figure 1A).

In the primary screen, the Z score metric, (normalized regeneration − 1)/(SD for all genes), reveals a positive hit rate slightly less than 3%; 479 genes increased axonal regeneration by more than two SDs from control (Figure 1B; Table S1). Suppression of 100 genes showed decreased axon regeneration by more than two SDs, though either decreased survival or decreased axonal growth per se may explain this phenotype. We focused on genes whose suppression stimulates regeneration (Z score > 2.0), because future development of pharmacological reagents is feasible when antagonists might promote regeneration. The top 122 genes from the full screen were retested for the validity and reproducibility of the screen (Figure 1C). Even with correction for 122 pairwise comparisons, 63% of the retested hits showed strong statistical significance ($p < 0.0001$), and 82% achieved statistically significant increases in axon regeneration. Thus, the screen faithfully identifies genes for which loss of function enhances regeneration in our in vitro assay.

Axon Regeneration Genes Are Distinct from Expression Surveys or Invertebrate Screens

We asked whether the genes we found to functionally affect regeneration of cultured vertebrate CNS neurons after injury (Table S1) are similar to genes identified by other functional methods. Loss-of-function studies in vivo in

peripheral nervous system (PNS) neurons (motor and sensory) completed in C. elegans have analyzed several thousand genes with 214 significant phenotypes (Chen et al., 2011; Nix et al., 2014). Murine orthologs for the 214 worm genes were identified bioinformatically and compared with the mouse regeneration gene lists (Figure 2A). There is a statistically significant overlap of these lists, with 16 of the 214 orthologs also affecting regeneration in our screen, suggesting that to some extent regeneration mechanisms are conserved between these two systems. Differences in neuron type, experimental method, or species may limit the degree of overlap that were detected.

Next, we asked whether the genes we found to functionally affect regeneration of cultured vertebrate CNS neurons after injury are similar to genes found to change expression after injury. Such expression changes have been hypothesized to include genes that are functionally important for regeneration. The 500 most differentially expressed (DE) genes from a cultured dorsal root ganglion (DRG) neuron study of the effect of preconditioning axotomy (Tedeschi et al., 2016) were extracted from RNA sequencing (RNA-seq) data of the GEO repository. This list was compared with the functional shRNA cortical axon regeneration gene lists (Figure 2B). A total of 12 and 6 genes overlapped between the functional and expression studies, and this rate was not statistically significant on the basis of chi-square analysis of sampling across the mouse genome. A broad range of alternate expression studies have been performed (Chandran et al., 2016). Previously, we assessed lumbar DRG expression in vivo by Affymetrix array at 7 days post-sciatic nerve crush, identifying 279 genes with

significantly altered expression (Tanabe et al., 2003). This study avoided any issues related to tissue culture prior to expression analysis, but the overlap with functional axon regeneration genes remained minimal with 5 genes in total, and was non-significant (Figure S2A). The functional regeneration genes were identified here in cortical neurons, so we also assessed overlap with our RNA-seq expression profile of sprouting corticospinal neurons after pyramidotomy (Fink et al., 2017). This expression survey also revealed minimal and statistically insignificant overlap with functional effects on axon regeneration, though the absolute numbers were higher than for the DRG studies (Figure S2B). Overall, we conclude that our functional screen identified genes largely distinct from analyses of gene expression after axon injury, suggesting that inhibition of regeneration is mediated largely by genes that are constitutively expressed rather than by injury-induced transcription.

To further assess any connection between our functional assay hits and differentially expressed genes, we examined expression levels from the RNA-seq GEO dataset analyzed in Figure 2B for each of the functional axon regeneration genes with Z scores > 2 and selected those with the most strongly altered expression (Figure 2C). Clearly some genes functionally limiting regeneration do show altered expression, even though they are not the most prominently altered in expression, and the directional effect on expression can be either increased or decreased.

Pathway Analysis of Functional Axonal Regeneration Genes

The 479 genes limiting axon regeneration with Z scores > 2.0 in the primary screen were analyzed bioinformatically to identify cellular pathways that limit regeneration. Three major pathways emerged from this analysis. Most strikingly, using Cytoscape and BINGO software (Maere et al., 2005; Shannon et al., 2003), the top Gene Ontology molecular function pathway enrichments include "transport" and "receptor binding" with a Bonferroni-corrected family-wise error rate (FWER) p value < 0.01 (Figure 3A). The protein-protein interactions, shared domain, and co-localization between the 99 genes linked to transport (false discovery rate [FDR] = 1.12E-05 by STRING; Szklarczyk et al., 2017) were assessed using GeneMania software (Montojo et al., 2010) (Figure 3B). Prominent among the transport group are the Rab GTPases, as detailed below. Also included are SNARES, ion channels, and transporters. The Rab GTPases are analyzed below. As a pathway, "transport" has not been associated with axonal regeneration mechanisms previously.

Second, we found numerous protein-protein, domain, and co-localization associations between the 50 receptor binding genes with axon regeneration phenotypes (FDR = 4.83E-07 by STRING; Figure 3C). Prominent among the receptor binding group are several growth factors, including Fgf family members. It may be that suppression of growth factors promotes differentiation and axon growth in this cortical neuron culture system.

Finally, analysis of KEGG pathway (Kanehisa et al., 2017) enrichment highlighted a role of cytokine and Jak-Stat signaling (FDRs = 2.82E-04 and 7.84E-03 by STRING; Figure 3D). These findings are consistent with previous

work identifying Stat3 and Socs as critical regulators of regeneration in vivo (Qiu et al., 2005; Smith et al., 2009). Thus, our screen successfully identified known regeneration mechanisms, in addition to identifying a large number of genes and functions not previously associated with regeneration.

The presence of transcription factor binding sites within 2 kb of the translation start site or microRNA binding sites within the 3′UTR as collected by MSigDB was also analyzed using GeneMania for the axonal regeneration genes (Figure S3A). Binding sites for SP1, ATF3, MEF2, and FAC1 were each significantly enriched among the genomic sequence near the transcriptional start sites of the axon regeneration genes. The genes with binding site for these factors are illustrated in Figure S3A. Because ATF3 overexpression has been associated with greater axonal regeneration (Seijffers et al., 2006; Tanabe et al., 2003), the presence of these sites in genes limiting regeneration implies that ATF3 suppresses their expression, that increased transcription by ATF3 for these genes tends to counteract ATF3 action through other sites, or that ATF3 binding sites are non-functional in these genes.

The presence of binding sites for one microRNA binding site in the 3′UTR was enriched among axonal regeneration genes, namely miR-202, which may regulate both Stat3 and Pten expression (Figure S3B). This has the potential to provide a strong synergistic action in promoting axonal regeneration.

Pharmacological Targets in Axonal Regeneration

Among the axon regeneration gene list, a subset includes the targets of existing pharmacological agents. One such gene encodes inositol polyphosphate phosphatase-like 1, Inppl1, which was revalidated by a second production of Inppl1-shRNA-expressing lentivirus (Figure 4A). Innpl1 encodes Ship2 protein, which is known to decrease phosphatidylinositol-3,4,5, trisphosphate levels and whose function may overlap with PTEN (Vinciguerra and Foti, 2006). Innpl1 is also required for signaling by other regeneration genes identified here, such as the HGF receptor Met (Koch et al., 2005). The Ship2 inhibitor AS1949490 (Suwa et al., 2009) dose-dependently increased cortical axon regeneration (Figures 4B and 4C). Therefore, Ship2 is a potential drug target for axonal regeneration therapy. Although the in vivo effect of Ship2 inhibition is unknown, these data suggest that combining genetic screening and drug testing in our in vitro regeneration assay can be used to identify targets and compounds that increase regeneration.

Socs Specificity in Axonal Regeneration

Next, we asked whether regeneration genes uncovered in our screen would have similar effects on axon regeneration in the CNS in vivo. We first analyzed the function of cytokine signaling, as its regeneration function in titrating axonal growth is documented in previous work. In the present dataset, Socs4 had the most prominent effect across the Socs family (Figure 4D), even though published studies have focused on Socs3 (Smith et al., 2009). The results are obtained from three to five different shRNA species for each gene, so knockdown

efficiency could account for minor differences in regeneration results among Socs genes. Suppression of Socs2, Socs5, and Socs7 levels also yielded significantly increased cortical axon regeneration. These findings confirm the significance of the gene family and highlight the importance of a member not previously studied with respect to regeneration. We validated the regeneration role of Socs4 in vivo by creating an AAV2/2 vector expressing the Socs4 shRNA species with the most prominent effect and testing by optic nerve regeneration. Virus expressing Socs4 shRNA or non-targeting control was injected intravitreally 2 weeks prior to retro-orbital optic nerve crush. On day 14 after crush, the axonal tracer cholera toxin β (CTB) conjugated to a fluorescent dye was injected intravitreally, and optic nerve anatomy was assessed 3 days later. Few retinal ganglion cell axons regenerate to 500 μm past the crush in control mice, but 4 times greater axon regeneration is detected in the socs4-suppressed optic nerves (Figures 4E and 4F). We conclude that Socs4 contributes to limited axonal regeneration in the adult optic nerve and that our in vitro screen identified genes that modulate CNS regeneration in vivo.

Transport Pathway and GTPase Family Members Limit Axonal Regeneration

As noted, our network analysis identified intracellular transport as a key process that inhibits regeneration, and within this network were multiple Rab and Rab-related proteins (Figure 3B). Thus, we focused on Rabs and closely related monomeric GTPases involved in organelle traffic. Axon regeneration after

suppression of each Rab or members of related Arf (ADP-ribosylation factor) and Arl (Arf-like) families from the primary full screen is shown in Figure S4A. The genes required for Rab prenylation (Rabggta, Rabggtb, Chm, and Chml) are also included. The 19 Rab and related genes for which axonal regeneration was >1.3 times control in the full screen were retested in the axonal regeneration assay (Figures 5A and 5B). The data from primary screening merged with a re-produced shRNA lentivirus study show that 15 Rab and related genes out of 19 genes exhibit statistically significant increased axon regeneration compared with non-targeting shRNA control. The GTPase enzymology allows the creation of point mutants that are constitutively active (CA) or dominant negative (DN), on the basis of oncogenic mutations for related Ras proteins. We generated a DN and CA form for each of six Rab and related proteins and assessed their effect on axonal regeneration. Compared with the DN form, neurons nucleofected with an expression vector for the CA form exhibit significantly suppressed axonal regeneration in Rab3b ($p < 0.01$), Rab3c ($p < 0.005$), and Rab27b ($p < 0.005$) but not Rab18 ($p > 0.57$), Rab31 ($p > 0.9$), and Arf4 ($p > 0.15$) (Figure S4B). Thus, activation of several Rab family members limits cortical axon regeneration.

Rab27b Suppresses Axonal Regeneration In Vitro

In selecting a gene to advance to in vivo studies, we were concerned that manipulating expression of a single Rab3 gene might not show a strong phenotype because of compensation by paralogs because Rab3 has four isoforms, Rab3a, Rab3b, Rab3c, and Rab3d, and it is thought their functions are

overlapping and redundant (Schlüter et al., 2004). Rab27 has two isoforms, Rab27a and Rab27b, but the predominant form is Rab27b in cortical neurons (Figure S4C). On the basis of these considerations, we focused subsequent analysis on Rab27b.

In the primary screen, the regenerating Z score was combined three to five shRNA species per gene, and the knockdown efficiency was not verified across the genome. For further validation, we generated two different shRNA constructs in an AAV transfer vector targeting Rab27b and evaluated the reduction of endogenous protein expression levels in shRNA nucleofected neurons. Each of the shRNA constructs shows a drastic reduction of endogenous protein levels compared with control (Figure S4D). We also used these constructs in axonal regeneration assays for further confirmation. Rab27b-knockdown neurons showed significantly enhanced axonal regeneration compared with non-targeting control (Figures S4E and S4F).

Rab27b deletion mice are viable (Tolmachova et al., 2007), so we cultured Rab27b−/− cortical neurons. Consistent with the shRNA data, axonal regeneration from Rab27b−/− mouse neurons is enhanced significantly relative to wild-type (WT) ($p < 0.05$, Student's t test) (Figures 5C, 5D, and S4G). Critically, this enhancement is rescued to WT levels by exogenous expression of FLAG-Rab27b WT in Rab27b−/− cortical neurons (Figures S4H and S4I). These data confirm that Rab27b is a suppressor of axonal regeneration after axotomy in vitro.

Localization of Rab27b in Regenerating Neuron

As mentioned above, neurons nucleofected with Rab27b T32N (DN) mutant show enhanced axonal regeneration mimicking the shRNA result (Figures 5E and S4J). In contrast, either Rab27b WT and Q78L (CA) mutant suppress regeneration (Figures 5E and S4J). Subcellular localization of Rab GTPase proteins to specific compartments is crucial to their function. To examine the axonal Rab27b localization, we examined the localization of FLAG-tagged Rab27b T32N and Q78L. Rab27b expressing neurons were axotomized mechanically on DIV 8 and incubated a further 3 days to allow regeneration. The inactive FLAG-Rab27b DN protein is highly enriched in regenerating growth cones and strongly co-localizes with F-actin visualized by rhodamine-conjugated phalloidin but not microtubules in the axon shaft detected by anti-βIII tubulin (Figures 5F and 5G). In marked contrast, the activated Rab27b CA mutant is most prominent in regenerating axon shafts and largely excluded from F-actin-positive growth cone structures (Figures 5H and 5I). Rab27b WT is present at similar intensity in both growth cones and axon shafts of regenerating axons (data not shown). Thus, the regenerating axon contains Rab27b and redistributes the protein on the basis of guanine nucleotide binding and activation state.

Increased Axonal Regeneration in *C. elegans* Lacking *rab-27*

On the basis of the in vitro primary neuron findings, we sought to determine whether Rab27b regulates neural repair in vivo. C. elegans provide a robust system to score single axon regeneration, and we focused on GABAergic axons

filled with a GFP reporter protein (Figure 6A). Two different rab-27 hypomorphic alleles were crossed onto the commissural neuron GABAergic reporter line and worms subjected to laser axotomy at the dorsal-ventral midline in young adult animals. No developmental aberration in axonal guidance was detected (not shown). Twenty-four hours after axotomy, the extent of regeneration was measured as the fraction of axon length from the dorsal nerve cord to the ventral nerve cord (Figures 6B–6D). Both rab-27 alleles, sa24 and sa699, significantly increase regeneration, with a majority of axons regenerating fully to the ventral surface. In contrast, the median axon length from control worms after cutting at the length of 0.5 reaches only a length of 0.6. Thus, endogenous rab-27 expression limits axon regeneration.

The rab-27 regeneration phenotype might be due to autonomous action within the injured GABA neuron or might be secondary to action in other cells. RAB-27 was overexpressed selectively in GABA neurons under the Punc-47 promotor to assess cell autonomy. High levels RAB-27 in GABA neurons generate no significant change in regeneration (Figure 6E). However, this expression significantly rescues the rab27 (sa24) increased regeneration phenotype. We conclude that RAB-27 acts cell-autonomously to restrict axon regeneration in worm GABA neurons.

Optic Nerve Axon Regeneration in Rab27b−/−

In order to evaluate the in vivo function of Rab27b in mammals, we used the optic nerve crush model of axon regeneration. Rab27b−/− mice are viable and

fertile without any reported abnormalities (Tolmachova et al., 2007). Strong Rab27b expression is observed in WT retinal tissue but not in Rab27b−/− retina (Figure S5A). We subjected WT and Rab27b−/− mice to optic nerve crush injury and injected the anterograde tracer CTB into the retina 14 days after crush. At 3 days after crush, Rab27b protein levels in retina were similar for uninjured and injured WT mice (Figures S5B and S5C). Animals were sacrificed 3 days after CTB injection and dissected to collect the optic nerves. The total number of CTB-positive axons regenerating beyond the injury site in Rab27b−/− optic nerve is significantly increased compared with WT (Figure 6F). We examined synergy of this phenotype with zymosan-induced inflammation (Figures 6F and 6G). Substantial numbers of regenerating fibers are observed in zymosan-injected optic nerve up to 2,000 μm distal to the injury site. The number of CTB-labeled regenerating axon at 500 or 10,000 μm distal to the injury site in Rab27b−/− optic nerve after zymosan injection is significantly increased compared with WT with zymosan. Thus, Rab27b limits vertebrate axonal regeneration not only in vitro but also in vivo.

Enhanced Behavioral Recovery in Rab27b−/− Mice after T7 Dorsal Hemisection

Because suppression of Rab27b expression enhanced neural repair in vitro and in vivo, we sought to determine whether functional recovery from traumatic spinal cord injury might be enhanced by Rab27b deletion. We verified that Rab27b protein is expressed in adult motor cortex (Figure S6A). Furthermore, motor cortex Rab27b protein levels were equal in uninjured and injured WT animals 7 days after spinal cord injury (Figures S6B and S6C). WT and Rab27b−/− mice

received dorsal hemisection of the midthoracic spinal cord (n = 19 per genotype). Unfortunately, 2 of 19 Rab27b−/− animals died 1 day after surgery, presumably because of hemorrhagic complications of systemic platelet function (Tolmachova et al., 2007). The Basso Mouse Scale (BMS) score is the most reliable test to monitor locomotion in the open field after dorsal hemisection surgery (Basso et al., 2006). Recovery of hindlimb function is significantly improved in the BMS test of Rab27b−/− animals between 5 and 10 weeks after axotomy (at indicated days, $p < 0.05$, Student's t test; between groups, $p < 0.05$, repeated-measures ANOVA) (Figure 7A). The same cohorts were subjected to additional functional outcomes. In the gridwalk test, uninjured mice made similar numbers of missed steps as did WT mice ($p > 0.13$), consistent with normal CNS development (Figure S6D). After injury and consistent with the BMS scores, Rab27b−/− mice group show a reduced rate of missed steps on the grid at 55 days post-lesion (dpl) compared with the WT group ($p < 0.05$, Student's t test) (Figure 7B). The Rab27b−/− mice at 48 dpl are able to stay on the rotating rotarod drum longer than WT animals ($p < 0.05$, Student's t test) (Figure 7C), although performance is equal before injury ($p > 0.29$) (Figure S6E). The behavioral improvement in Rab27b−/− mice are not due to differences in the degree of injury or in tissue sparing, because intact tissue was identical in the two groups by histological assessment with anti-GFAP staining at the end of the experiment ($p > 0.74$, Student's t test) (Figure 7D).

The raphespinal serotonergic (5HT) axonal tract possesses a known ability for injury-induced axonal growth and contributes substantially to locomotion and is

significantly lesioned by the dorsal hemisection trauma (Kim et al., 2004). Because of the in vitro regenerative efficacy and the improved behavioral performance after deletion of Rab27b, we assessed 5HT staining for axonal growth after injury. The density of proximal 5HT-positive fibers in the ventral horn rostral to the lesion site is similar between groups on day 70 after dorsal hemisection injury (Figure 7E). Caudal to the lesion site, the density of ventral horn distal 5HT-positive fibers is twice as great in the Rab27b−/− group compared with WT ($p < 0.005$, Student's t test) (Figures 7F and 7G). This phenotype is not secondary to development changes, because the 5HT fibers in the ventral horn of either cervical or lumbar cord in uninjured WT and Rab27b−/− mouse is indistinguishable (Figures S6F and S6G).

We also examined the projection of corticospinal axons in Rab27b−/− after spinal cord injury. Biotin-dextran amine (BDA) anterograde tracing from injections in the motor cortex was conducted 8 weeks after spinal cord injury. BDA-labeled axons were visualized in fixed tissue collected 2 weeks after tracer injection using streptavidin Alexa Fluor 568. Equivalent numbers of BDA-labeled CST axons were detected rostral to the injury site in both groups, but no regenerating axons reached the caudal spinal cord in either genotype (Figures S6H and S6I). Immediately rostral to the injury epicenter, significantly greater numbers of CST axons were observed Rab27b−/− mice compared with WT mice (Figures S6H–S6J). The increased CST axon density in this region for spinal cord injury mice lacking Rab27b may be due either to reduced dieback from the axotomy site or to short range regeneration after dieback from spinal cord injury. Taken together,

the improved functional recovery and greater descending axonal length of serotonin and CST fibers demonstrate that deletion of Rab27b is beneficial for neural repair after spinal cord injury.

DISCUSSION

In the present study, we screened the mouse genome for factors with a role in restricting axonal regeneration by suppression of expression. Importantly, our unbiased screen was based on functional analyses of regeneration after gene knockdown: we assess the ability of cultured cortical neurons to regrow after injury. We found approximately 500 genes that show a regeneration phenotype, and validation studies on more than 120 genes confirm reproducible effect axon regeneration in our in vitro system. Among these genes, most have not previously been linked to axonal regeneration or neural repair. Transport, receptor binding and cytokine signaling are enriched pathways. Most highly enriched was the membrane trafficking Rab GTPase family, and Rab27b was studied in detail. The inactive Rab27b protein is localized to regenerating growth cones and inhibition of regeneration requires the active GTP conformation. Adult worms and mice lacking this protein exhibit greater axonal regeneration. Moreover, mice null for Rab27b recover greater motor function after spinal cord trauma. The many other genes and cellular pathways identified in our screen await in vivo study, but for one of them (Inppl1), we found that a small-molecule inhibitor was able to replicate the in vitro regeneration effect.

Despite the limited data regarding a role for Rabs themselves in axonal regeneration prior to this work, there is pre-existing evidence that membrane traffic plays a key role in axonal extension. Rab 11 has been implicated in regulating the traffic of inhibitory proteins from axons to dendrites (Koseki et al., 2017). There is a link between endoplasmic reticulum (ER) and endosome contact in mediating axonal extension (Raiborg et al., 2015). Semaphorins, as extracellular cues inhibiting extension and collapsing growth cones, stimulate local and massive macropinocytosis at the growth cone (Fournier et al., 2000). Inpp5f regulates both axon regeneration and membrane traffic (Nakatsu et al., 2015; Zou et al., 2015). In C. elegans, loss of function in any of three endocytosis genes (unc-26/synaptojanin, unc-57/endophilin, and unc-41/stonin) results in decreased regeneration (Chen et al., 2011). Multiple studies have demonstrated that new membrane is added to the distal axon tip during growth, and the growth cone is known to be highly enriched in endomembranous stacks (Cheng and Reese, 1987; Diefenbach et al., 1999; Hazuka et al., 1999; Kolpak et al., 2009; Lockerbie et al., 1991; Tojima et al., 2007). Dendritic branching in Drosophila is intimately connected with Golgi outposts (Ye et al., 2007). Thus, Rab regulation of distal membrane traffic may be crucial for effective regeneration via regulation of membrane addition, a hypothesis that we favor. An alternative hypothesis stems from the role of retrograde transport to the cell soma for signaling from distal extracellular cues (Cosker and Segal, 2014). For both synaptic vesicle and non-synaptic vesicle Rabs, gene suppression is hypothesized to allow a net diversion of membrane delivery to axonal extension. This hypothesis explains the

observation that suppression of multiple different intracellular trafficking events supports greater axonal extension. In this light, it is important to note that the surface area of the axon membrane of mature mammalian projection neuron of the corticospinal tract may be 300 times that of the cell soma, so that regeneration requires very substantial plasma membrane delivery.

Multiple Rab-family proteins have regeneration phenotypes when expression is suppressed. This includes Rab3b and Rab3c proteins, which are known to share synaptic vesicle regulation with Rab27b. As an effector, Rabphilin3 has been linked to Rab3s as well as Rab27b, and suppression of its expression phenocopies Rab27b loss of function both in vitro and in vivo. In addition, Arf4, Rab18, and Rabif were validated by repeat testing among 25 Rab-related genes identified as hits in the original screen. We expect that Rab27b and other regenerating-controlling Rabs are likely to play a role in modifying membrane delivery and retrieval to the cell surface in the distal axons. Although Rab27b and the Rab3s have been implicated in synaptic vesicle exocytosis in the distal axon (Fukuda, 2008; Pavlos et al., 2010), a loss of these Rabs may shift membrane traffic from synaptic function to permit greater plasma membrane addition for axon extension. Rab27b has also been associated with melanosome traffic, platelet degranulation and exosome release (Chen et al., 1997; Fukuda, 2008; Mizuno et al., 2007; Tolmachova et al., 2007). For both synaptic vesicle and non-synaptic vesicle Rabs, gene suppression is hypothesized to allow a net diversion of membrane delivery to axonal extension. This hypothesis explains the observation that suppression of multiple different intracellular trafficking events

supports greater axonal extension. These findings highlight the critical role of membrane traffic for successful axonal extension. In this light, it is important to note that the surface area of the axon membrane of mature mammalian projection neuron of the corticospinal tract may be 300 times that of the cell soma, so that regeneration requires very substantial plasma membrane delivery. Although Rab proteins and intracellular membrane traffic were highlighted bioinformatically as most enriched gene set among regeneration genes, many non-Rab-related genes were identified as limiting axonal regeneration. These do not constitute a single pathway but cover a range of pathways, some of which have been connected with axonal regeneration and many of which have not previously been identified as participating in axonal regeneration. Of the top hits revalidated by rescreening, xylt1, encoding xylosyl transferase, is central for chondroitin sulfate synthesis (Baker et al., 1972), so its role may fit with well-documented role of CSPG to inhibit regeneration. Hif3a encodes an inactive subunit that titrates Hif1 and Hif2 signaling in protective responses to hypoxic stress. The ability of Hif3a suppression to increase regeneration is consistent with HIF1 signaling in C. elegans axon regeneration (Alam et al., 2016). Parp1 was previously reported to have a role in C. elegans and mouse regeneration (Byrne et al., 2016), but in vivo evaluation of its role as a target for neural repair in mammals were disappointing (Wang et al., 2016).

We focused on those genes whose suppression increased regeneration. By our screening criteria, about 100 genes reduced axon regeneration when expression was suppressed. It is possible that these genes are required for endogenous

regenerative potential. However, we have not excluded cell toxicity as a cause for the reduced number of βIII-tubulin regenerating axons in these cases. Thus, this group may contain both essential regeneration genes and genes required for cell survival non-specifically. Further studies will investigate these possibilities. Importantly, our screen was based on functional analyses with loss of function. In contrast, the most common approach to identifying genes involved in regeneration has focused on expression surveys, most commonly at the mRNA level (Belin et al., 2015; Bonilla et al., 2002; Chandran et al., 2016; Fink et al., 2017; Tanabe et al., 2003; Tedeschi et al., 2016). Such previous work has the premise that genes involved in regulating regeneration are controlled transcriptionally by injury. Although this can be the case, there is no a priori basis for this assumption, and especially for those genes limiting regeneration, their physiological function and regulation may relate to alternate cellular functions, which must be suppressed for successful axon regrowth. As hypothesized above, this may the case with Rab proteins.

The approach described here examined one gene at a time for effects on functional axon regeneration. However, it is highly likely the combinations of different genes may have far greater effects in many cases, and examples of successful combinations have been reported (Bei et al., 2016; Benowitz et al., 2017; Sun et al., 2011; Wang et al., 2012; Zai et al., 2011). The screen identifies genes with unrelated cellular functions, thereby predicting that additive effects on regeneration may exist. For genes related to a single pathway, the consequence of dual suppression is not obvious. To the extent that the factors in the same

pathway are redundant, dual inhibition is expected to be synergistic, while to the extent that they are epistatic, one will occlude that other's effect.

Both the comprehensive screening results and the specific data for Rab trafficking events provide new directions for research and therapy based on axonal regeneration and neural plasticity after injury. Because a number of genes not previously associated with neural repair have been nominated by the loss of function screen, methods for rapid in vivo evaluation is essential. In this regard, species conservation allows implementation of secondary studies in tractable genetic organisms, and CNS regional conservation permits evaluation of genes relevant for spinal cord injury in more accessible injury models, such as optic nerve regeneration. The present study broadens the horizons for successful neural repair and neurological recovery after trauma.

EXPERIMENTAL PROCEDURES

Further details and an outline of resources used in this work can be found in Supplemental Experimental Procedures. All animal studies were conducted with approval of the Yale Institutional Animal Care and Use Committee. All behavioral measurements and all imaging quantifications were conducted by experimenters unaware of experimental group. No data were excluded from the analysis. Both male and female mice were included, as mice were collected from sequential littermates of the appropriate genotypes in tissue culture experiments. Spinal cord injury studies were performed only with female mice to facilitate bladder management. Both male and female mice were used of optic nerve crush studies. The age of mice is specified in each figure legend, and for CNS injury was introduced at 10 weeks.

Primary Cortical Neuron Culture and Axon Regeneration Assay

Primary cortical neuron axon regeneration assay was performed as described previously (Huebner et al., 2011). For the shRNA-based regeneration screen, lentiviral particles targeting 16,007 mouse genes with 83,106 unique shRNA clones (Mission TM TRC Mouse Lentiviral shRNA Library 10180801; Sigma-Aldrich) were added to the neurons on DIV 3. On DIV 8, 96-well cultures were scraped and fixed on DIV 10.

C. elegans Laser Axotomy Studies

Laser axotomy was performed on late L4 C. elegans larvae as previously described (Byrne et al., 2011).

Mice and Surgery

Age-matched adult (10 weeks) C57BL/6 WT female mice or Rab27b−/− mice (Tolmachova et al., 2007) were subjected to dorsal hemisection as described previously (Zou et al., 2015). For optic nerve crush injury study, both male and female C57BL/6J mice or Rab27b−/− mice were used. AAV serotype 2/2 was produced and purified >1 × 1012 genome copies per milliliter and then injected intraorbitally to WT animals 2 weeks prior to crush surgery. The optic nerve was exposed intraorbitally with care taken to avoid damage to the ophthalmic artery. Alexa 555-CTB was injected intravitreally to trace axons 14 days after injury.

Quantification and Statistical Analyses

One-way ANOVA with post hoc Tukey pairwise comparisons, repeated-measures ANOVA, and Student's t test as specified in the figure legends were performed using GraphPad Prism version 5.0d and SPSS Statistics version 22. Mean ± SEM and specific n values are reported in each figure legend. Data are considered to be statistically significant if $p < 0.05$. The assumption of Gaussian distribution was checked using the D'Agostino-Pearson omnibus test.

Supplementary Material

Refer to Web version on PubMed Central for supplementary material

Acknowledgments

We thank Stefano Sodi, Tomoko Sekine, Kristin DeLuca, and Yram Foli for expert technical assistance. This work was supported by grants from the Falk Medical Research Trust to S.M.S. and from the NIH (R35NS097283 and R01NS098817) to M.H. and S.M.S.

REFERENCES

Alam, T., Maruyama, H., Li, C., Pastuhov, S.I., Nix, P., Bastiani, M., Hisamoto, N., and Matsumoto, K. (2016). Axotomy-induced HIF-serotonin signalling axis promotes axon regeneration in C. elegans. Nat. Commun. 7, 10388.

Baker, J.R., Rode´ n, L., and Stoolmiller, A.C. (1972). Biosynthesis of chondroitin sulfate proteoglycan. Xylosyl transfer to Smith-degraded cartilage proteoglycan and other exogenous acceptors. J. Biol. Chem. 247, 3838–3847.

Basso, D.M., Fisher, L.C., Anderson, A.J., Jakeman, L.B., McTigue, D.M., and Popovich, P.G. (2006). Basso Mouse Scale for locomotion detects differences in recovery after spinal cord injury in five common mouse strains. J. Neurotrauma 23, 635–659.

Bei, F., Lee, H.H.C., Liu, X., Gunner, G., Jin, H., Ma, L., Wang, C., Hou, L., Hensch, T.K., Frank, E., et al. (2016). Restoration of visual function by enhancing conduction in regenerated axons. Cell 164, 219–232.

Belin, S., Nawabi, H., Wang, C., Tang, S., Latremoliere, A., Warren, P., Schorle, H., Uncu, C., Woolf, C.J., He, Z., and Steen, J.A. (2015). Injury-induced decline of intrinsic regenerative ability revealed by quantitative proteomics. Neuron 86, 1000–1014.

Benowitz, L.I., He, Z., and Goldberg, J.L. (2017). Reaching the brain: advances in optic nerve regeneration. Exp. Neurol. 287, 365–373.

Blackmore, M.G., Moore, D.L., Smith, R.P., Goldberg, J.L., Bixby, J.L., and Lemmon, V.P. (2010). High content screening of cortical neurons identifies novel regulators of axon growth. Mol. Cell. Neurosci. 44, 43–54.

Bonilla, I.E., Tanabe, K., and Strittmatter, S.M. (2002). Small proline-rich repeat protein 1A is expressed by axotomized neurons and promotes axonal outgrowth. J. Neurosci. 22, 1303–1315.

Buchser, W.J., Slepak, T.I., Gutierrez-Arenas, O., Bixby, J.L., and Lemmon, V.P. (2010). Kinase/phosphatase overexpression reveals pathways regulating hippocampal neuron morphology. Mol. Syst. Biol. 6, 391.

Byrne, A.B., Edwards, T.J., and Hammarlund, M. (2011). In vivo laser axotomy in C. elegans. J. Vis. Exp. (22), 2707.

Byrne, A.B., McWhirter, R.D., Sekine, Y., Strittmatter, S.M., Miller, D.M., and Hammarlund, M. (2016). Inhibiting poly(ADP-ribosylation) improves axon regeneration. eLife 5, 5.

Chandran, V., Coppola, G., Nawabi, H., Omura, T., Versano, R., Huebner, E.A., Zhang, A., Costigan, M., Yekkirala, A., Barrett, L., et al. (2016). A systems-level analysis of the peripheral nerve intrinsic axonal growth program. Neuron 89, 956–970.

Chen, D., Guo, J., Miki, T., Tachibana, M., and Gahl, W.A. (1997). Molecular cloning and characterization of rab27a and rab27b, novel human rab proteins shared by melanocytes and platelets. Biochem. Mol. Med. 60, 27–37.

Chen, L., Wang, Z., Ghosh-Roy, A., Hubert, T., Yan, D., O'Rourke, S., Bowerman, B., Wu, Z., Jin, Y., and Chisholm, A.D. (2011). Axon regeneration pathways identified by systematic genetic screening in C. elegans. Neuron 71, 1043–1057.

Cheng, T.P., and Reese, T.S. (1987). Recycling of plasmalemma in chick tectal growth cones. J. Neurosci. 7, 1752–1759.

Cosker, K.E., and Segal, R.A. (2014). Neuronal signaling through endocytosis. Cold Spring Harb. Perspect. Biol. 6, 6.

Diefenbach, T.J., Guthrie, P.B., Stier, H., Billups, B., and Kater, S.B. (1999). Membrane recycling in the neuronal growth cone revealed by FM1-43 labeling. J. Neurosci. 19, 9436–9444.

El Bejjani, R., and Hammarlund, M. (2012). Neural regeneration in Caenorhabditis elegans. Annu. Rev. Genet. 46, 499–513.

Fink, K.L., López-Giráldez, F., Kim, I.J., Strittmatter, S.M., and Cafferty, W.B.J. (2017). Identification of intrinsic axon growth modulators for intact CNS neurons after injury. Cell Rep. 18, 2687–2701.

Fournier, A.E., Nakamura, F., Kawamoto, S., Goshima, Y., Kalb, R.G., and Strittmatter, S.M. (2000). Semaphorin3A enhances endocytosis at sites of receptor-F-actin colocalization during growth cone collapse. J. Cell Biol. 149, 411–422.

Fukuda, M. (2008). Regulation of secretory vesicle traffic by Rab small GTPases. Cell. Mol. Life Sci. 65, 2801–2813.

Hammarlund, M., Nix, P., Hauth, L., Jorgensen, E.M., and Bastiani, M. (2009). Axon regeneration requires a conserved MAP kinase pathway. Science 323, 802–806.

Hazuka, C.D., Foletti, D.L., Hsu, S.C., Kee, Y., Hopf, F.W., and Scheller, R.H. (1999). The sec6/8 complex is located at neurite outgrowth and axonal synapse-assembly domains. J. Neurosci. 19, 1324–1334.

Huebner, E.A., Kim, B.G., Duffy, P.J., Brown, R.H., and Strittmatter, S.M. (2011). A multi-domain fragment of Nogo-A protein is a potent inhibitor of cortical axon regeneration via Nogo receptor 1. J. Biol. Chem. 286, 18026– 18036.

Kanehisa, M., Furumichi, M., Tanabe, M., Sato, Y., and Morishima, K. (2017). KEGG: new perspectives on genomes, pathways, diseases and drugs. Nucleic Acids Res. 45 (D1), D353–D361.

Kim, J.E., Liu, B.P., Park, J.H., and Strittmatter, S.M. (2004). Nogo-66 receptor prevents raphespinal and rubrospinal axon regeneration and limits functional recovery from spinal cord injury. Neuron 44, 439–451.

Koch, A., Mancini, A., El Bounkari, O., and Tamura, T. (2005). The SH2-domian-containing inositol 5-phosphatase (SHIP)-2 binds to c-Met directly via tyrosine residue 1356 and involves hepatocyte growth factor (HGF)-induced lamellipodium formation, cell scattering and cell spreading. Oncogene 24, 3436–3447.

Kolpak, A.L., Jiang, J., Guo, D., Standley, C., Bellve, K., Fogarty, K., and Bao, Z.Z. (2009). Negative guidance factor-induced macropinocytosis in the growth cone plays a critical role in repulsive axon turning. J. Neurosci. 29, 10488–10498.

Koseki, H., Donegá, M., Lam, B.Y., Petrova, V., van Erp, S., Yeo, G.S., Kwok, J.C., Ffrench-Constant, C., Eva, R., and Fawcett, J.W. (2017). Selective rab11 transport and the intrinsic regenerative ability of CNS axons. eLife 6, 6.

Lockerbie, R.O., Miller, V.E., and Pfenninger, K.H. (1991). Regulated plasmalemmal expansion in nerve growth cones. J. Cell Biol. 112, 1215–1227.

Loh, S.H., Francescut, L., Lingor, P., Bähr, M., and Nicotera, P. (2008). Identification of new kinase clusters required for neurite outgrowth and retraction by a loss-of-function RNA interference screen. Cell Death Differ. 15, 283–298.

Maere, S., Heymans, K., and Kuiper, M. (2005). BiNGO: a Cytoscape plugin to assess overrepresentation of gene ontology categories in biological networks. Bioinformatics 21, 3448–3449.

Mizuno, K., Tolmachova, T., Ushakov, D.S., Romao, M., Abrink, M., Ferenczi, M.A., Raposo, G., and Seabra, M.C. (2007). Rab27b regulates mast cell granule dynamics and secretion. Traffic 8, 883–892.

Montojo, J., Zuberi, K., Rodriguez, H., Kazi, F., Wright, G., Donaldson, S.L., Morris, Q., and Bader, G.D. (2010). GeneMANIA Cytoscape plugin: fast gene function predictions on the desktop. Bioinformatics 26, 2927–2928.

Moore, D.L., Blackmore, M.G., Hu, Y., Kaestner, K.H., Bixby, J.L., Lemmon, V.P., and Goldberg, J.L. (2009). KLF family members regulate intrinsic axon regeneration ability. Science 326, 298–301.

Nakatsu, F., Messa, M., Nández, R., Czapla, H., Zou, Y., Strittmatter, S.M., and De Camilli, P. (2015). Sac2/INPP5F is an inositol 4-phosphatase that functions in the endocytic pathway. J. Cell Biol. 209, 85–95.

Nix, P., Hammarlund, M., Hauth, L., Lachnit, M., Jorgensen, E.M., and Bastiani, M. (2014). Axon regeneration genes identified by RNAi screening in C. elegans. J. Neurosci. 34, 629–645.

Park, K.K., Liu, K., Hu, Y., Smith, P.D., Wang, C., Cai, B., Xu, B., Connolly, L., Kramvis, I., Sahin, M., and He, Z. (2008). Promoting axon regeneration in the adult CNS by modulation of the PTEN/mTOR pathway. Science 322, 963–966.

Pavlos, N.J., Grønborg, M., Riedel, D., Chua, J.J., Boyken, J., Kloepper, T.H., Urlaub, H., Rizzoli, S.O., and Jahn, R. (2010). Quantitative analysis of synaptic vesicle Rabs uncovers distinct yet overlapping roles for Rab3a and Rab27b in Ca2+-triggered exocytosis. J. Neurosci. 30, 13441–13453.

Qiu, J., Cafferty, W.B., McMahon, S.B., and Thompson, S.W. (2005). Conditioning injury-induced spinal axon regeneration requires signal transducer and activator of transcription 3 activation. J. Neurosci. 25, 1645–1653.

Raiborg, C., Wenzel, E.M., Pedersen, N.M., Olsvik, H., Schink, K.O., Schultz, S.W., Vietri, M., Nisi, V., Bucci, C., Brech, A., et al. (2015). Repeated ER-endosome contacts promote endosome translocation and neurite outgrowth. Nature 520, 234–238.

Schlüter, O.M., Schmitz, F., Jahn, R., Rosenmund, C., and Südhof, T.C. (2004). A complete genetic analysis of neuronal Rab3 function. J. Neurosci. 24, 6629–6637.

Seijffers, R., Allchorne, A.J., and Woolf, C.J. (2006). The transcription factor ATF-3 promotes neurite outgrowth. Mol. Cell. Neurosci. 32, 143–154.

Sepp, K.J., Hong, P., Lizarraga, S.B., Liu, J.S., Mejia, L.A., Walsh, C.A., and Perrimon, N. (2008). Identification of neural outgrowth genes using genome-wide RNAi. PLoS Genet. 4, e1000111.

Shannon, P., Markiel, A., Ozier, O., Baliga, N.S., Wang, J.T., Ramage, D., Amin, N., Schwikowski, B., and Ideker, T. (2003). Cytoscape: a software environment for integrated models of biomolecular interaction networks. Genome Res. 13, 2498–2504.

Smith, P.D., Sun, F., Park, K.K., Cai, B., Wang, C., Kuwako, K., Martinez-Carrasco, I., Connolly, L., and He, Z. (2009). SOCS3 deletion promotes optic nerve regeneration in vivo. Neuron 64, 617–623.

Sun, F., Park, K.K., Belin, S., Wang, D., Lu, T., Chen, G., Zhang, K., Yeung, C., Feng, G., Yankner, B.A., and He, Z. (2011). Sustained axon regeneration induced by co-deletion of PTEN and SOCS3. Nature 480, 372–375.

Suwa, A., Yamamoto, T., Sawada, A., Minoura, K., Hosogai, N., Tahara, A., Kurama, T., Shimokawa, T., and Aramori, I. (2009). Discovery and functional characterization of a novel small molecule inhibitor of the intracellular phosphatase, SHIP2. Br. J. Pharmacol. 158, 879–887.

Szklarczyk, D., Morris, J.H., Cook, H., Kuhn, M., Wyder, S., Simonovic, M., Santos, A., Doncheva, N.T., Roth, A., Bork, P., et al. (2017). The STRING database in 2017: quality-controlled protein-protein association networks, made broadly accessible. Nucleic Acids Res. 45 (D1), D362–D368.

Tanabe, K., Bonilla, I., Winkles, J.A., and Strittmatter, S.M. (2003). Fibroblast growth factor-inducible-14 is induced in axotomized neurons and promotes neurite outgrowth. J. Neurosci. 23, 9675–9686.

Tedeschi, A., Dupraz, S., Laskowski, C.J., Xue, J., Ulas, T., Beyer, M., Schultze, J.L., and Bradke, F. (2016). The calcium channel subunit Alpha2delta2 suppresses axon regeneration in the adult CNS. Neuron 92, 419–434.

Tojima, T., Akiyama, H., Itofusa, R., Li, Y., Katayama, H., Miyawaki, A., and Kamiguchi, H. (2007). Attractive axon guidance involves asymmetric membrane transport and exocytosis in the growth cone. Nat. Neurosci. 10, 58–66.

Tolmachova, T., Abrink, M., Futter, C.E., Authi, K.S., and Seabra, M.C. (2007). Rab27b regulates number and secretion of platelet dense granules. Proc. Natl. Acad. Sci. U S A 104, 5872–5877.

Vinciguerra, M., and Foti, M. (2006). PTEN and SHIP2 phosphoinositide phosphatases as negative regulators of insulin signalling. Arch. Physiol. Biochem. 112, 89–104.
Wang, Z., and Jin, Y. (2011). Genetic dissection of axon regeneration. Curr. Opin. Neurobiol. 21, 189–196.

Wang, X., Hasan, O., Arzeno, A., Benowitz, L.I., Cafferty, W.B., and Strittmatter, S.M. (2012). Axonal regeneration induced by blockade of glial inhibitors coupled with activation of intrinsic neuronal growth pathways. Exp. Neurol. 237, 55–69.

Wang, X., Sekine, Y., Byrne, A.B., Cafferty, W.B., Hammarlund, M., and Strittmatter, S.M. (2016). Inhibition of poly-ADP-ribosylation fails to increase

axonal regeneration or improve functional recovery after adult mammalian CNS injury. eNeuro 3, 3.

Yan, D., Wu, Z., Chisholm, A.D., and Jin, Y. (2009). The DLK-1 kinase promotes mRNA stability and local translation in C. elegans synapses and axon regeneration. Cell 138, 1005–1018.

Ye, B., Zhang, Y., Song, W., Younger, S.H., Jan, L.Y., and Jan, Y.N. (2007). Growing dendrites and axons differ in their reliance on the secretory pathway. Cell 130, 717–729.

Zai, L., Ferrari, C., Dice, C., Subbaiah, S., Havton, L.A., Coppola, G., Geschwind, D., Irwin, N., Huebner, E., Strittmatter, S.M., and Benowitz, L.I. (2011). Inosine augments the effects of a Nogo receptor blocker and of environmental enrichment to restore skilled forelimb use after stroke. J. Neurosci. 31, 5977–5988.

Zou, Y., Stagi, M., Wang, X., Yigitkanli, K., Siegel, C.S., Nakatsu, F., Cafferty, W.B., and Strittmatter, S.M. (2015). Gene-silencing screen for mammalian axon regeneration identifies Inpp5f (Sac2) as an endogenous suppressor of repair after spinal cord injury. J. Neurosci. 35, 10429–10439.

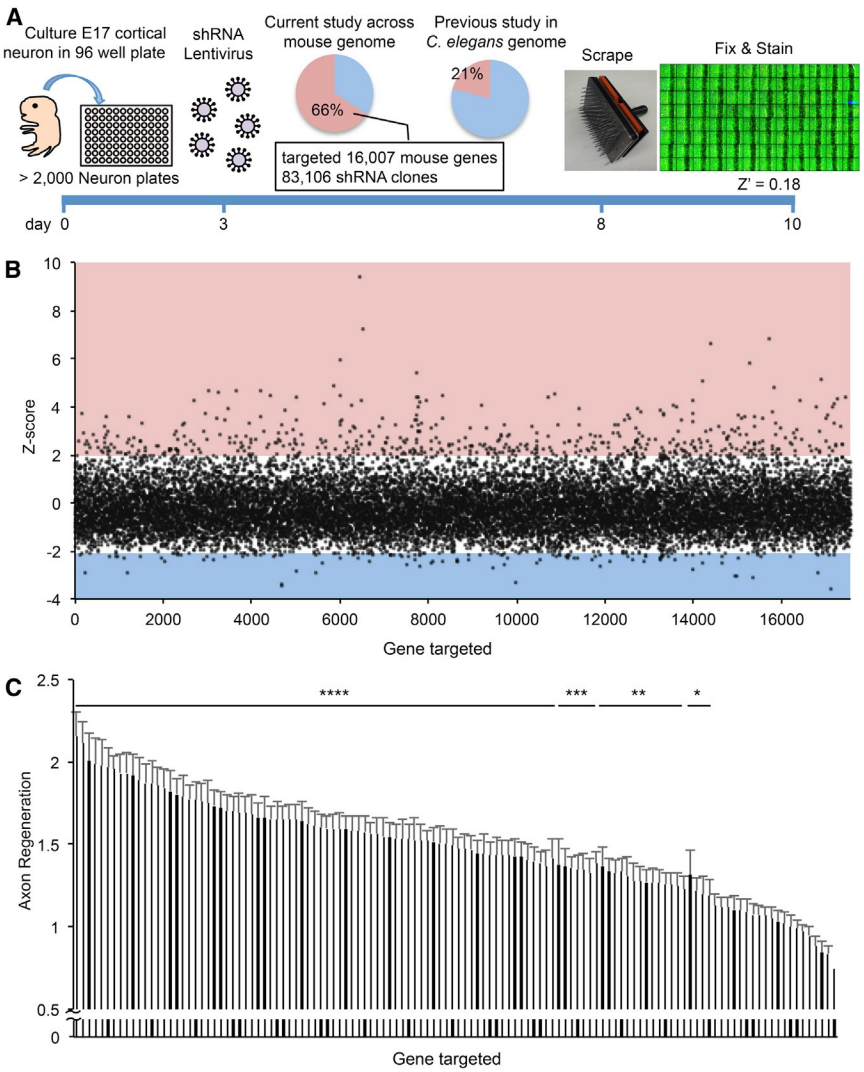

Figure 1. Mouse Cortical Axon Regenera- tion Analysis in a Genome-wide Loss-of-Function Screen.

(A) Schematic time line for this screen. (B) The Z score for axonal regeneration is plotted from all measurements for each of 16,007 genes normalized to control shRNA. Red square shows Z score > 2.0, and blue square shows Z score < -2.0. (C) The top 122 genes from the first screen were retested for validation (see also Table S1). Data are mean with SEM for n = 16–20, four replicates of four or five shRNA species. Results for each gene were compared with non-targeting virus wells using ANOVA with the two-stage linear step-up procedure of Benjamini, Krieger and Yekutieli. *p < 0.05, **p < 0.01, ***p < 0.001, ****p < 0.0001.

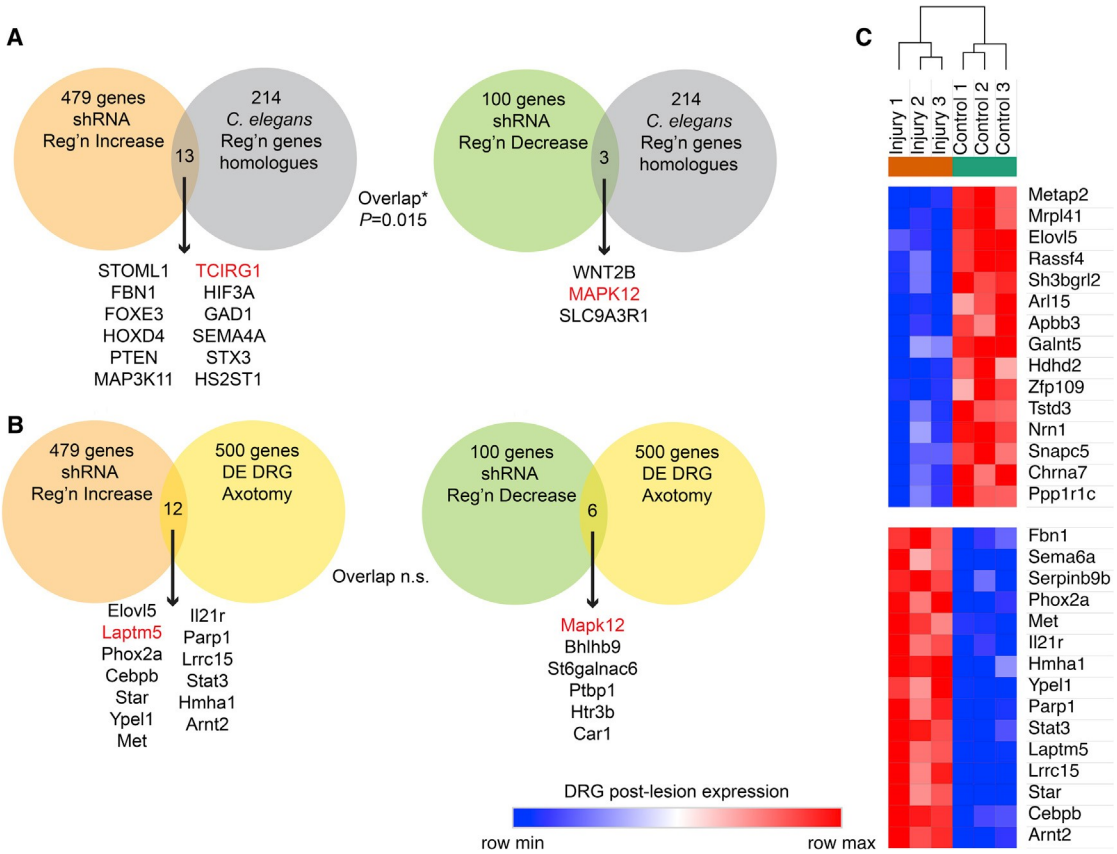

Figure 2. Functional Regeneration Genes Are Distinct from Those Identified by Expression Profiling (A) The functional axonal regeneration gene list from Figure 1 was compared with the mouse orthologs of genes with axonal regeneration phenotypes in *C. elegans* (Chen et al., 2011; Nix et al., 2014). The genome-wide significance of the overlap between lists was compared using a chi-square test. Individual genes in both datasets are listed. Genes in red were also detected in other comparisons from Figure 2 or Figure S1.

(B) The functional axonal regeneration gene list from Figure 1 was compared with the list of genes differentially expressed in cultured DRG neurons precondi- tioned by sciatic nerve injury (Tedeschi et al., 2016). The genome-wide significance of the overlap between lists was compared using a chi-square test ($p > 0.05$). Individual genes in both datasets are listed. Genes in red were also detected in other comparisons from Figure 2 or Figure S1. (C) For the functional axonal regeneration genes with Z scores > 2.0 from Figure 1, the expression level in cultured DRG neurons with or without preconditioning sciatic nerve injury was assessed from published values (Tedeschi et al., 2016). The top markers of injury-induced differential DRG expression within this set of 479 genes were identified by signal-to-noise ratio using the Morpheus website and plotted as a row-normalized expression map. Among genes limiting axonal regeneration, both up- and downregulated DRG genes are detected.

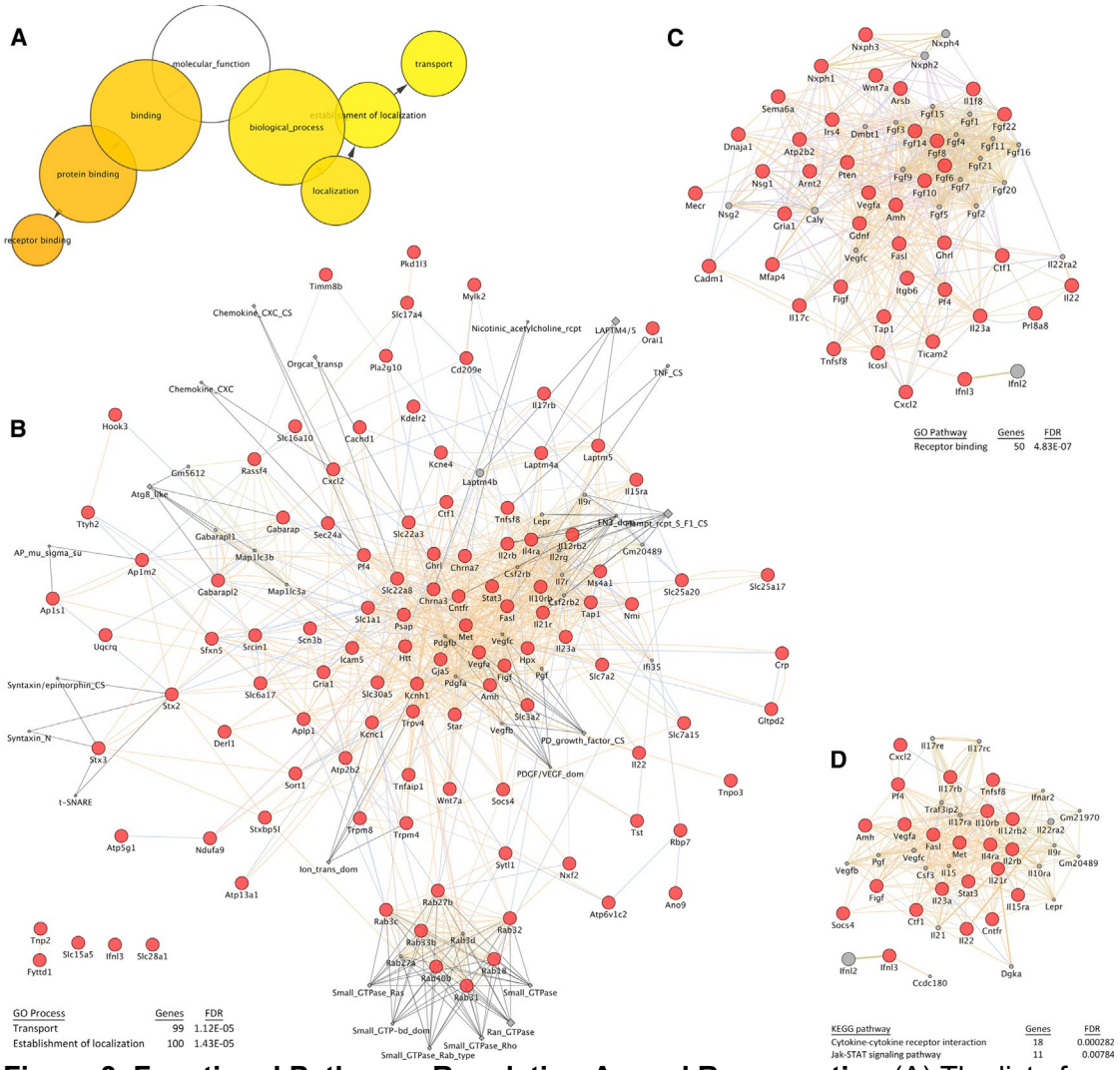

Figure 3. Functional Pathways Regulating Axonal Regeneration (A) The list of regeneration genes from Figure 1 and Table S1 with Z scores > 2.0 was assessed for Gene Ontology (GO) pathway enrichment using BINGO software (Maere et al., 2005; Shannon et al., 2003). Those pathways significantly enriched (Bonferroni-corrected family-wise error rate [FWER] $p < 0.01$) are shown with colored circles of greater intensity for greater significance. The size of each circle reflects the number of genes in that category. (B) The list of regeneration genes from Figure 1 and Table S1 with Z scores > 2.0 that are in the ‘‘transport’’ GO function group was analyzed using GeneMania software (Montojo et al., 2010) for interactions. Each red circle is regeneration gene, each gray diamond is a protein domain, and each gray circle is predicted regeneration gene on the basis of sequence homology. Protein-protein interactions, co-localization, and co-expression are shown by connecting lines. The ‘‘transport’’ pathways includes multiple Rab proteins. Statistical significance for enrichment of this process by genome-wide false discovery rate (FDR) was calculated using the STRING database (Szklarczyk et al., 2017). (C) Similar analysis as in (B) but for the ‘‘receptor binding’’ GO process. (D) Similar analysis as in (B) but for the ‘‘cytokine’’ plus ‘‘Jak-Stat signaling’’ KEGG pathways.

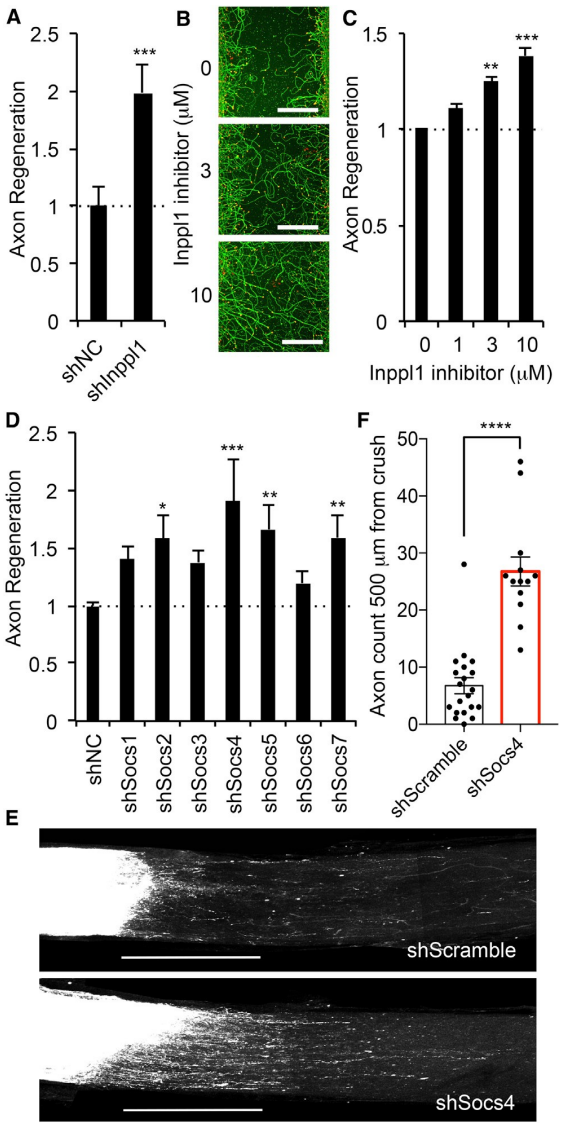

Figure 4. Functional Analysis of Identified Protein Families for Axonal Regeneration

(A) Quantification of axonal regeneration in shNC and shInppl1 transduced neuron is shown with SEM, n = 128 for shNC and n = 32 for shInppl1 from eight replicates of four shRNA species. ***p < 0.005, Student's t test. (B) Representative pictures of regenerated axons 3 days after axotomy with indicated amount of Inppl1 inhibitor. Neurons were stained with bIII tubulin (green) and phalloidin of F-actin (red) to illustrate growth cones. Scale bars represent 200 mm.

(C) The graph shows quantification of axonal regeneration. Neurons were treated with indicated amount of Inppl1 inhibitor right after axotomy for 3 days. Error bars represent SEM, n = 3 biological replicates. **p < 0.01 and ***p < 0.005, one-way ANOVA followed by Tukey's test.

(D) The graph shows quantification of axonal regeneration after axotomy in shNC and shSocs transduced neurons. Error bars represent SEM, n = 30–116 from 10 replicates of four or five shRNA species. *p < 0.05, **p < 0.01, and ***p < 0.005, one-way ANOVA followed by Dunnett's test. (E) Representative confocal images of optic nerve at 17 days after crush injury from shScramble and shSocs4 AAV-injected mice. AAV was injected intra- ocularly 2 weeks before injury. The CTB-labeled RGC axons are

white. The eye is to the left and the brain is to the right. Scale bars represent 500 mm. (F) Quantification of regenerating axons at 500 mm distances distal to the lesion sites at 17 days after injury. Data are presented as mean with SEM for n = 20 shScramble and n = 13 shSocs4. ****p < 0.001, Student's t test.

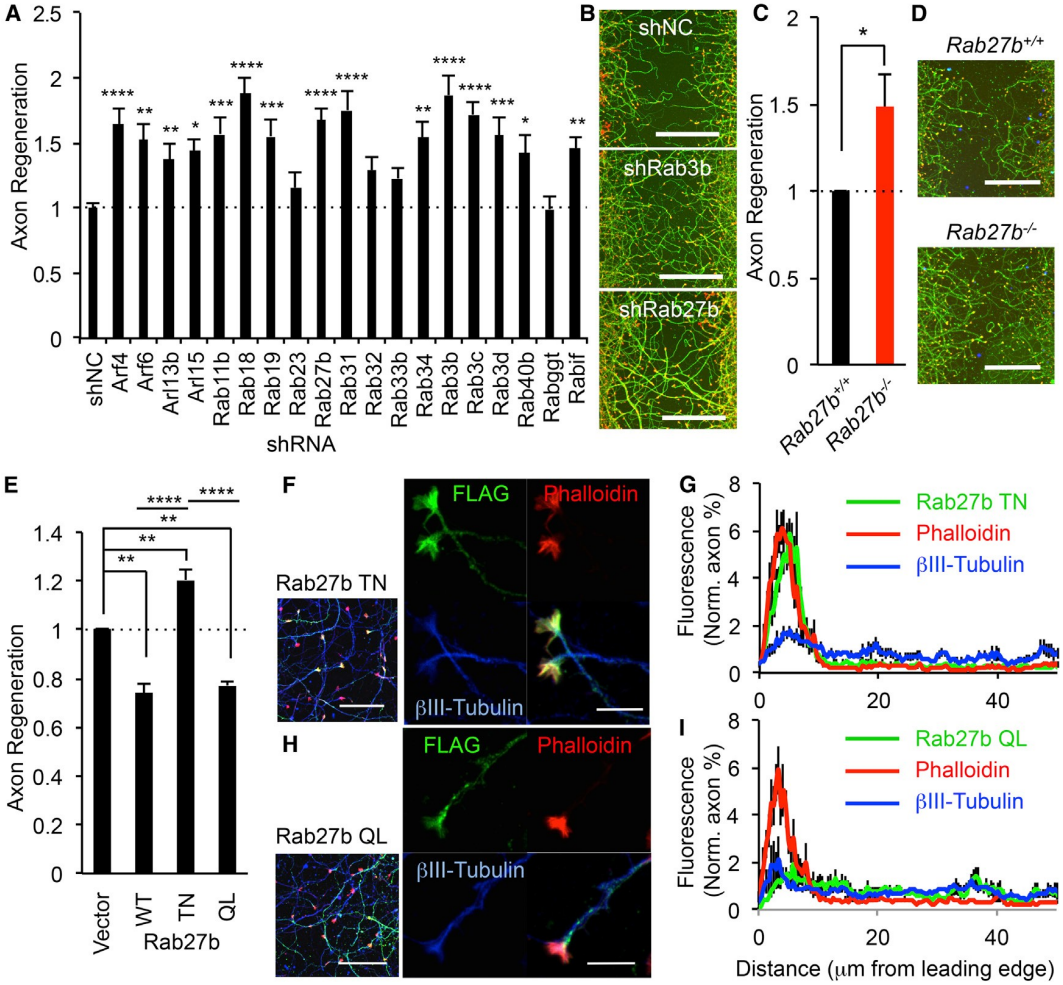

Figure 5. Transport Pathway and Rab Proteins Limit Axonal Regeneration (A) Nineteen Rab-related proteins, with axon regeneration > 1.3 from genome-wide screen, were retested in the axonal regeneration scrape assay. Results for each gene were compared with control using ANOVA with Dunnett's multiple comparisons test. n = 31–116; *p < 0.05, **p < 0.01, ***p < 0.001, ****p < 0.0001. Error bars represent SEM. (B) Photomicrographs of regenerating axons in shNC, shRab3b, and shRab27b transduced neurons stained with bIII tubulin (green) and phalloidin of F-actin (red) to illustrate growth cones. Scale bars represent 200 mm. (C) Quantification of axonal regeneration in Rab27b+/+ and Rab27b-/- neurons is shown with SEM, n = 5 biological replicates. *p < 0.05, Student's t test. (D) Microphotographs of axonal regeneration assay in Rab27b+/+ and Rab27b-/- neuron. Scale bars represent 200 mm. (E) Cortical neurons were nucleofected with vector, Rab27b WT, T23N, or Q78L. Neurons were scraped at DIV 8 and regenerated for 3 days. The graph shows quantification of axonal regeneration. Error bars represent SEM, n = 3 biological replicates. **p < 0.005 and ****p < 0.0001, one-way ANOVA followed by Tukey's test. (F–I) Localization of Rab27b TN and QL in regenerating neurons. (F and H) Cortical neurons were nucleofected with FLAG-Rab27b T23N or Q78L. Neurons were scraped at DIV 8 and regenerated for 3 days. Confocal microscope images of FLAG-Rab27b (FLAG; green), axon (bIII-tubulin; blue), and

growth cones (rhodamine-phalloidin; red) are taken. Left pictures are 633 objective lens images, and scale bars represent 50 mm. Right pictures are 633 objective lens plus 33 digital zoom images, and scale bars represent 10 mm. (G and I) The graphs show quantification of distribution of Rab27b, bIII-tubulin, and F-actin in regenerating axon 3 days after axotomy. Data are presented as mean ± SE, n = 9.

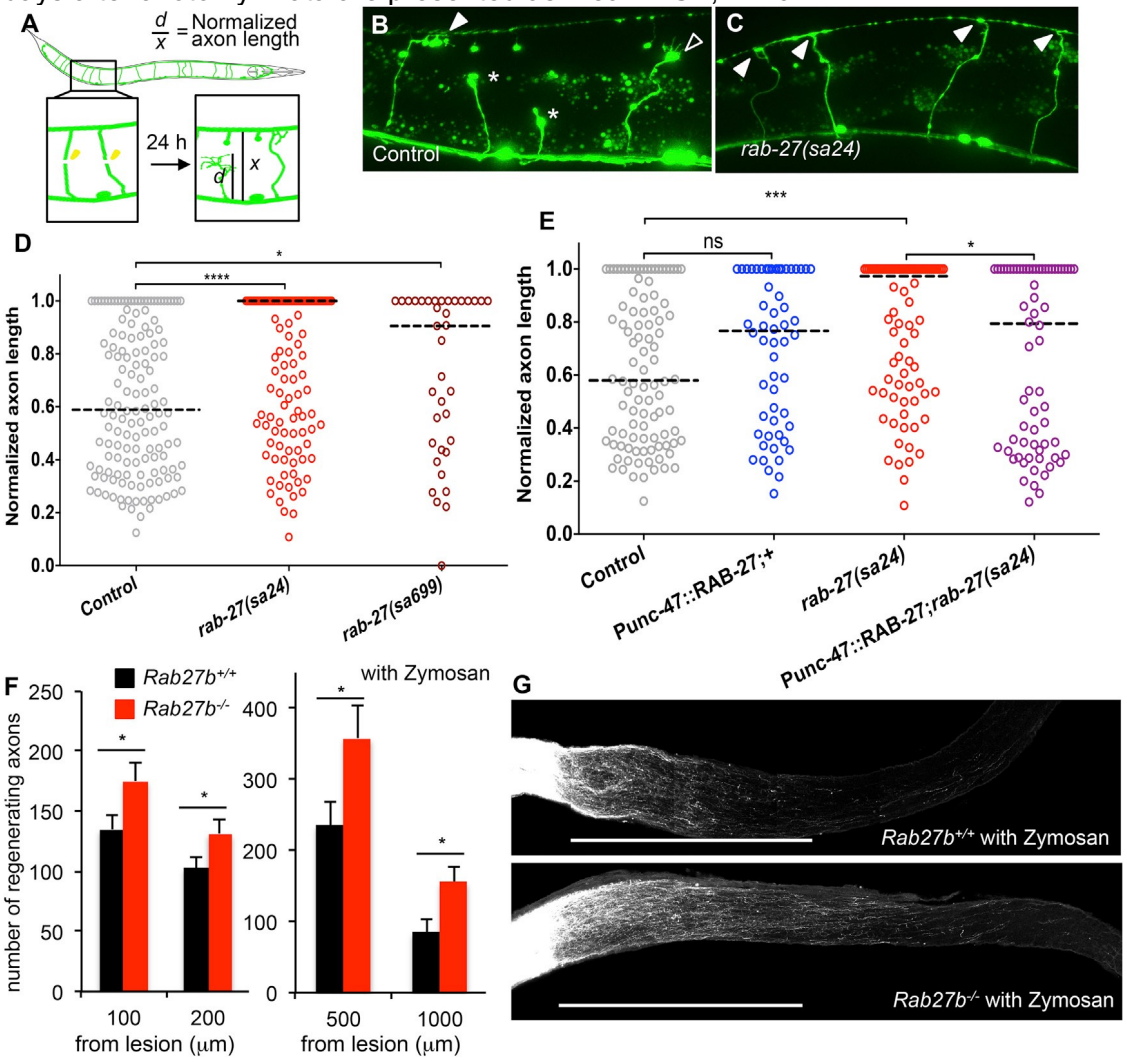

Figure 6. Rab27 Inhibits Axonal Regeneration In Vivo (A) Commissural axons of the GABAergic DD/VD neurons are severed using a pulsed laser, and regeneration is assessed after 24 hr in young adult (L4 stage + 24 hr at 200C) animals. (B) Normalized axon length in control and rab-27 mutant animals. Number of axons cut per genotype, left to right: 142, 148, and 37. (C and D) Regenerating GABA axons 24 hr after axotomy in control (C) and rab-27-null (D) animals. Filled arrows indicate fully regenerated axons reaching the dorsal nerve cord, empty arrows indicate partial regeneration, and stars indicate nonregenerating axon stumps. All animals express Punc-47::GFP, which drives GFP expressing specifically in the GABA motor neurons. (E)Normalized axon length in control, rab-27 mutants, and animals specifically expressing rab-27 cDNA in GABA neurons, in control and rab-27 mutant animals. Number of axons cut per genotype, left to right: 98, 56, 84, and 68. Kolmogorov-Smirnov test was used. ns, not significant; *p < 0.05, ***p < 0.0005, ****p < 0.0001. (F) Age-matched (9–10 weeks old without zymosan, 14 weeks old with zymosan) animals underwent optic nerve crush (ONC). Quantification of regenerating RGC axons at indicated distances distal to the lesion sites at 17 days

after injury from WT control mouse and Rab27b-/- mice. Data are presented as mean with SEM. Without zymosan, n = 29 Rab27b+/+ and n = 28 Rab27b-/-, and with zymosan, n = 10 Rab27b+/+ and n = 8 Rab27b-/- mice. *p < 0.05, Student's t test. (G) Representative confocal images of optic nerve at 17 days after crush injury with zymosan injection from WT control mouse and Rab27b-/- mouse. The CTB-labeled RGC axons are white. The eye is to the left and the brain is to the right. Scale bars represent 1,000 mm.

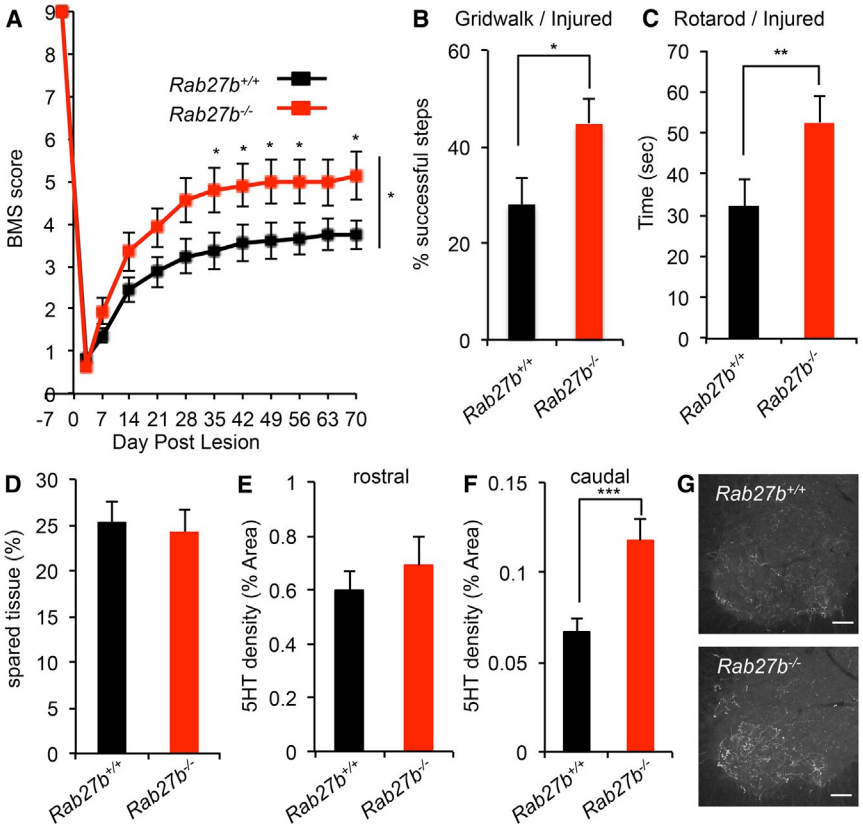

Figure 7. Improvement of Functional Recovery after Spinal Cord Injury in Rab27b-/- Mouse. (A) Open-field locomotion performance measured by BMS of Rab27b+/+ and Rab27b-/- mice. Animals were scored on day post-lesion (DPL) -3, 3, 7, 14, 21, 28, 35, 42, 49, 56, 63, and 70 by two experienced observers blinded to group. Data are mean ± SEM for n = 19 Rab27b+/+ and n = 17 Rab27b-/-. *p < 0.05, significant difference between genotypes through DPL 35 to 70, one- way repeated-measure ANOVA across time series followed by Student's t test between genotypes at indicated times. (B and C) Gridwalk test at DPL 55 (B) and RotaRod performance at DPL 48 (C) of Rab27b+/+ and Rab27b-/- mice. Data are mean with SEM for n= 19 Rab27b+/+ and n = 17 Rab27b-/-. *p < 0.05 and **p < 0.01, Student's t test. (D) Sagittal sections of thoracic cord were stained with anti-GFAP antibody, and the extent of spared tissue at the injury site was quantified. Data are presented as mean with SEM for n = 19 Rab27b+/+ and n = 17 Rab27b-/-. No significant differences between groups with Student's t test. (E and F) Serotonergic (5HT+) fiber density at coronal sections of rostral to the lesion (E) and caudal to the lesion (F) from Rab27b+/+ and Rab27b-/- mice 70 days after hemisection were quantified. Data are presented as mean with SEM for n = 19 Rab27b+/+ and n = 17 Rab27b-/-. No significant differences between groups with Student's t test (E). *p < 0.05, Student's t test (F). (G) Representative image of raphespinal fibers stained with anti-5HT antibody in the spinal ventral horn.

Preface to: *rab-27* acts in an intestinal secretory pathway to inhibit axon regeneration in *C. elegans*

This work covers much of my dissertation research subsequent to the work covered in Sekine et al. 2018 and following the initial identification of *Rab27b/rab-27* as a novel *in vitro* and *in vivo* inhibitor of axon regeneration.

Our initial findings on RAB-27 pointed to a cell-intrinsic role in axon regeneration inhibition, a role supported by *in vitro* and *in vivo* results in mammalian neuron models. In spite of this result, we were not able to identify a neuronal function for RAB-27 in *C. elegans* that was sufficient to explain its potent inhibitory effect, either through regulation of neuronal RAB-27 activity or identification of RAB-27 genetic interactors. Instead, I found that RAB-27 functions in the *C. elegans* intestine to inhibit axon regeneration. While signaling pathways linking the gut to the nervous system have been identified, the intestine was a tissue not previously known to regulate axon growth. This work identifies the intestine as an important source of inhibitory signals for axon regeneration, and describes a pathway of inhibition mediated through the maturation and RAB-27-dependent secretion of inhibitory signals including the neuropeptide NLP-40.

rab-27 acts in an intestinal secretory pathway to inhibit axon regeneration in *C. elegans*

Alexander T. Lin-Moore[1], Motunrayo J. Oyeyemi[2], Marc Hammarlund[1,3]*

[1]Department of Genetics, Yale University School of Medicine, New Haven, CT USA
[2]Yale College, New Haven, CT USA
[3]Department of Neuroscience, Yale University School of Medicine, New Haven, CT USA
*Correspondence to: marc.hammarlund@yale.edu

ABSTRACT

Injured axons must regenerate to restore nervous system function, and regeneration is regulated in part by external factors from non-neuronal tissues. Many of these extrinsic factors act in the immediate cellular environment of the axon to promote or restrict regeneration, but the existence of long-distance signals regulating axon regeneration has not been clear. Here we show that the Rab GTPase *rab-27* inhibits regeneration of GABAergic motor neurons in *C. elegans* through activity in the intestine as well as the nervous system. Re-expression of RAB-27, but not the closely related RAB-3, in the intestine of *rab-27* mutant animals is sufficient to rescue normal regeneration. Several additional components of an intestinal neuropeptide secretion pathway also inhibit axon regeneration, including NPDC1/*cab-1*, SNAP25/*aex-4*, KPC3/*aex-5*, and the neuropeptide *nlp-40*. Together these data indicate that RAB-27-dependent neuropeptide secretion from the intestine inhibits axon regeneration, and point to distal tissues as potent extrinsic regulators of regeneration.

INTRODUCTION

Unlike many other tissues, where cells respond to injury through proliferation and replacement, cells in the nervous system are not usually replaced following axon damage. Instead, neurons rely on axon regeneration to restore the connectivity necessary for function. Despite its importance, however, axon regeneration is often inhibited *in vivo*, leading to permanent loss of nervous system function after injury.

A neuron's axon regeneration capacity is extensively regulated by contacts with the extracellular environment of the injured axon. In the mammalian central nervous system, myelin-associated transmembrane signals Nogo, MAG and OMgp potently inhibit post-injury growth through direct interaction with neuronal receptors like Ngr1 and PTPσ (Liu et al. 2006, Cheah & Andrews 2016). In *C. elegans*, which lacks myelin-associated regeneration inhibitors, the peroxidasin PXN-2 and syndecan (SDN-1) control the integrity and signaling topography of the extracellular matrix to negatively or positively regulate regeneration success, respectively (Gotenstein et al. 2010, Edwards & Hammarlund 2014). Thus, a neuron's local environment and neighbor cells influence its regenerative capacity.

In addition to responding to their local environment and neighbors, neurons respond to secreted, long-range signals from distant tissues, which can regulate neuronal programs ranging from synapse patterning to complex behaviors (Klassen & Shen 2007, Sawa & Korswagen 2013, Holzer & Farzi 2014). But for axon regeneration, the existence of long-range inhibitory signals *in vivo* has not

been clear. We have previously identified the Rab GTPase *rab-27* as a conserved inhibitor of axon regeneration (Sekine et al. 2018), and previous evidence pointed to a cell-autonomous role for *rab-27* in regeneration inhibition. Here we show that *rab-27* inhibits regeneration of D-type motor neurons in *C. elegans* through activity in the intestine. We further show that inhibition of axon regeneration involves an intestinal secretory pathway involved in neuropeptide secretion, and that regeneration is inhibited in part by the neuropeptide NLP-40. Together these results indicate that the *C. elegans* intestine inhibits axon regeneration, and point to long-distance, extrinsic signaling as a novel mechanism of axon regeneration regulation.

RESULTS

An intestinal function for RAB-27 in axon regeneration

C. elegans provides a robust system to investigate in vivo axon regeneration at single-neuron resolution (Hammarlund & Jin 2014). Previously, Rab27 was identified in a large-scale screen as a key inhibitor of regeneration (Sekine et al. 2018). This work demonstrated that Rab27B/*rab-27* inhibits regeneration in both mouse and *C. elegans* models, and indicated that one site of function for RAB-27 in *C. elegans* is in the injured neurons. However, in *C. elegans*, *rab-27* is highly expressed in the anterior- and posterior-most cells of the intestine as well as the nervous system (Mahoney et al. 2006, Cao et al. 2017). A potential function of *rab-27* in the intestine was not previously tested.

To study *rab-27*'s function in axon regeneration, we used the same regeneration assay as described in previous work (Sekine et al. 2018). We used the GABAergic neurons as our model system, lesioning individual axons with a pulsed laser and measuring subsequent regeneration (Fig. 1A). As shown previously, loss of *rab-27* resulted in high regeneration, with significant regeneration enhancement occurring as early as 12 hours after axotomy (Fig. 1B). *rab-27* mutants produced growth cones earlier and at a higher proportion than in controls, and axons of *rab-27* mutant animals that initiated regeneration grew further and reached the dorsal nerve cord earlier compared to control axons (Fig. 1C,D).

Next, to determine whether intestinal *rab-27* might function in regeneration, we expressed *rab-27* in either the intestine or the neurons of mutant animals. The intestine is known to signal to the *C. elegans* nervous system to regulate the defecation motor program (Thomas 1990, Mahoney et al. 2008, Wang et al. 2013). However, signals from the intestine, which must travel through the pseudocoelom to reach the GABAergic neurons, have not previously been implicated in regulation of axon regeneration. We expected that expression in a tissue where it functions would restore normal, lower levels of regeneration. Surprisingly, re-expression of *rab-27* in the intestine of mutants was sufficient to significantly reduce regeneration compared to *rab-27* mutant animals (Fig. 1E, G, I-K), indicating that the intestine is a major site of *rab-27* function in inhibiting axon regeneration. Expression of *rab-27* in the GABA neurons of *rab-27* mutants also reduced regeneration relative to *rab-27* mutant animals, as previously

described (Sekine et al. 2018). Thus, *rab-27* can function in both the intestine and in GABA neurons to inhibit axon regeneration.

Expression of *rab-27* in GABA neurons had a significant effect on regeneration but was not sufficient to fully suppress regeneration to control levels (Fig. 1F, Fig. S1A). By contrast, we previously found that expressing *rab-27* in GABA neurons restores regeneration to control levels (Sekine et al. 2018). Our current strategy to express *rab-27* only in GABA neurons used an expression construct that contained the *rab-3* 3'UTR, while our previous efforts used the *unc-54* 3'UTR. The *unc-54* UTR sequence can itself drive expression in the posterior gut because it contains regulatory and coding sequence for the intestinal gene *aex-5* (Silva-García et al. 2019). We hypothesized that a requirement for intestinal expression accounts for the different effects of the UTR. Intestine-specific *rab-27* rescue constructs containing the *rab-3* 3'UTR rescued axon regeneration identically to those containing the *unc-54* 3'UTR (Fig. S1B). Use of the *rab-3* 3' UTR in the intestine-specific RAB-27 rescue construct also produced a much stronger rescue of *rab-27* mutants' *aex* phenotype, with nearly full restoration of the pBoc/expulsion ratio, compared to only a partial rescue by constructs containing the *unc-54* 3' UTR (Fig. S2). Thus, *rab-27* can act in either neurons or the intestine to suppress regeneration, but intestinal expression is necessary for complete function. Overall, these tissue-specific experiments raise the question of whether similar or different cellular mechanisms mediate *rab-27*'s regeneration function in these two tissues.

RAB-27's synaptic vesicle tethering cofactors do not inhibit regeneration

In neurons, *rab-27* is thought to function similar to the well-studied Rab family member *rab-3*. Phylogenetic analysis of the *C. elegans* Rab family shows that *rab-27* and *rab-3* are each other's closest paralog (Gallegos et al. 2012). RAB-3 and RAB-27 are both enriched in the nerve ring of *C. elegans* (Mahoney et al. 2006), suggesting synaptic localization, and both Rabs colocalize at synapses in mammalian neurons (Pavlos et al. 2010). Consistent with these studies, we found that tagged *rab-3* and

rab-27 colocalize at synapses in *C. elegans* GABA neurons (Fig. 2A). *rab-3* regulates synaptic vesicle tethering and synaptic transmission (Mahoney et al. 2006), and *rab-27* is thought to play an auxiliary role in this process (Mahoney et al. 2006, Pavlos et al. 2010). Further, both *rab-27* and *rab-3* are regulated by a common GEF MADD/*aex-3*, and *aex-3* is required for normal synaptic transmission (Mahoney et al. 2006). However, despite these similarities, other data suggest that *rab-27* and *rab-3* also have different functions. In *C. elegans*, the Rab effector protein Rabhilin/*rbf-1* genetically interacts with *rab-27* but not *rab-3* (Mahoney et al. 2006, Mesa et al. 2011, Barclay et al. 2012). Further, *rab-27* and *rbf-1*, but not *rab-3*, are required for tethering and secretion of dense core vesicles in neurons (Ch'ng et al. 2008, Feng et al. 2012, Laurent et al. 2018). Finally, *rab-27*, unlike *rab-3* or Rabphilin/*rbf-1*, is expressed in both neurons and intestine (Mesa et al. 2011, Cao et al. 2017). Consistent with this, *rab-27* mutants but not *rab-3* or Rabphilin/*rbf-1* mutants have a constipated phenotype due to a

defect in dense core vesicle release from the intestine and resulting disruption of the defecation motor program (DMP) (Riddle et al. 1997, Mahoney et al. 2008). These data raise the question of what the relationship is between *rab-27* and *rab-3* in axon regeneration.

We used genetic analysis to determine the relationship between *rab-27, rab-3* and the effector Rabphilin/*rbf-1* in axon regeneration. Loss of *rab-3* did not affect axon regeneration (Fig. 2B). Thus, unlike for synaptic vesicle release, where *rab-3* predominates (Mahoney et al. 2006), *rab-27* rather than *rab-3* is the major factor in axon regeneration. Loss of Rabphilin/*rbf-1* also did not affect regeneration. However, double mutants for either *rab-27;rab-3* or *rab-27;rbf-1* suppressed the high regeneration phenotype of *rab-27* single mutants (Fig. 2B). We conclude that a neuronal function mediated by *rab-3* and Rabphilin/*rbf-1* is required for enhanced regeneration in *rab-27* mutants, though this neuronal function is dispensable for normal regeneration.

A major site of *rab-27* function in axon regeneration is the intestine (Fig. 1G), where *rab-3* is not expressed (Nonet et al. 1997). Given the close evolutionary and functional relationship between *rab-27* and *rab-3*, it is possible that *rab-3* could function in the intestine to inhibit axon regeneration, but is simply not expressed there. To test this idea, we ectopically expressed RAB-3 in the intestine of *rab-27* mutants to see whether RAB-3 could compensate for loss of *rab-27*. Intestinal expression of RAB-3 in *rab-27* mutants was not sufficient to rescue high regeneration (Fig. 2C). Intestinal RAB-3 also failed to rescue DMP defects in *rab-27* mutants. Thus, for the two distinct phenotypes of axon

regeneration and DMP, *rab-27* mutants expressing intestinal RAB-3 were indistinguishable from non-transgenic *rab-27* mutants. By contrast, *rab-27* mutants expressing intestinal RAB-27 significantly rescued the DMP (Fig. 2D, Fig. S2), as well as restoring normal levels of axon regeneration (Fig. 2C). Together, these results indicate that despite their similarity and shared function in synaptic vesicle tethering, RAB-27 and RAB-3 are functionally distinct, and raise the question of what mechanisms act with RAB-27 to mediate its intestinal function in axon regeneration.

Intestinal components of a neuropeptide signaling pathway inhibit regeneration

In the intestine, *rab-27* acts to facilitate the tethering and fusion of dense core vesicles during the defecation motor program (DMP) (Mesa et al. 2011). At the expulsion ('Exp') step of the DMP, a neuropeptide ligand packaged into DCVs is secreted from the intestine. This peptide signal is sensed by receptors on the GABAergic neurons AVL and DVB, which in drive contractions of the enteric muscles and eventually waste expulsion (Riddle et al. 1997, Mahoney et al. 2008, Wang et al. 2013). Packaging and fusion of these intestinal DCVs involves *rab-27*, together with the pro-protein convertase KPC3/*aex-5*, the t-SNARE protein SNAP25/*aex-4*, the Munc13-like SNARE regulator *aex-1*, the Rab GEF recruitment factor NPDC1/*cab-1*, and the Rab GEF MADD/*aex-3*. Of these pathway components, SNAP25/*aex-4*, Munc13-b/*aex-1*, and KPC3/*aex-5* are primarily expressed in the intestine and excluded from the nervous system (Cao

et al. 2017, Taylor et al. 2019).The neuronal receptor that responds to neuropeptide release from the intestine is the GPCR *aex-2*, which is expressed in a small subset of neurons including the excitatory GABAergic neurons AVL and DVB, which are required for DMP (Taylor et al. 2019). Loss of function in any of these genes disrupts the DMP and results in a constipation phenotype (Riddle et al. 1997, Mahoney et al. 2008, Wang et al. 2013).

We hypothesized that this same DCV secretion mechanism may account for *rab-27*'s function in axon regeneration. Consistent with this hypothesis, we found that KPC3/AEX-5, SNAP25/AEX-4, NPDC1/CAB-1, and NLP-40 itself all inhibit axon regeneration to varying degrees (Fig. 3B, Fig. 4A, Fig. 5), suggesting that a conserved neuropeptide signaling pathway links the intestine to the nervous system to regulate both waste expulsion and axon regeneration. However, loss of the Rab GEF MADD/*aex-3*, Munc13-b/*aex-1*, or the GPCR *aex-2* did not affect regeneration (Fig. 3B), pointing to a significant separation in pathway subunits between these two pathways. Altogether, these results indicate that secretion of the neuropeptide NLP-40 from the intestine inhibits axon regeneration, and that RAB-27 is an essential part of the secretion mechanism. However, this secretory pathway is genetically separable from the defecation motor program as a whole, suggesting that regulation of axon regeneration involves a distinct, specialized pool of secretory vesicles.

The identity of additional secreted signals or their receptors are presently unknown. Over 250 distinct neuropeptides have been identified in *C. elegans* (Li & Kim 2008), of which approximately fifty are believed to be expressed in the

intestine (Nathoo et al. 2001, Pierce et al. 2001, Li et al. 2003, Cao et al. 2017). A small candidate screen of intestinally-expressed neuropeptide-like proteins (NLPs) that are expressed in the intestine and are processing targets of KPC3/AEX-5 (Husson et al. 2006) did not identify any additional neuropeptide inhibitors of regeneration (Fig. 6). Similarly, the *C. elegans* has between 125 to 150 G-protein coupled neuropeptide receptor homologs (Frooninckx et al. 2012, Koelle 2018), of which approximately 20 are expressed in the DD/VD GABAergic motor neurons (Taylor et al. 2019). Of these, we find that the GPCR AEX-2 does not inhibit regeneration, although it does respond to peptide signals from the intestine in the context of the DMP (Wang et al. 2013). The identity of the peptide signal or signals, and the potential receptor remain unknown. Further work is required to identify these components of the intestine-neuron signaling axis that inhibits axon regeneration.

Multiple Rab GTPases affect axon regeneration

rab-27 was initially identified as a candidate regeneration inhibitor in a functional genome-wide screen for regeneration inhibitors done in mammalian cortical neurons *in vitro* that identified 19 Rab GTPases as potential regeneration inhibitors (Sekine et al. 2018). *C. elegans* has a drastically reduced cohort of functional Rabs compared to mammals (Gallegos et al. 2012), attributable in large part to decreases in redundancy. Compared to the results seen in mammalian cell culture, a few Rabs in *C. elegans* affect regeneration (Fig. 5A). In addition to *rab-27* and the previously identified *rab-6.2* (Zeng et al. 2018), loss

of *rab-18* significantly decreases regeneration success, while loss of *glo-1* leads to a modest increase in regeneration. Unlike other high-regenerating Rab mutants, *glo-1* mutants specifically show an increase in full regeneration after 24 hours of recovery, though not an increase in the likelihood of regeneration initiation during that period (Fig. 6B,C). GLO-1 is expressed specifically in the intestine, where it localizes to and is required for the biogenesis of the lysosome-like gut granules (Hermann et al. 2005). Along with *rab-27*, the effect of *glo-1* on regeneration suggests that the intestine may play a previously unknown but important role in regulation of axon regeneration.

DISCUSSION

Axon regeneration is tightly regulated by pathways from within the injured neuron as well as by interactions with the local environment, but the existence of long-range regulatory signals has remained unclear. Here we show that in *C. elegans*, RAB-27 acts in the intestine to inhibit regeneration of severed axons of the DD/VD GABAergic motor neurons. This inhibition occurs independently of *rab-27*'s known role in neurons, where it regulates synaptic vesicle fusion and also functions in axon regeneration (Mahoney et al. 2006, Sekine et al. 2018).

We find that multiple factors involved in dense core vesicle (DCV) packaging and secretion from the intestine inhibit regeneration along with *rab-27*. Loss of NPDC1/*cab-1*, which regulates intestinal DCV trafficking and fusion (E. Jorgensen, pers. comm.) or the intestine-specific SNAP25 homolog *aex-4* both lead to improvements in regeneration (Fig. 3, Fig. 4A) highly reminiscent of, and

in the case of *cab-1* genetically linked to (Fig. 4B), *rab-27* loss. Loss KPC3/*aex-5*, which processes multiple intestinally-produced neuropeptides (Husson et al. 32006) or the neuropeptide *nlp-40* also inhibit regeneration (Fig. 3, Fig. 5), though not as strongly as NPDC1/*cab-1*, SNAP25/*aex-4* or *rab-27*. These data suggest a model in which axon regeneration is regulated by a neuropeptide signal, processed by KPC3/AEX-5, that is packaged into dense core vesicles, tether to the basal membrane of intestinal cells via RAB-27-dependent interactions, and secreted via SNAP25/AEX-4-dependent SNARE activity. An attractive hypothesis is that a neuronal neuropeptide receptor responds to this signal to limit regeneration. Additionally, the strongly inhibitory phenotypes of a subset of these components suggests that additional inhibitory signals, independent of KPC3/AEX-5 processing but requiring NPDC1/*cab-1*, SNAP25/AEX-4 and RAB-27, may be generated in and secreted from the intestine.

Surprisingly we find no role for Munc-13b/*aex-1* in regeneration. Munc13 proteins are involved in SNARE-mediated vesicle docking and fusion (Hammarlund et al. 2007, Lai et al. 2017), and Munc13-b/*aex-1* is required for DCV fusion in the intestine during the DMP (Yamashita et al. 2009). These data suggest that the intestinal DCV population that mediates regeneration is distinct from DCVs that mediate the DMP. Presumably the “regeneration DCVs” rely on a different factor than the “DMP DCVs” to mediate SNARE-directed fusion. However, we did not detect a role in regeneration for CAPS/*unc-31*(Fig. S3),

another factor that mediates SNARE-directed membrane fusion (Hammarlund et al. 2008). One possibility is that Munc-13b/AEX-1 may function redundantly with other vesicle docking regulators to mediate DCV fusion for axon regeneration.

In the nervous system, RAB-27 regulates synaptic vesicle tethering in coordination with the closely related RAB-3, upstream of the effector Rabphilin/RBF-1 (Mahoney et al. 2006, Mesa et al. 2011). While neuronal RAB-27 inhibits regeneration (Fig. 1H), loss of *rab-3* or Rabphilin/*rbf-1* does not affect regeneration (Fig. 2B). Similarly, the shared GEF for RAB-3 and RAB-27 MADD/*aex-3* does not affect regeneration (Fig. 3), despite being intestinally-expressed and required for both intestinal dense core vesicle secretion and synaptic transmission (Mahoney et al. 2006). These data suggest that neuronal RAB-27 inhibits axon regeneration independent of its role in synaptic vesicle tethering. As it does in diverse tissues across species, RAB-27 also regulates the tethering and fusion of non-synaptic vesicles in *C. elegans* neurons (Feng et al. 2012), and similar to the intestine, neuronal RAB-27 may regulate the secretion of an unknown ligand or ligands through dense core vesicles to inhibit regeneration. Several possibilities could explain neuronal RAB-27's incomplete rescue of high regeneration compared to intestinal RAB-27: the two tissue-specific RAB-27-dependent pathways may be regulating the release of different inhibitory ligands, with the intestine secreting a more potent inhibitor. Alternatively, intestinal and neuronal RAB-27 could be promoting release of the same inhibitory ligand or ligands, with these ligands highly secreted from the intestine but only marginally expressed in neurons.

While loss of *rab-3*Rabphilin/*rbf-1* alone does not affect regeneration, loss of either in a *rab-27* mutant background completely suppresses the *rab-27* mutant high regeneration phenotype (Fig. 2B). However, these double mutants, which show severe defects in synaptic transmission (Mahoney et al. 2006), do not show any defects in regeneration beyond the suppression of the *rab-27* mutant phenotype (Fig 2B). These data suggest that robust synaptic vesicle fusion is required only for enhanced regeneration. Significant loss of vesicle fusion below a certain threshold may restrict high regeneration by restricting the available pool of membrane required for enhanced outgrowth (Futerman & Banker 1996). Alternatively, loss of synaptic vesicle tethering and fusion could disrupt specific pro-regeneration pathways that are normally inhibited during regeneration, but that are released following loss of inhibitory upstream regulatory signals such as RAB-27. Thus, neuronal RAB-27 appears to have dual roles in the regulation of axon regeneration: a pro-high regenerative role mediated through synaptic vesicle fusion and co-regulated by RAB-3 and Rabphilin/RBF-1, and an inhibitory role mediated by the secretion of an anti-regeneration signal from DCV fusion.

Rab GTPases are emerging as key regulators of axon regeneration *in vitro* and *in vivo*. *C. elegans* provides an excellent system to probe the “rabome” for novel pathways affecting axon regeneration. In *C. elegans*, *rab-6.2* was previously shown to affect regeneration (Zeng et al. 2018), as was *rab-27* function in neurons (Sekine et al. 2018). This work probed the function of RAB-27 outside the nervous system, revealing an unexpected role for DCV fusion in the intestine in regulation of axon regeneration. Rabs mediate many complex

biological processes, such as Parkinson's disease pathogenesis (Gao et al. 2018) and cancer metastasis through regulation of exosome secretion (Li et al. 2018). This study adds to our understanding of Rab function by identifying a novel role for RAB-27 in mediating a long-range signal that inhibits the ability of neurons to regenerate after injury.

Materials and Methods

C. elegans strains

Strains were maintained at 20C, as described in Brenner (Brenner, 1974), on NGM plates seeded with OP50. Some strains were provided by the CGC, which is funded by the NIH Office of Research Infrastructure Programs (P40 OD010440). The following strains were purchased from the CGC: NM791[*rab-3(js49)*], RT2[*rab-10(e1747)*], RB1638[*rab-18(ok2020*], RB1537[*rab-19(ok1845*], JT24[*rab-27(sa24)*], JT699[*rab-27(sa699)*], JJ1271[*glo-1(zu391)*], VC2505[*rab-28(gk1040)*], MT1093[*unc-108(n501)*], JT23[*aex-5(sa23)*], JT3[*aex-2(sa3)*], JT5[*aex-3(sa5)*], JT9[*aex-1(sa9)*], KY46[*cab-1(tg46)*], NM1278[*rbf-1(js232)*], NM2777 [*aex-6(sa24);rab-3(js49)*]. The following strains were purchased from the NBRP: *rab-8(tm2526).*

List of generated strains:

rab-27(*sa24*) I; *oxIs12*[P*unc-47*::GFP;*lin-15*+] X	XE1873
wpEx434[P*spl-1*::RAB-27::SL2::mCherry::RAB-3 3' UTR]; *oxIs12*[P*unc-47*::GFP;*lin-15*+] X	XE2524
wpEx417[P*spl-1*::RAB-27::SL2::mCherry::RAB-3 UTR];*rab*-27(*sa24*) I; *oxIs12*[P*unc-47*::GFP;*lin-15*+] X	XE2452
wpEx418[P*unc-47*::RAB-27::SL2::mCherry::RAB-3 3' UTR]; *oxIs12*[P*unc-47*::GFP;*lin-15*+] X	XE2451

wpEx436[P*unc-47*::RAB-27::SL2::mCherry::RAB-3 3' UTR];*rab-27*(*sa24*) I; *oxIs12*[P*unc-47*::GFP;*lin-15*+] X	XE2525
wpEx287[P*unc-47*::RAB-27::SL2::mCherry::UNC-54 3' UTR]; *oxIs12*[P*unc-47*::GFP;*lin-15*+] X	XE1874
wpEx287[P*unc-47*::RAB-27::SL2::mCherry::UNC-54 3' UTR];*rab-27*(*sa24*) I; *oxIs12*[P*unc-47*::GFP;*lin-15*+] X	XE1890
wpEx405[P*spl-1*::RAB-27::SL2::mCherry::UNC-54 3' UTR]; *oxIs12*[P*unc-47*::GFP;*lin-15*+] X	XE2353
wpEx405[P*spl-1*::RAB-27::SL2::mCherry::UNC-54 3' UTR];*rab-27*(*sa24*) I; *oxIs12*[P*unc-47*::GFP;*lin-15*+] X	XE2354
wpEx288[P*unc-47*::EGFP::RAB-27::UNC-54 3' UTR]; *wpIs40*[P*unc-47*::*mCherry*] V	XE1904
wpEx435[P*unc-47*::EGFP::RAB-27::UNC-54 3' UTR; P*unc-47*::mCherry::RAB-3::UNC-54 3' UTR]	XE2523
rab-3(*js49*) II; *oxIs12*[P*unc-47*::GFP;*lin-15*+] X	XE1871
rbf-1(*js232*) III; *oxIs12*[P*unc-47*::GFP;*lin-15*+] X	XE1901
rab-27(*sa24*) I; *rab-3*(*js49*) II; *oxIs12*[P*unc-47*::GFP;*lin-15*+] X	XE2514
rab-27(*sa24*) I; *rbf-1*(*js232*) III; *oxIs12*[P*unc-47*::GFP;*lin-15*+] X	XE2515
wpEx406[P*spl*-1::RAB-3::SL2::mCherry::UNC-54 3' UTR];*rab-27*(*sa24*) I; *oxIs12*[P*unc-47*::GFP;*lin-15*+] X	XE2351
wpEx406[P*spl-1*::RAB-3::SL2::mCherry::UNC-54 3' UTR]; *oxIs12*[P*unc-47*::GFP;*lin-15*+] X	XE2352
aex-1(*sa9*) I; *oxIs12*[P*unc-47*::GFP;*lin-15*+] X	XE2511

aex-2(*sa3*) X; *juIs76*[P*unc-25*::GFP;*lin-15*+] II	XE2517
aex-3(*sa5*) X; *juIs76*[P*unc-25*::GFP;*lin-15*+] II	XE2510
aex-4(*sa22*) X; *juIs76*[P*unc-25*::GFP;*lin-15*+] II	XE2516
aex-5(sa23); *oxIs12*[P*unc-47*::GFP;*lin-15*+] X	XE2509
unc-31(*e928*) IV; *oxIs12*[P*unc-47*::GFP;*lin-15*+] X	XE1905
cab-1(*tg46*) X; *juIs76*[P*unc-25*::GFP;*lin-15*+] II	XE2512
cab-1(*tg46*) X;*rab-27*(*sa24*) I; *juIs76*[P*unc-25*::GFP;*lin-15*+] II	XE2513
unc-108/rab-2(*n501*) I; *oxIs12*[P*unc-47*::GFP;*lin-15*+] X	XE2518
rab-6.2(*ok2254*) X;*juIs76*[P*unc-25*::GFP;*lin-15*+] II	XE1560
rab-8(*tm2526*) I; *oxIs12*[P*unc-47*::GFP;*lin-15*+] X	XE2519
rab-10(*q373*) I;*oxIs12*[P*unc-47*::GFP;*lin-15*+] X	XE1804
rab-18(*ok2020*) III; *oxIs12*[P*unc-47*::GFP;*lin-15*+] X	XE1872
rab-19(*ok1845*) IV; *oxIs12*[P*unc-47*::GFP;*lin-15*+] X	XE2522
rab-21(*gk500186*) II; *oxIs12*[P*unc-47*::GFP;*lin-15*+] X	XE2521
rab-28(*gk1040*) IV; *oxIs12*[P*unc-47*::GFP;*lin-15*+] X	XE1806
glo-1(*zu391*) X; *juIs76*[P*unc-25*::GFP;*lin-15*+] II	XE2520
nlp-1(*ok1469*) X; *juIs76*[P*unc-25*::GFP;*lin-15*+] II	XE2409
nlp-8(*ok1799*) I; *juIs76*[P*unc-25*::GFP;*lin-15*+] II	XE2407
nlp-20(*ok1591*) IV; *juIs76*[P*unc-25*::GFP;*lin-15*+] II	XE2408
nlp-40(tm4085) I; *juIs76*[P*unc-25*::GFP;*lin-15*+] II	XE2560

Constructs and cloning

Transgenic constructs were generated with Gateway recombination (Invitrogen). Fluorescent-tagged RAB-27 was generated through fusion PCR (Hobert 2002)

Laser axotomy

Laser axotomy was performed as previously described in Byrne et al. 2011. L4 animals were immobilized using 0.05 μm polystyrene beads (Polybead Microspheres, Polysciences Cat #08691-10) or in 0.2mM Levamisole (Sigma) on a pad of 3% agarose dissolved in M9 buffer on a glass slide. Worms were visualized using a Nikon Eclipse 80i microscope with a 100x Plan Apo VC lens (1.4 NA). Fluorescently-labeled D-type motor neuron commissures were targeted at the dorsoventral midline using a 435 nm Micropoint laser with 10 pulses at 20 Hz. In all cases no more than four of the seven posterior commisures were cut per animal to minimize possible adverse locomotion or behavioral effects. Animals were recovered to NGM plates seeded with OP50 and allowed to recover.

Fluorescence microscopy and regeneration scoring

Animals with cut axons were immobilized using 0.25–2.5 mM levamisole (Santa Cruz, sc-205730) and mounted on a pad of 3% agarose in M9 on glass slides. All animals were imaged to visualize regeneration using an Olympus DSU mounted on an Olympus BX61 microscope, with a Hamamatsu ORCA-Flash4.0 LT camera, and Xcite XLED1 light source with BDX, GYX and RLX LED

modules. Images were acquired as 0.6 um z-stacks using consistent exposure time, camera sensitivity and light intensity. Images were exported as tiff files and analyzed in ImageJ. Cut axons were scored based on regeneration status and length, and each individual axon was given a designation showing presence of a growth cone indicative of regeneration initiation (Y,N), its general elongation status (no regeneration, GC below midline, GC at midline, GC above midline, full regeneration to DNC), and the measured axon length (absolute axon growth relative to the distance between dorsal and ventral nerve cords). Significance is indicated by and asterisk (*$p<0.05$, Kolmogorov-Smirnov test).

For imaging of GFP::RAB-27 in cut axons (Fig. S1C-E) and GFP::RAB-27; mCherry::RAB-3 in intact axons (Fig. 2A), worms were immobilized as described above, and imaged using the vt-iSIM system mounted on a Leica DMi8 inverted platform, with a Hammamatsu ORCA-Flash 4.0 camera. Images were acquired as 0.6 um z-stacks using consistent exposure time, camera sensitivity and light intensity.

Fecundity

L4 worms of each genotype were singled onto NGM plates seeded with 100µL OP50 for 48 hours. Adult worms were removed, and surviving progeny (L1 or older animals) were counted after an additional 24 hours. Unhatched eggs were not counted.

References

Barclay JW, Morgan A, Burgoyne RD. 2012. Neurotransmitter release mechanisms studied in *Caenorhabditis elegans*. *Cell Calcium* 52: 289-295.

Brenner, S. 1974. The genetics of *Caenorhabditis elegans*. *Genetics* 77: 71-94.

Byrne AB, Edwards TJ, Hammarlund M. 2011. In vivo laser axotomy in *C. elegans. Journal of Visualized Experiments*: JoVE. DOI: https://doi.org/10.3791/2707, PMID: 21633331.

Cao J., Packer JS, Ramani V, Cusanovich DA, Huynh C, Daza R, Qiu X, Lee C, Furlan SN, Steemers FJ, Adey A, Waterston BH, Trapnell C, Shendure J. 2017. Comprehensive single-cell transcriptional profiling of a multicellular organism. *Science* 357:661-667.

Ch'ng Q, Sieburth D, Kaplan JM. 2008. Profiling synaptic proteins identifies regulators of insulin secretion and lifespan. *PLoS Genet* 4:e1000283

Cheah M, Andrews MR. 2016. Targeting cell surface receptors for axon regeneration in the central nervous system. *Neural Regeneration Research* 11:1884-1887.

Chen L, Wang Z, Ghosh-Roy A, Hubert T, Yan D, O'Rourke S, Bowerman B, Wu Z, Jin Y, Chisholm AD. 2011. Axon regeneration pathways identified by systematic genetic screening in *C. elegans*. *Neuron* 71:1043-1057.

Doi M, Iwasaki K. 2002. Regulation of retrograde signaling at neuromuscular junctions by the novel C2 domain protein AEX-1. *Neuron* 33: 249-259.

Edwards TJ, Hammarlund M. Syndecan promotes axon regeneration by stabilizing growth cone migration. *Cell Reports* 8:272-283.

Feng W, Liang T, Yu J, Zhou W, Zhang Y, Wu Z, Xu T. 2012. RAB-27 and its effector RBF-1 regulate the tethering and docking steps of DCV exocytosis in *C. elegans*. *Sci China Life Sci* 55:228-235.

Futerman AH, Banker GA. 1996. The economics of neurite outgrowth - the addition of new membrane to growing axons. *TINS* 19: 144-149.

Frooninckx L, Van Rompay L, Temmerman L, Van Sinay E, Beets I, Janssen T, Husson SJ, Schoofs L. 2012. Neuropeptide GPCRs in *C. elegans*. *Front Endocrinol* 3: 1-18.

Gallegos ME, Balakrishnan S, Chandramouli P, Arora S, Azameera A, BAbushekar A, Bargoma E, Bokhari A, Chava SK, Das P, Desai M, Decena D,

Saramma SDD, Dey B, Doss A, Gor N, Gudiputi L, Guo C, Hande S, Jensen M, Jones S, Jones N, Jorgens D, Karamchedu P, Kamrani K, Kolora LD, Kristensen L, Kwan K, Lau H, Maharaj P, Mander N, Mangipudi K, Menakuru H, Mody V, Mohanty S, Mukkamala S, Mundra SA, Nagaraju S, Narayanaswamy R, Ndungu-Case C, Noorbakshsh , Patel J, Patel P, Pendem SV, Ponakala A, Rath M, Robles MC, Rokkam D, Roth C, Sasidharan P, Shah S, Tandon S, Suprai J, Truong TQN, Uthayaruban R, Varma A, Ved U, Wang Z, Yu Z. 2012. The *C. elegans* Rab family: identification, classification and toolkit construction. PLoS One: 7:e49387.

Gotenstein , JR, Swale, RE, Fukuda T, Wu Z, Girumescu CA, Goncharov A, Jin Y, Chisholm AD. 2010. The *C. elegans* peroxidasin PXN-2 is essential for embryonic morphogenesis and inhibits adult axon regeneration. *Development* 137: 3606-3613

Hammarlund M, Palfreyman MT, Watanabe S, Olsen S, Jorgensen EM. Open syntaxin docks synaptic vesicles. *PLoS Biol* 5: e198.

Hammarlund M, Watanabe S, Schuske K, Jorgensen EM. 2008. CAPS and syntaxin dock dense core vesicles to the plasma membrane in neurons. *JCB* 180: 483-491.

Hammarlund M, Jin Y. 2014. Axon regeneration in *C. elegans*. *Curr Opin Neurobiol* 27:199-207

Hermann GJ, Schroeder LK, Hieb CA, Kershner AM, Rabbitts BM, Fonarev P, Grant BD, Priess JR. 2005. Genetic analysis of lysosomal trafficking in *Caenorhabditis elegans*. *MBoC* 16: 3273-3288.

Hobert, O. 2002. PCR fusion-based approach to create reporter gene constructs for expression analysis in transgenic *C. elegans*. *BioTechniques* 32: 728-730.

Holzer P., Farzi A. 2014. Neuropeptides and the Microbiota-Gut-Brain Axis. In: Lyte M., Cryan J. (eds) Microbial Endocrinology: The Microbiota-Gut-Brain Axis in Health and Disease. Advances in Experimental Medicine and Biology, vol 817. Springer, New York, NY

Husson SJ, Clynen E, Baggerman G, Janssen T, Schoofs L. 2006. Defective processing of neuropeptide precursors in *Caenorhabditis elegans* lacking proprotein convertase 2 (KPC-2/EGL-3): mutant analysis by mass spectrometry. *J Neurochem* 98: 1999-2012.

Iwasaki K, Tonoyaga R. 2000. The Rab3 GDP/GTP exchange factor homolog AEX-3 has a dual function in synaptic transmission. *EMBO J* 19:4806-4816.

Klassen MP, Shen K. 2007. Wnt signaling positions neuromuscular connectivity by inhibiting synapse formation in *C. elegans*. *Cell* 130: 704-716.

Koelle M.R. Neurotransmitter signaling through heterotrimeric G proteins: insights from studies in *C. elegans*. (December 11, 2018), *WormBook*, ed. The *C. elegans* Research Community, WormBook, doi/10.1895/wormbook.1.75.2, http://www.wormbook.org.

Lai Y, Choi UB, Leitz J, Rhee HJ, Lee C, Altas B, Zhao M, Pfuetzner RA, Wang AL, Brose N, Rhee JS, Brunger AT. 2017. Molecular mechanisms of synaptic vesicle priming by Munc13 and Munc18. Neuron 95:591-607.

Laurent P, Ch'ng Q, Jospin M, Chen C, Lorenzo R, de Bono M. 2018. Genetic dissection of neuropeptide cell biology at high and low activity in a defined sensory neuron. *PNAS* 115:E6890–E6899

Li C, Kim K. Neuropeptides. In: WormBook: The Online Review of C. elegans Biology [Internet]. Pasadena (CA): WormBook; 2005-2018. Available from: https://www.ncbi.nlm.nih.gov/books/NBK116087/

Li C, Hisamoto N, Nix P, Kanao S, Mizuno T, Bastiani M, Matsumoto K. 2012. The growth factor SVH-1 regulates axon regeneration in *C. elegans* via the JNK MAPK cascade. *Nature Neuroscience* 15:551-557.

Liu BP, Cafferty WB, Budel SO, Strittmatter SM. 2006. Extracellular regulators of axonal growth in the adult central nervous system. *Philosophical Transactions of the Royal Society B* 361:1593-1610.

Mahoney TR, Liu Q, Itoh T, Luo S, Hadwiger G, Vincent R, Wang ZW, Fukuda M, Nonet ML. 2006. Regulation of synaptic transmission by RAB-3 and RAB-27 in *Caenorhabditis elegans*. *Mol Biol Cell* 17:3617-2625.

Mahoney TR, Luo S, Round EK, Brauner M, Gottschalk A, Thomas JH, Nonet ML. Intestinal signaling to GABAergic neurons regulates a rhythmic behavior in *Caenorhabditis elegans*. *PNAS* 105:16350-16355.

Mesa R, Luo S, Hoover CM, Miller K, Minniti A, Inestrosa N, Nonet ML. 2011. HID-1, a new component of the peptidergic signaling pathway. Genetics 187:467-483.

Nonet ML, Staunton JE, Kilgard MP, Fergestad T, Hartwieg E, Horvitz HR, Jorgensen EM, Meyer BJ. 1997. *Caenorhabditis rab-3* mutant synapses exhibit impaired function and are partially depleted of vesicles. *J Neurosci* 17: 8061-8073.

Pavlos NJ, Grønborg M, Riedel D, Chua JJE, Boyken J, Kloepper TH, Urlaub H, Rizzoli SO, Jahn R. 2010. Quantitative analysis of synaptic vesicle rabs uncovers distinct yet overlapping roles for Rab3a and Rab27b in Ca^{2+}-triggered exocytosis. *J Neurosci* 30: 13441-13453.

Pavlos NJ, Jahn R. 2011. Distinct yet overlapping roles of Rab GTPases on synaptic vesicles. *Small GTPases* 2:77-81.

Riddle DLBT., BJ Meyer, JR Priess. Defecation motor program. In *C. elegans II, 2nd ed.*; Cold Spring Harbor Laboratory Press: Cold Spring Harbor, NY, USA, 1997.

Sawa H., Korswagen H. C. Wnt signaling in *C. elegans* (December 9, 2013), *WormBook*, ed. The *C. elegans* Research Community, WormBook, doi/10.1895/wormbook.1.7.2, http://www.wormbook.org.

Sekine Y, Lin-Moore A, Chenette DM, Wang X, Jiang Z, Cafferty WB, Hammarlund M, Strittmatter SM. 2018. Functional genome-wide screen identifies pathways restricting central nervous system axonal regeneration. *Cell Reports* 23:415-428.

Silva-García CG, Lanjuin A, Heintz C, Dutta S, Clark NM, Mair WB. 2019. Sing-copy knock-in loci for defined gene expression in *Caenorhabditis elegans*. *G3* 9: 2195-8.

Staunton J, B Ganetzky, ML Nonet. 2001. Rabphilin potentiates Soluble N-Ethylamide Sensitive Factor Attachment Protein Receptor function independent of Rab3. *J Neurosci* 21: 9255-64.

Taylor SR, Santpere G, Reilly M, Glenwinkel L, Poff A, McWhirter R, Xu C, Weinreb A, Basavaraju M, Cook SJ, Barrett A, Abrams A, Vidal B, Cros C, Rafi I, Sestan N, Hammarlund M, Hobert O, Miller III DM. 2019. Expression profiling of the mature *C. elegans* nervous system by single-cell RNA sequencing. bioRxiv 737577; doi: https://doi.org/10.1101/737577

Thomas JH. 1990. Genetic analysis of defecation in *Caenorhabditis elegans*. *Genetics* 124:855-872.

Tsuboi T, Fukuda M. 2005. The C2B domain of rabphilin directly interacts with SNAP-25 and regulates the docking step of dense core vesicle exocytosis in PC12 cells. *JCB* 280:39253-39259.

Wang H, Girskis K, Janssen T, Chan JP, Dasgupta K, Knowles JA, Schoofs L, Sieburth D. 2013. Neuropeptide secreted from a pacemaker activates neurons to control a rhythmic behavior. *Curr Biol* 23:746-754.

Xia Z, Chen Y, Sheng Y, Yi Y, Song E, Xu T. 2014. Whole genome RNAi screen in *C. elegans* identifies CAB-1 as a novel regulator of DCV secretion. *PIBB* 41:787095.

Yamashita M, Iwasaki K, Doi M. 2009. The non-neuronal syntaxin SYN-1 regulates defecation behavior and neural activity in *C. elegans* through interaction with the Munc13-like protein AEX-1. Biochem Biophys Res Commun 378:404-408.

Zeng L, El Bejjani R, Hammarlund M. 2018. The amyloid precursor-like protein APL-1 regulates axon regeneration.
bioRxiv 305284; doi: https://doi.org/10.1101/305284.

Acknowledgements: We thank WormBase and the Caenorhabditis Genetics Center (CGC), which is funded by the National Institutes of Health (NIH) Office of Research Infrastructure Programs (P40 OD010440). We also thank Tyler Page and Erik Jorgensen for suggestions and feedback regarding *cab-1*. This research was supported by NIH grants (R01 NS098817 and R01 NS094219) to M.H.
Author contributions: A.L.M. and M.H. designed experiments. A.L.M. and R.J.O. performed experiments and data analysis.

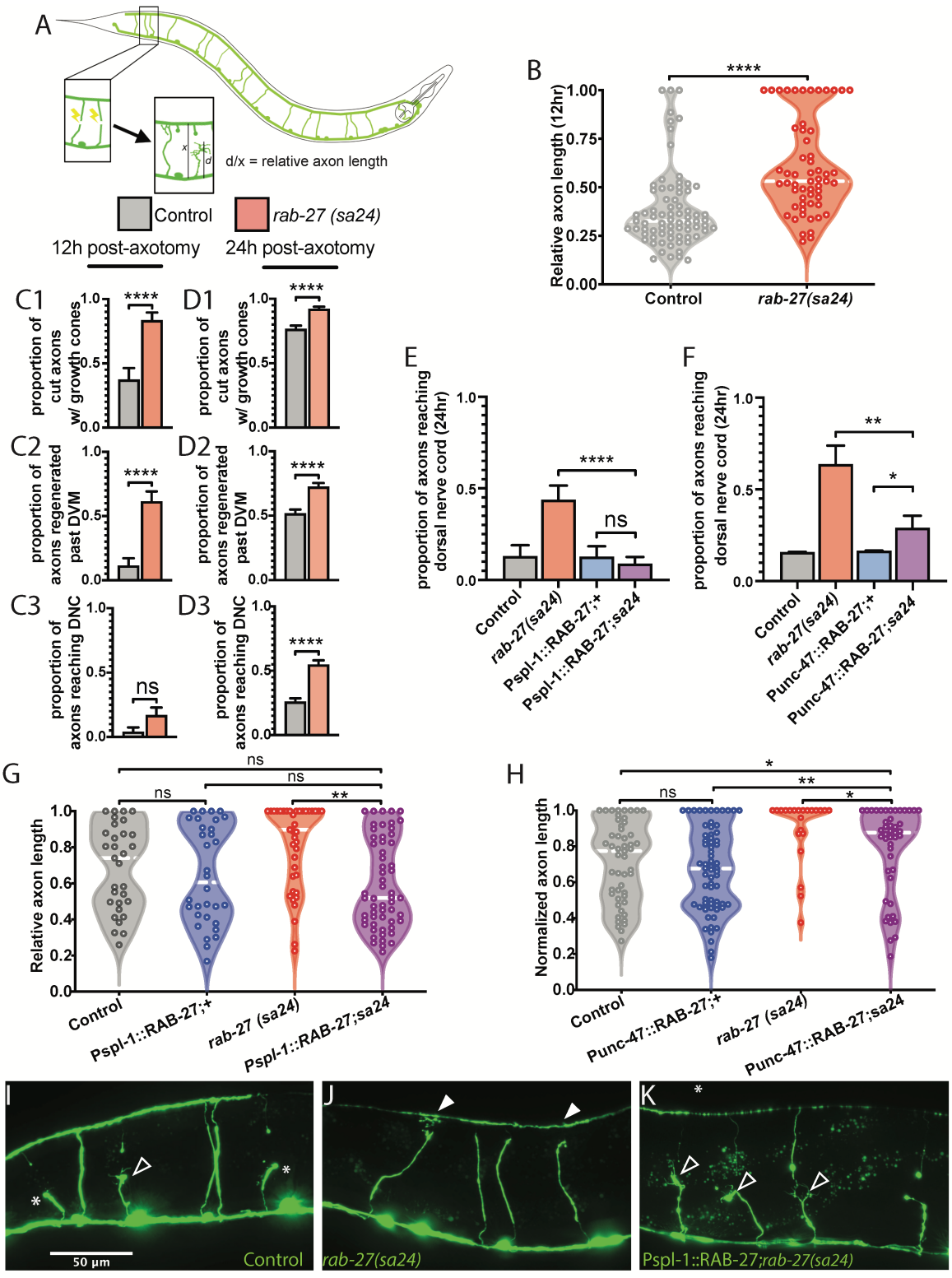

Figure 1. RAB-27 expression in the intestine inhibits axon regeneration. (A) Posterior DD/VD commissural axons in the GABAergic nervous system of L4 animals were severed using a pulsed laser, and regeneration was measured after a 24 hour recovery window. (B) Relative axon length in control (*oxIs12*) animals and *rab-27*(*sa24*) mutants after 12 hours of recovery after axotomy. Axons cut per genotype, L to R: 27, 36. Kolmogorov-Smirnov test was used. ns, not

significant, * $p < 0.05$, *** $p < 0.0005$. (C). Proportion of cut axons forming growth cones (C1), regeneration past the dorsoventral midline (DVM) (C2), or full regeneration back to the dorsal nerve cord (DNC) (C3) in control (*oxIs12*) and *rab-27*(*sa24*) mutant animals after 12 hours of recovery post-axotomy. Axons cut per genotype, L to R: 27, 36. Unpaired t-test was used. ns, not significant, **** $p < 0.0001$. Error bars represent SEM. (D). Proportion of cut axons forming growth cones (D1), regeneration past the dorsoventral midline (DVM) (D2), or full regeneration back to the dorsal nerve cord (DNC) (D3) in control (*oxIs12*) and *rab-27*(*sa24*) mutant animals after 24 hours of recovery post-axotomy. Axons cut per genotype, L to R: 233, 198. Unpaired t-test was used. ns, not significant, **** $p < 0.0001$. Error bars represent SEM. (E) Proportion of cut axons showing signs of regeneration in control (*oxIs12*) and *rab-27*(*sa24*) mutant animals, and animals expressing RAB-27 cDNA under an intestine-specific promoter (Pspl-1) and stabilized with *rab-3* 3' UTR sequence, in both control and *rab-27* mutant backgrounds. Axons were scored after 24 hours of recovery post-axotomy. Axons cut per genotype, L to R: 31, 39, 32, 57. Unpaired t-test was used. ns, not significant, **** $p < 0.0001$. Error bars represent SEM. (F) Proportion of cut axons showing signs of regeneration in control (*oxIs12*) and *rab-27*(*sa24*) mutant animals, and animals expressing RAB-27 cDNA under a GABA neuron-specific promoter (Punc-47) and stabilized with *rab-3* 3' UTR sequence, in both control and *rab-27* mutant backgrounds. Axons were scored after 24 hours of recovery post-axotomy. Axons cut per genotype, L to R: 51, 22, 67, 45. Unpaired t-test was used. ns, not significant, * $p < 0.05$, ** $p < 0.005$. Error bars represent SEM. (G) Relative axon length in control (*oxIs12*) animals, *rab-27*(*sa24*) mutants, and animals expressing RAB-27 cDNA under an intestine-specific promoter and stabilized with *rab-3* 3' UTR sequence, in both control and *rab-27* mutant backgrounds. Number of axons cut per genotype, L to R: 31, 32, 39, 57. Kolmogorov-Smirnov test was used. ns, not significant, * $p < 0.05$, ** $p < 0.005$. (H) Relative axon length in animals expressing RAB-27 cDNA under a GABA neuron-specific promoter, in both control (*oxIs12*) and *rab-27* mutant backgrounds. Number of axons cut per genotype, L to R: 51, 67, 22, 45. Kolmogorov-Smirnov test was used. ns, not significant, * $p < 0.05$, ** $p < 0.005$, *** $p < 0.0005$. (I-K). Representative micrographs of regeneration in Day 1 adults 24 hours after axotomy in *oxIs12* control (I), *rab-27* mutant (J), and intestinal *rab-27* rescue (K) animals. Filled arrows indicate fully regenerated axons reaching the dorsal nerve cord, empty arrows indicate partially regenerated axons, and stars indicate non-regenerating axon stumps. All animals express Punc-47::GFP (*oxIs12*).

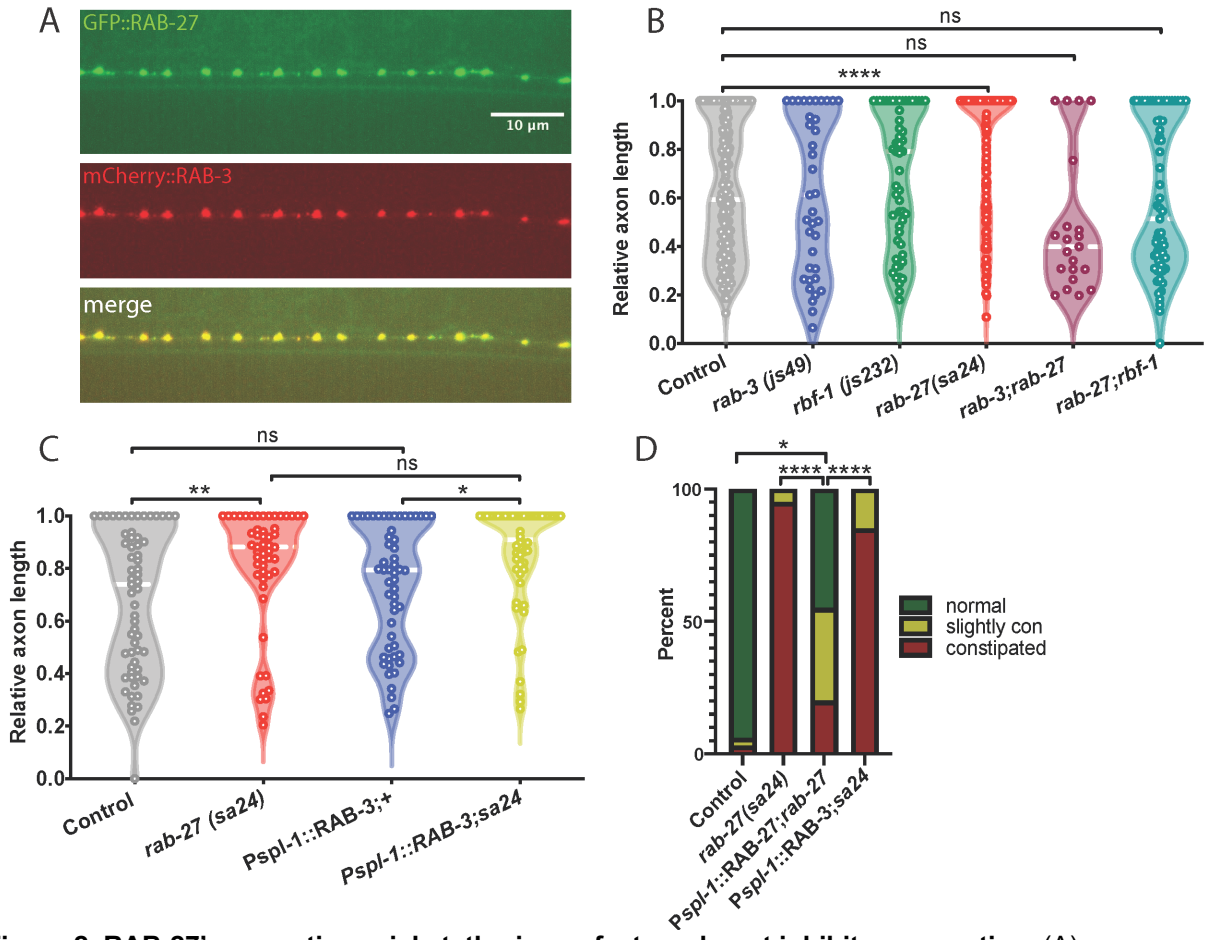

Figure 2. RAB-27's synaptic vesicle tethering cofactors do not inhibit regeneration. (A) Colocalization of transgenic GFP::RAB-27 and mCherry::RAB-3 at synapses of DD/VD neurons. GFP::RAB-27 and mCherry::RAB-3 were expressed as multicopy arrays at an injection concentration of 7.5ng/µL. GFP::RAB-27 was expressed as multicopy array with a soluble mCherry transcriptional reporter at an injection concentration of 7.5ng/µL. (B) Relative axon length in control (*oxIs12*) animals, *rab-3*(*js49*), rbr-1(*js232*), *rab-27*(*sa24*), *rab-3*(*js49*);*rab-7*(*sa24*) mutants. Axons cut per genotype, L to R: 183, 37, 55, 196, 21, 69. Kolmogorov-Smirnov test was used. ns, not significant, * $p < 0.05$, *** $p < 0.0005$. (C) Relative axon length in control animals, *rab-27*(*sa24*) mutants, and animals expressing RAB-3 cDNA under an intestine-specific promoter, in control and *rab-27* mutant backgrounds. Number of axons cut per genotype, L to R: 61, 55, 53, 50. Kolmogorov-Smirnov test was used. ns, not significant, * $p < 0.05$, ** $p < 0.005$. (D) Percent stacked bar graph for visual scoring of Aex phenotype rescue. Animals were randomized on plates and scored by phenotype, then genotyped. Animals were scored as normal (no gut distention, strong pBoc contraction with accompanying expulsion), constipated (severe posterior gut distention, weak pBoc with no expulsion), or slightly con (some possible gut distention, normal pBoc, weak expulsion). Fisher's Exact test was used. * $p < 0.05$, **** $p < 0.0001$. (E). Visualization of Aex phenotype and rescue in control and transgenic animals. Distention of the intestinal lumen, caused by failure to expel waste is characteristic of *rab-27* mutant animals, and was partially rescued by intestinal expression of RAB-27 cDNA, but not by RAB-3.

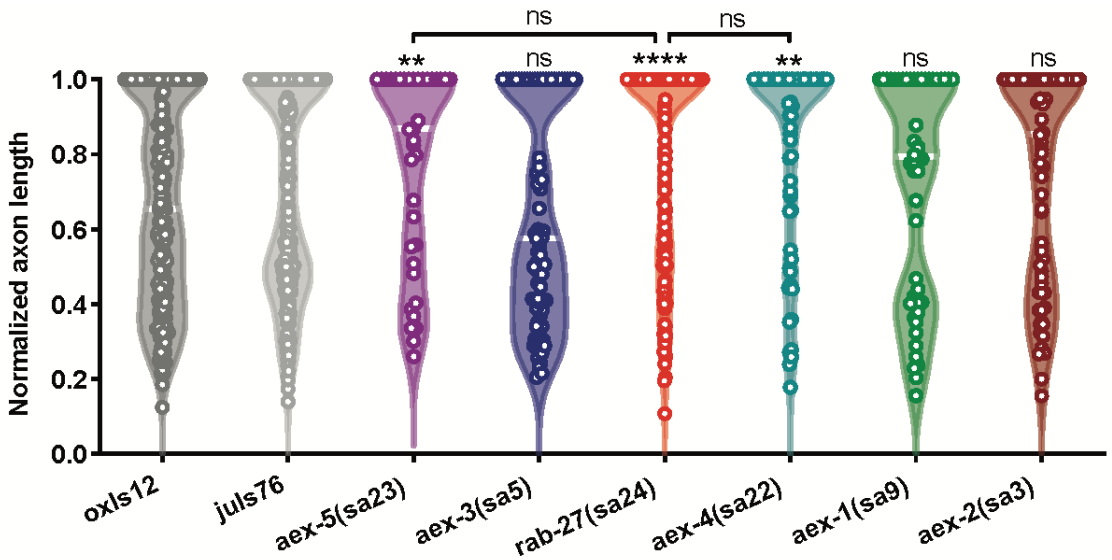

Figure 3. AEX-4 and AEX-5 inhibit axon regeneration. (A) Relative axon length in control animals expressing GABAergic neuron-specific GFP (*oxIs12* & *juIs76*), and *aex-1*(sa9), *aex-2*(*sa3*), *aex-3*(*sa5*), *aex-4*(*sa22*), *aex-5*(*sa23*) and *rab-27*(*sa24*) mutants. *aex-1*, *aex-5*, and *rab-27* are compared against *oxIs12*, while *aex-2*, *aex-3*, while *aex-4* are compared against *juIs76*. Axons cut per genotype, L to R: 238, 199, 37, 83, 148, 69, 50, 66. Kolmogorov-Smirnov test was used. ns, not significant, * $p < 0.05$, ** $p < 0.005$ **** $p < 0.0001$.

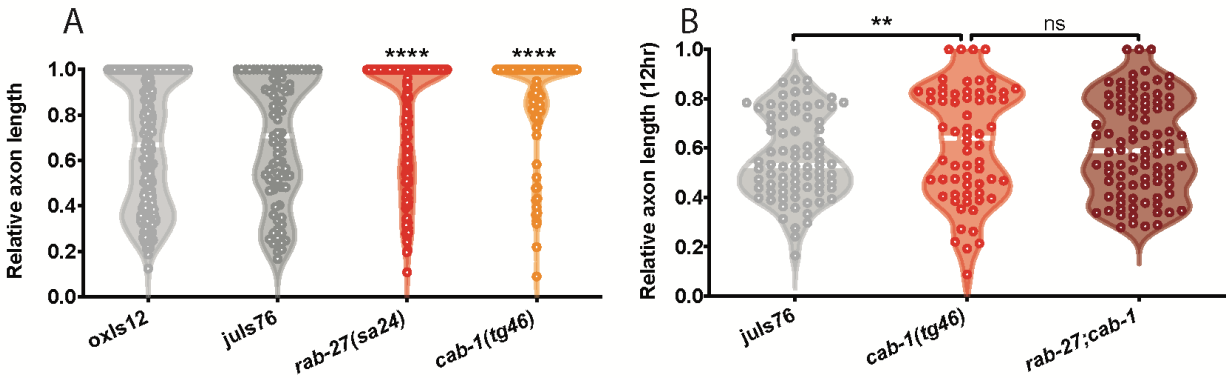

Figure 4. CAB-1 inhibits axon regeneration. (A) Relative axon length in control animals expressing GABAergic neuron-specific GFP (*oxIs12* & *juIs76*), and *rab-27*(*sa24*) and *cab-1*(*tg46*) mutants. *rab-27* is compared against *oxIs12*, while *cab-1* is compared against *juIs76*. Axons cut per genotype, L to R: 200, 81, 164, 91. Kolmogorov-Smirnov test was used. ns, not significant, **** $p < 0.0001$. (B) Relative axon length in control animals expressing GABAergic neuron-specific GFP (*juIs76*), *rab-27*(*sa24*) mutants and *rab-27*(*sa24*);*cab-1*(*tg46*) double mutants. L to R: 78, 64, 90. Kolmogorov-Smirnov test was used. ns, not significant, ** $p < 0.005$. Regeneration was scored after 12 hours of recovery to more easily visualize enhanced regeneration in the *rab-27* and *rab-27*;*cab-1* double mutants, which show nearly full regeneration after the usual 24 hour recovery window.

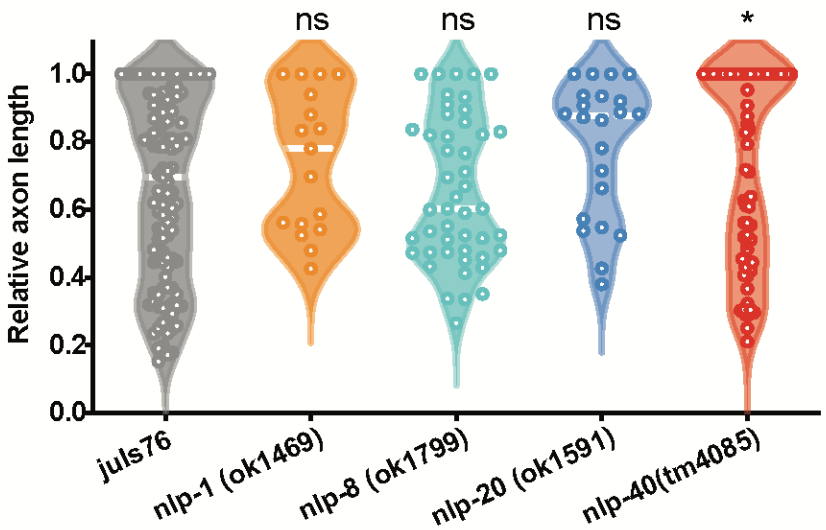

Figure 5. The neuropeptide NLP-40 inhibits axon regeneration. Relative axon length in control animals expressing GABAergic neuron-specific GFP (*juIs76*), and mutants of several intestinally-expressed neuropeptides: *nlp-1*(*ok1469*), *nlp-8*(*ok1799*), *nlp-20*(*ok1591*) and *nlp-40*(*tm4085*). Axons cut per genotype, L to R: 117, 17, 47, 22, 67. Kolmogorov-Smirnov test was used. ns, not significant, **** $p < 0.0001$.

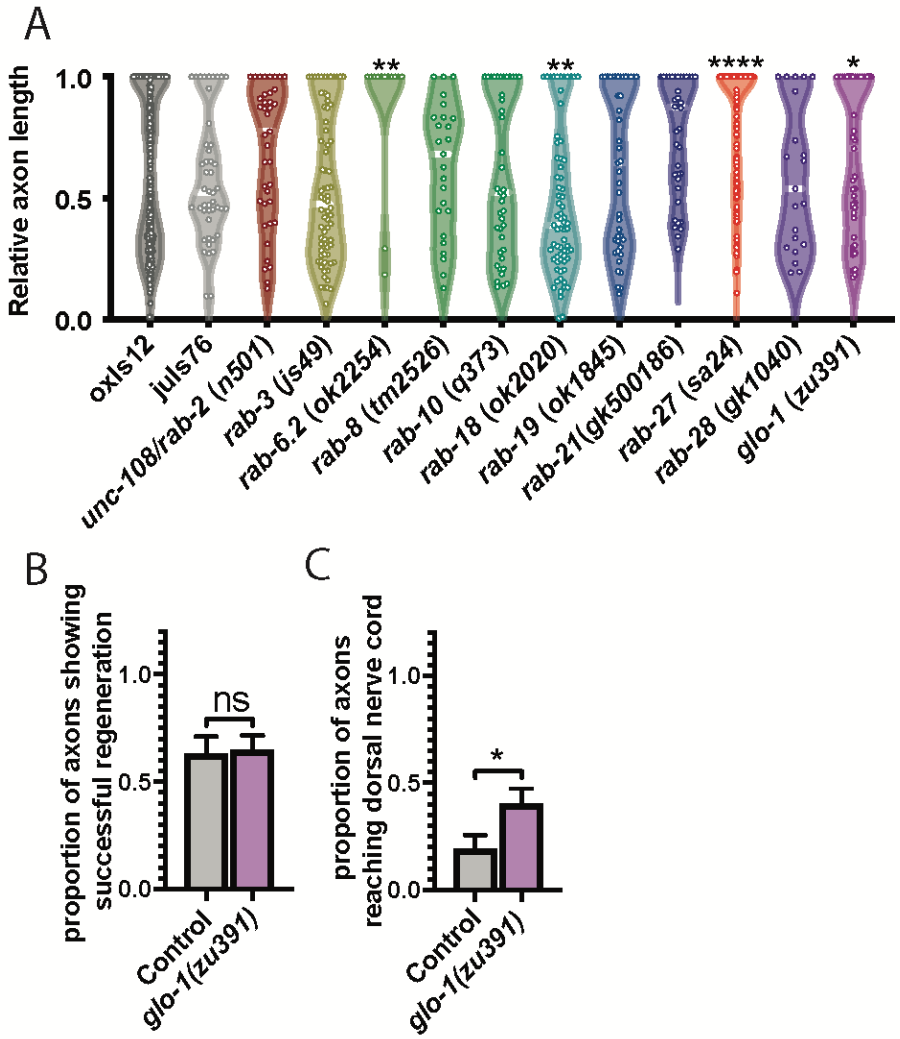

Figure 6. Multiple Rab GTPases affect axon regeneration. (A) Relative axon length in control animals expressing GABAergic neuron-specific GFP (*oxIs12* & *juIs76*), and unc-108/rab-2(n501), *rab-3*(*js49*), *rab-6.2*(*ok2254*), *rab-8*(*tm2526*), *rab-10*(*q373*), *rab-18*(*ok2020*), *rab-19*(*ok1845*), *rab-21*(*gk500186*), *rab-27*(*sa24*), *rab-28*(*gk1040*), and *glo-1*(*zu391*). *unc-108*/*rab-2*, *rab-3*, *rab-8*, *rab-10*, *rab-18*, *rab-19*, *rab-21*, *rab-27* and *rab-28* are compared against *oxIs12*, while *rab-6.2* and *glo-1* are compared against *juIs76*. Axons cut per genotype, L to R: 396, 46, 39, 72, 13, 25, 41, 69, 43, 38, 123, 21, 45, 64. Kolmogorov-Smirnov test was used. ns, not significant, * $p < 0.05$, ** $p < 0.005$ **** $p < 0.0001$. (B) Proportion of cut axons showing signs of regeneration in control (*juIs76*) and *glo-1*(*zu391*) mutant animals. Axons cut per genotype, L to R: 32, 45. Unpaired t-test was used. ns, not significant. Error bars represent SEM. (C) Proportion of cut axons showing full regeneration back to the dorsal nerve cord in control (*juIs76*) and *glo-1*(*zu391*) mutant animals. Axons cut per genotype, L to R: 32, 45. Unpaired t-test was used. ns, not significant. Error bars represent SEM.

Supplemental Figures

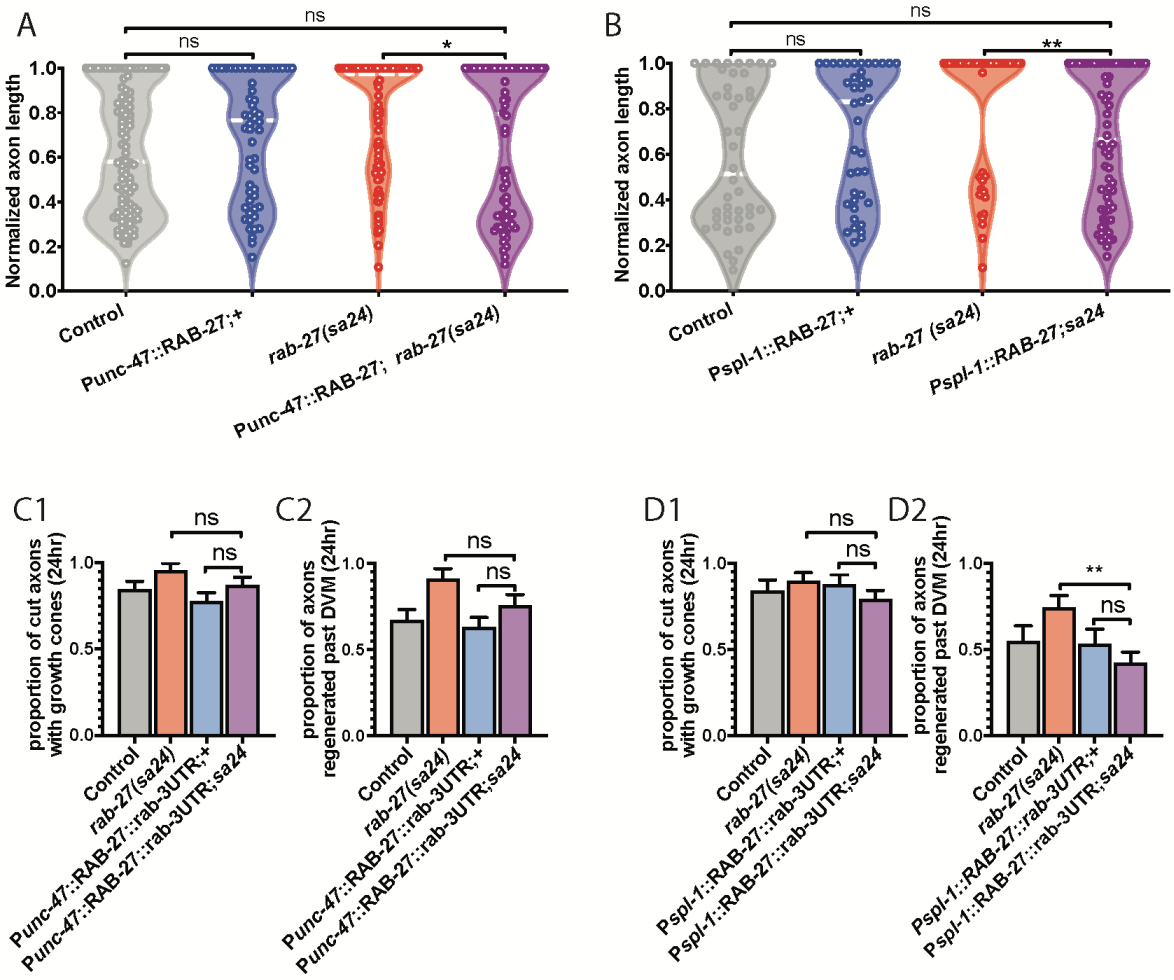

Figure S1. Use of *unc-54* 3' UTR sequence in constructs containing RAB-27 cDNA inhibits regeneration. (A-B) Relative axon length in animals expressing RAB-27 cDNA under a GABA neuron-specific (A) or intestine-specific (B) promoter and with *unc-54* 3' UTR sequence, in both control (*oxIs12*) and *rab-27* mutant backgrounds. Number of axons cut per genotype, L to R: 51, 67, 22, 45. Kolmogorov-Smirnov test was used. ns, not significant, * $p < 0.05$, ** $p < 0.005$, *** $p < 0.0005$. (C) Proportion of cut axons showing signs of successful regeneration initiation (C1) or regeneration past the dorsoventral midline (C2) in control (*oxIs12*) and *rab-27(sa24)* mutant animals, and animals expressing *rab-27* cDNA under a GABA neuron-specific promoter (Punc-47) and the *rab-3* 3' UTR sequence, in both control and *rab-27* mutant backgrounds. Axons were scored after 24 hours of recovery post-axotomy. Axons cut per genotype, L to R: 51, 22, 67, 45. Unpaired t-test was used. ns, not significant. Error bars represent SEM. (D) Proportion of cut axons showing signs of successful regeneration initiation (D1) or regeneration past the dorsoventral midline (D2) in control (*oxIs12*) and *rab-27(sa24)* mutant animals, and animals expressing *rab-27* cDNA under an intestine-specific promoter (Pspl-1) and the *rab-3* 3' UTR sequence, in both control and *rab-27* mutant backgrounds. Axons were scored after 24 hours of recovery post-axotomy. Axons cut per genotype, L to R: 31, 39, 32, 57. Unpaired t-test was used. ns, not significant, ** $p < 0.005$. Error bars represent SEM.

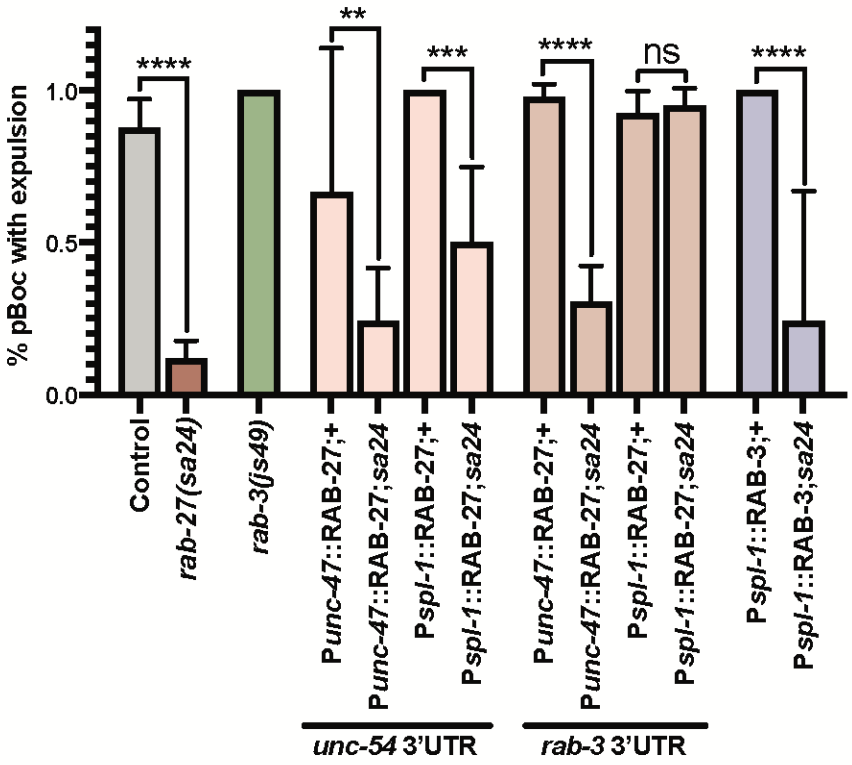

Figure S2. Rescue of the defecation motor program by intestinal *rab-27* expression. Mutants in the *aex* pathway display a defect in the defecation motor program, visualized by a loss of waste expulsion (Exp) following posterior body contraction (pBoc). Animals were randomly selected and observed for 5 DMP cycles, and the ratio of Exp/pBoc was plotted. Intestinal (P*spl-1*) but not GABA neuron-specific (P*unc-47*) expression of *rab-27* cDNA was sufficient to rescue DMP in *rab-27* mutant worms. This rescue was enhanced in animals expressing constructs with a *rab-3* 3' UTR compared to animals expressing constructs with a *unc-54* 3' UTR. Expression of *rab-3* cDNA in the intestine of *rab-27* mutant animals did not rescue DMP defects. pBoc cycles observed, L to R: 49, 119, 30, 27, 25, 20, 18, 49, 62, 54, 56, 40, 58. Kolmogorov-Smirnov test was used. ns, not significant, * $p < 0.05$, ** $p < 0.05$, *** $p < 0.0005$, **** $p < 0.0001$, Fisher's Exact Test. Error bars represent SEM.

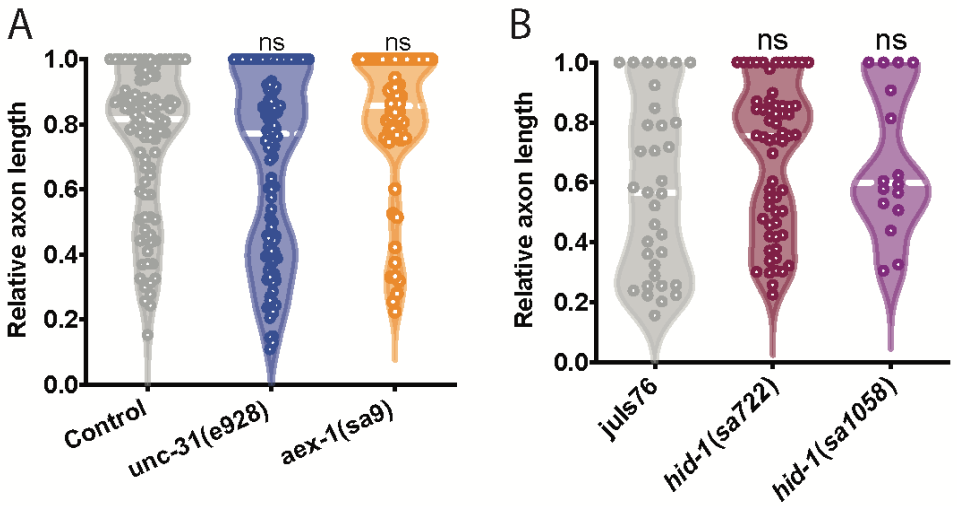

Figure S3. Two dense core vesicle tethering regulators do not affect axon regeneration. (A) Relative axon length in control (*juIs76*) animals, *unc-31(e928)* and *aex-1(sa9)* mutants. Axons cut per genotype, L to R: 91, 59, 116. Kolmogorov-Smirnov test was used. ns, not significant. (B) Relative axon length in control (*juIs76*) animals, and *hid-1* (*js722* and *js1058*) mutants. Axons cut per genotype, L to R: 34, 61, 16. Kolmogorov-Smirnov test was used. ns, not significant

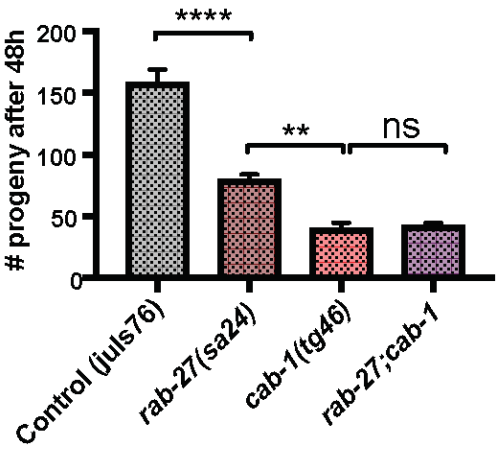

Figure S4. *cab-1* and *rab-27* show reduced fecundity. One-day adult worms were placed onto empty NGM plates seeded with OP50 and left for 48 hours. Adults were removed and progeny counted. *rab-27* mutants show significantly decreased brood size compared to control animals, and *cab-1* mutants show more severe defects. The low brood size of *cab-1* mutants is not increased in *rab-27;cab-1* double mutants. Worms sampled, L to R: 9, 10, 7, 8. One-way ANOVA test was used. ns, not significant, ** $p < 0.005$, **** $p < 0.0001$. Error bars represent SEM.

Unpublished experiments

This section describes various experiments that were motivated by and related to my dissertation work on RAB-27 and its role in axon regeneration. Several of these experiments outline attempts to identify potential pathways related to RAB-27 that could explain its incomplete neuronal role in regeneration, attempts to visually characterize intracellular RAB-27 or neuronal morphologies of *rab-27* mutants that could motivate the identification of inhibitory pathways, and baseline regeneration levels in DD/VD GABAergic neurons of several potential genes of interest moving forward. While these experiments did not directly lead to the primary findings of my dissertation work, they do provide interesting and important data on regeneration and cell biology in the greater context of RAB-27.

Visualizing neuronal RAB-27 and *rab-27* regeneration

In intact axons, RAB-27 localization is punctate, as it is predominantly localized to synaptic vesicles that are trafficked to the axon terminal. Accordingly, RAB-27+ puncta can be seen throughout the length of the commissure, and individual RAB-27+ vesicles can be tracked as they move through the axon. I was interested to observe both how RAB-27+ vesicles move in the axons, and whether this vesicle-associated, punctate localization pattern was disrupted during axon regeneration. Synaptic vesicle fusion machinery is believed to be an

important mechanism in membrane addition during axon outgrowth (Futerman & Banker 1996), and growth cone filopodia have been observed containing vesicles with synaptic vesicle proteins (Sabo & McAllister 2003), suggesting a potential localization mechanism for synaptic vesicle-bound RAB-27 in the regenerating growth cone.

In addition to visualizing RAB-27 in regenerating axons, I was interested to see whether the anatomy of regenerating axons was different in *rab-27* animals. Growth cone structure and stability is important for successful regeneration. Stabilization of growth cones is required for regeneration, as loss of the stabilizing heparin sulfate proteoglycan syndecan/*sdn-1* in the hypodermis leads to severely impairs successful regrowth (Edwards & Hammarlund, 2014). Like *sdn-1*, *rab-27* acts outside the neurons to regulate axon regeneration, and I investigated *rab-27* mutant animals for differences or abnormalities in growth cone structure.

GFP-tagging of RAB-27 was done as described by Hobert (2002). Briefly, GFP sequence was fused to the N-terminal of a validated RAB-27 cDNA sequence, which was then modified for tissue-specific expression by attaching the fusion sequence to a described, cell type-specific promoter. GFP was added to the N-terminal rather than the more typical C-terminal due to the presence of a pre-C-terminal effector binding domain in most Rabs, which is essential for their localization and function (Chavrier et al. 1991). To better understand GFP::RAB-27 localization in neurons, imaging of worms expressing these constructs was done with superresolution microscopy, using the vt-iSIM system.

Because growth cones in regenerating axons are variable in size and shape, I took a volumetric approach to measuring differences between *rab-27* mutant and wild-type growth cones. I imaged growth cones at superresolution using the vt-iSIM system, and calculated the surface area-to-volume ratio of each growth cone using the analysis software IMARIS (Bitplane).

Axonal GFP::RAB-27 was punctate (Fig. 1A,E), and individual puncta were mobile within the axon (Fig. 1A), with several puncta exhibiting rapid anterograde movement consistent with localization on synaptic vesicles. In regenerating axons, however, GFP::RAB-27 is diffuse, lacking any obvious puncta, and is generally excluded from the growth cone, except in areas with significant cytosolic accumulation (Fig. 1B-D). No punctate GFP signal is detectable in growth cone filopodia or elsewhere in the axon, suggesting that RAB-27-containing vesicles are not directly involved in the addition of membrane or other aspects of regrowth. Structurally, growth cones of *rab-27* mutants are not different than control growth cones (Fig. 1G), which supports that RAB-27's site of action for regeneration inhibition is not at the regeneration front of the injured axon.

Expression of a dominant-negative RAB-27 in the nervous system

Most Rabs must be activated by binding GTP before interacting with the effectors that mediate many Rab-dependent cellular processes. Activation of Rab GTPases can be suppressed not only through loss of their activating guanine nucleotide exchange factors (GEFs), but also by transgenic introduction of GTP-

binding-defective copies. These copies can be modified either to not bind GTP at all, or to bind GTP but not hydrolyze it into GDP, leaving the GTPase in a permanent on-state. While hydrolase-defective isoforms lead to a constitutively active Rab, non-activatable mutants produce a dominant negative effect by sequestering GEFs and other GTPase activating cofactors away from the native, functional Rab (Chen et al. 2002). Use of dominant negative isoforms of Ras superfamily GTPases is a common technique to determine whether GTPase activation is required for specific cellular processes (Zhang et al. 2016; Rodriguez et al. 2017). Expression of a dominant negative Rab should phenocopy loss of function mutants for both the Rab and its activating GEF.

Dominant negative Rab isoforms can be generated through a threonine-to-asparagine substitution in the N-terminal GTP-binding pocket (Gallegos et al. 2012). Based on sequences provided by Gallegos et al. (2008), I generated a dominant negative RAB-27 (RAB-27T21N) using PCR mutagensis, and expressed it under the GABA neuron-specific *unc-47* promoter to ensure RAB-27 knockdown specifically in the cell type that I cut.

Expression of RAB-27T21N did not enhance axon regeneration, suggesting that suppression of neuronal RAB-27 activity does not affect regeneration inhibition (Fig. 2). This result further supports the theory that neuronal RAB-27 is not the primary source of *rab*-27's regeneration inhibition phenotype. An alternative possibility is that expression of the dominant negative RAB-27T21N in neurons induced a double knockdown effect on both RAB-27 and RAB-3, which

share the GEF AEX-3. *rab-3;rab-27* double mutants suppress the high regeneration of *rab-27* single mutants.

Alternative roles for RAB-27 in regulating regeneration

Beyond its synaptic vesicle tethering in neurons and neuropeptide release in the *C. elegans* intestine, *rab-27* and its mammalian orthologs are involved in diverse secretory processes in many cell types, including secretion of exosomes (Ostrowski et al. 2010), insulin secretion from pancreatic beta-cells (Kimura & Niki, 2011), and transport of melanosomes (Ishida et al. 2014). Many of these functions have implications for cancer progression and metastasis (Li et al. 2017, Guo et al. 2019). I investigated one such alternative role of *rab-27* identified in the immune system, which included a Rab27 effector with a conserved ortholog in *C. elegans*.

In cytotoxic T lymphocytes (CTL), Rab27a is required for the fusion of cytotoxic granules (Ritter et al. 2017). Cytotoxic granule release at the plasma membrane is preceded by local decreases in the lymphocyte's cortical actin cytoskeleton, which is recovered following vesicle fusion. In Rab27a-deficient cells, in addition to loss of cytotoxic granule release, local loss of cortical actin is not recovered following vesicle docking (Ritter et al. 2017). The recovery of the cortical actin cytoskeleton is mediated by the actin-binding protein and Rab27a effector coronin 3 (Kimura et al. 2010). Unusually for a Rab effector, coronin 3 is recruited to GDP-bound, inactive Rab27a. Recruitment of coronin 3 to the membrane-bound Rab27a-GDP facilitates its activity in local actin assembly. In

C. elegans, coronins are represented by *cor-1*, but little is known about its activity or its relationship to *rab-27*. Given the identification of its mammalian ortholog as a Rab27a effector in non-neuronal tissues, I examined *cor-1* in the context of axon regeneration, to determine whether loss of *cor-1* improves regeneration, and if so, whether it is genetically related to *rab-27*.

cor-1 (*ok869*) mutants do not show any significant differences in axon regeneration success (Fig. 3), suggesting that *rab-27*'s mechanism of regeneration inhibition is not related to local actin cytoskeletal assembly, but the recruitment of coronin 3 to Rab27a-GDP does open the possibility for other pathways that rely on inactive *rab-27*.

The GTPase *arf-6* inhibits DD/VD axon regeneration

In addition to Rabs, other GTPases have been identified that regulate axon regeneration in *C. elegans*. The Arf GTPase *arf-6* was described as an regeneration inhibitor of axon regeneration in the PLM axon by Chen et al. (2011). We confirmed the conservation of this inhibitory phenotype in the GABAergic DD/VD neurons (Fig. 4A), and *arf-6*(*tm1447*) was used as a positive control for regeneration phenotypes while screening the *C. elegans* Rabome. The enhanced regeneration seen in *arf-6*(*tm1447*) mutants was similar to that of *rab-27*(*sa24*) mutants, with similarly significant improvements in regeneration after only 12 hours of recovery (Fig. 4B).

***sid-1* does not affect axon regeneration**

sid-1 encodes an RNA transmembrane transporter, best known for being required for systemic RNAi in *C. elegans* (Winston et al. 2010). While SID-1 expression can potentiate RNAi sensitivity when ectopically expressed in specific cell types (Calixto et al. 2010), we aimed to restrict RNAi sensitivity to the intestinal cells by using feeder RNAi on *sid-1*(*pk3321*) null worms. Before attempting this strategy, I examined *sid-1*(*pk3321*) mutants for any baseline differences in axon regeneration compared to control animals. *sid-1*(*pk3321*) mutants did not show any significant changes in regeneration success (Fig. 5). Subsequent use of *sid-1* mutants in *rab-27* RNAi was not able to recapitulate a high regeneration phenotype, although this may be due failure of the feeder RNAi to even reach the intestine, as some finding suggest that SID-1 is required for not only export from the digestive system, but also import of dsRNA into the intestine (Whangbo et al. 2017).

References

Calixto A, Chelur D, Topalidou I, Chen X, Chalfie M. 2010. Enhanced neuronal RNAi in *C. elegans* using SID-1. *Nat Methods* 7:554-559.

Chavrier P, Gorvel JP, Stelzer E, Simons K, Gruenberg J, Zerial M. 1991. Hypervariable C-terminal domain of rab proteins acts as a targeting signal. Nature. 353:769-72.

Chen L, Wang Z, Ghosh-Roy A, Hubert T, Yan D, O'Rourke S, Bowerman B, Wu Z, Jin Y, Chisholm A. 2011. Axon regeneration pathways identified by systematic genetic screening in *C. elegans*. *Neuron* 71:1043-1057.

Chen X, Edwards JAS, Logsdon CD, Ernst SA, Williams JA. 2002. Dominant negative Rab3D inhibits amylase secretin fr

Chen Y, Semaraweera P, Sun T, Kreibich G, Orlow SJ. 2002. Rab27b association with melanosomes: dominant negative mutants disrupt melanosomal movement. *J Invest Dermatol* 118:993-940.

Edwards TJ, Hammarlund M. 2014. Syndecan promotes axon regeneration by stabilizing growth cone migration. *Cell Rep* 8:272-283.

Futerman AH, Banker GA. 1996. The economics of neurite outgrowth – the addition of new membrane to growing axons. *TINS* 19:144-149.

Gallegos ME, Balakrishnan S, Chandramouli P, Arora S, Azameera A, BAbushekar A, Bargoma E, Bokhari A, Chava SK, Das P, Desai M, Decena D, Saramma SDD, Dey B, Doss A, Gor N, Gudiputi L, Guo C, Hande S, Jensen M, Jones S, Jones N, Jorgens D, Karamchedu P, Kamrani K, Kolora LD, Kristensen L, Kwan K, Lau H, Maharaj P, Mander N, Mangipudi K, Menakuru H, Mody V, Mohanty S, MukkamalaS, Mundra SA, Nagaraju S, Narayanaswamy R, Ndungu-Case C, Noorbakshsh , Patel J, Patel P, Pendem SV, Ponakala A, Rath M, Robles MC, Rokkam D, Roth C, Sasidharan P, Shah S, Tandon S, Suprai J, Truong TQN, Uthayaruban R, Varma A, Ved U, Wang Z, Yu Z. 2012. The *C. elegans* Rab family: identification, classification and toolkit construction. *PLoS One*: 7:e49387.

Guo D, Lui GYL, Lai SL, Wilmott JS, Tikoo S, Jackett LA, Quek C, Brown DL, Sharp DM, Kwan RYQ, Chacon D, Wong JH, Beck D, van Geldermalsen M, Holst J, Thompson JF, Mann GJ, Scolyer RA, Stow JL, Weninger W, Haass NK, Beaumont KA. 2019. RAB27A promotes melanoma cell invasion and metastasis via regulation of pro-invasive exosomes. *Int J Cancer*. 144:3070-3085.

Hobert O. 2002. PCR fusion-based approach to create reporter gene constructs for expression and analysis in transgentic *C. elegans. Biotechniques* 32:728-730.

Ishida M, Arai SP, Ohbayashi N, Fukuda M. 2014. The GTPase-deficient Rab27A(Q78L) mutant inhibits melanosome transport in melanocytes through trapping of Rab27A effector protein Slac2-a/melanophilin in their cytosol: development of a novel melanosome-targetinG tag. J Biol Chem. 289:11059-67.

Kimura T, Kaneko Y, Yamada S, Ishihara H, Senda T, Iwamatsu A, Niki I. 2010. The GDP-dependent Rab27a effector coronin 3 controls endocytosis of secretory membrane in insulin-secreting cell lines. *J Cell Sci* 121:3092-3098.

Kimura T., Niki I. 2011. Rab27a, actin and beta-cell endocytosis. *Endocr J.* 58:1-6.

Li Z, Fang R, Fang J, He S, Liu T. 2018. Functional implications of Rab27 GTPases in Cancer. *Cell Commun Signal*. 16:44.

Ostrowski M, Carmo NB, Krumeich S, Fanget I, Raposo G, Savina A, Moita CF, Schauer K, Hume AN, Freitas RP, Goud B, Benaroch P, Hacohen N, Fukuda M, Desnos C, Seabra MC, Darchen F, Amigorena S, Moita LF, Thery C. 2010. Rab27a and Rab27b control different steps of the exosome secretion pathway. *Nat Cell Biol*. 12:19-30.

Ritter AT, Kapnick SA, Murugesan S, Schwartzberg PL, Griffiths GM, Lippincott-Schwartz J. 2017. Cortical actin recovery at the immunological synapse leads to termination of lytic granule secretion in cytotoxic T lymphocytes. *PNAS* 114:E6586-E6594.

Rodriguez L, Mohamed NV, Desjardins A, Lippé R, Fon EA, Leclerc N. 2017. Rab7A regulates tau secretion. *J Neurochem*. 141:592-605

Sabo SL, McAllister AK. 2003. Mobility and cycling of synaptic protein-containing vesicles in axonal growth cone filopodia. *Nat Neurosci* 6:1264-1269.

Whangbo Js, Weisman AS, Chae J, Hunter CP. 2017. SID-1 domains important for dsRNA import in *Caenorhabiditis elegans*. *G3* 7:3887-3899.

Winston WM, Molodowitch C, Hunter CP. 2002. Systemic RNAi in *C. elegans* requires the putative transmembrane protein SID-1. *Science* 295:2456-2459.

Zhang D, Dubey J, Koushika SP, Rongo C. 2016. RAB-6.1 and RAB-6.2 promote retrograde transport in *C. elegans. PLoS One* 11: e0149314.

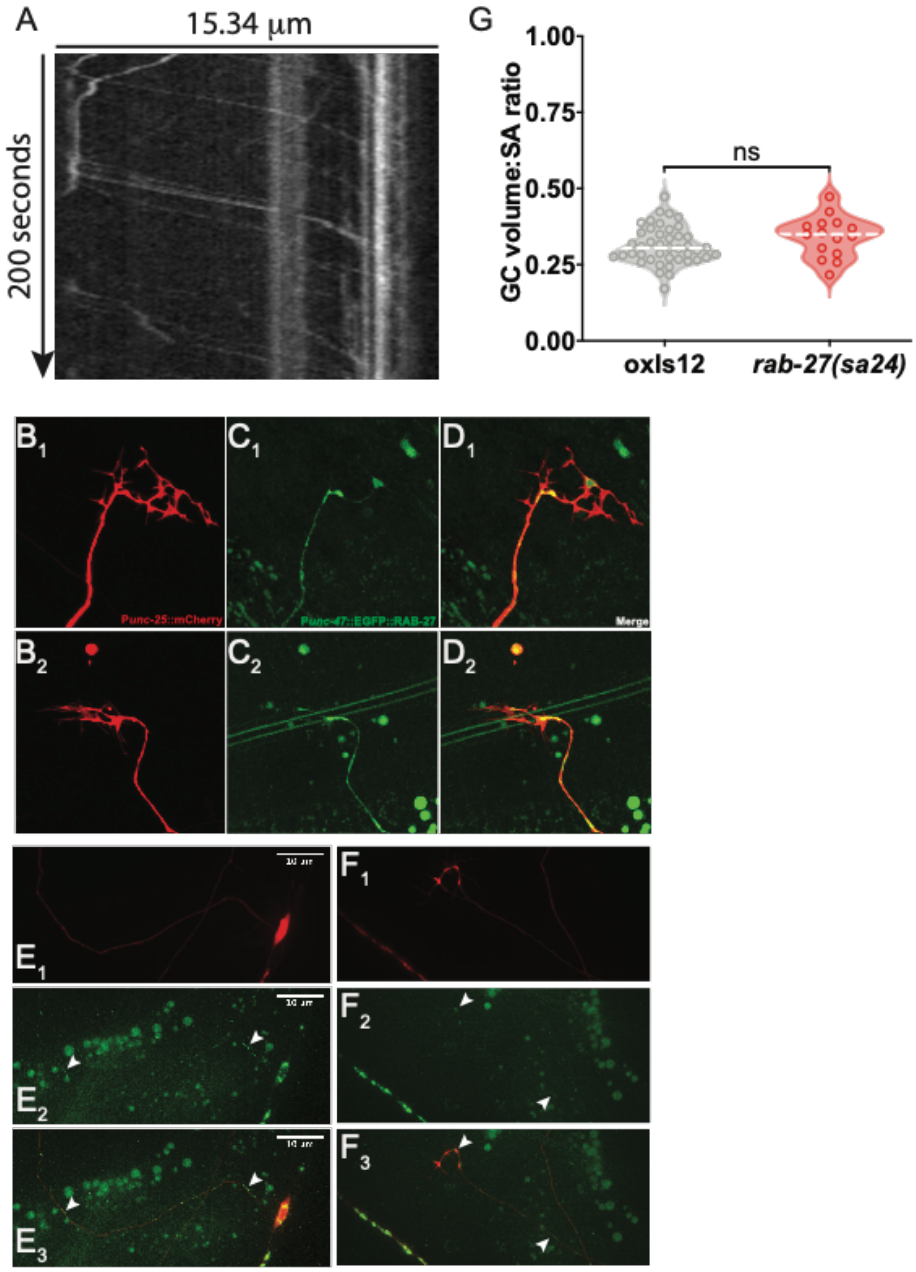

Figure 1. Visualization of neuronal RAB-27 in intact and regenerating axons. A) Kymograph of GFP::RAB-27 puncta in the commissure of a DD axon at 100x magnification. Dorsal nerve cord is oriented to the right of the image. Rapid anterograde movement of GFP-positive puncta was seen at several points throughout the 200s duration. B-D, F) Expression of GFP::RAB-27 in regenerating axons. GFP::RAB-27 was expressed as a multicopy array at an injection concentration of 7.5ng/µL in worms expressing GABA-specific mCherry as an integrated transgene (wpIs40[Punc-47::mCherry]). Imaging was done at 100x magnification 24h after axotomy. E) GFP::RAB-27 localization in intact axons. Experimental conditions were identical to above. F) Surface area-to-volume ratio of growth cones in regenerating axons of control (*oxIs12*) and *rab-27* mutant animals. Surface area and volume were calculated using IMARIS imaging software. Axons cut per genotype, L to R: 43, 15. Kolmogorov-Smirnov test was used. ns, not significant.

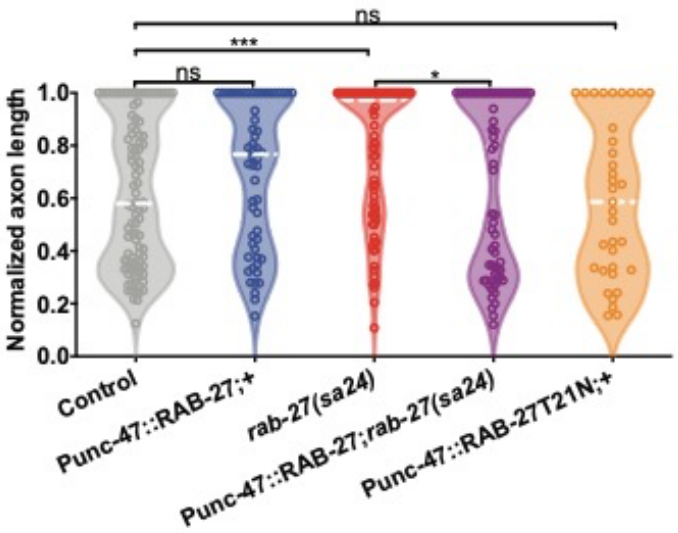

Figure 2. Expression of dominant negative RAB-27 in GABA neurons. Normalized regenerating axon length in animals expressing wildtype or dominant negative (T21N) RAB-27 cDNA under a GABA neuron-specific promoter in control (*oxIs12*) and *rab-27(sa24)* mutant backgrounds. Number of axons cut per genotype, L to R: 98, 56, 84, 68, 35. Kolmogorov-Smirnov test was used. ns, not significant, * $p < 0.05$, ** $p < 0.005$, *** $p < 0.0005$.

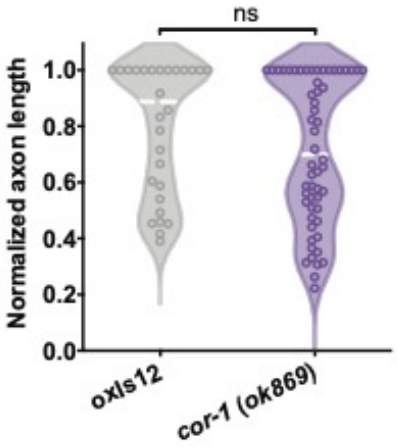

Figure 3. Axon regeneration in *cor-1(ok869)* mutants. Normalized regenerating axon length in control (*oxIs12*) and *cor-1(ok869)* mutant backgrounds. Number of axons cut per genotype, L to R: 28, 56. Kolmogorov-Smirnov test was used. ns, not significant.

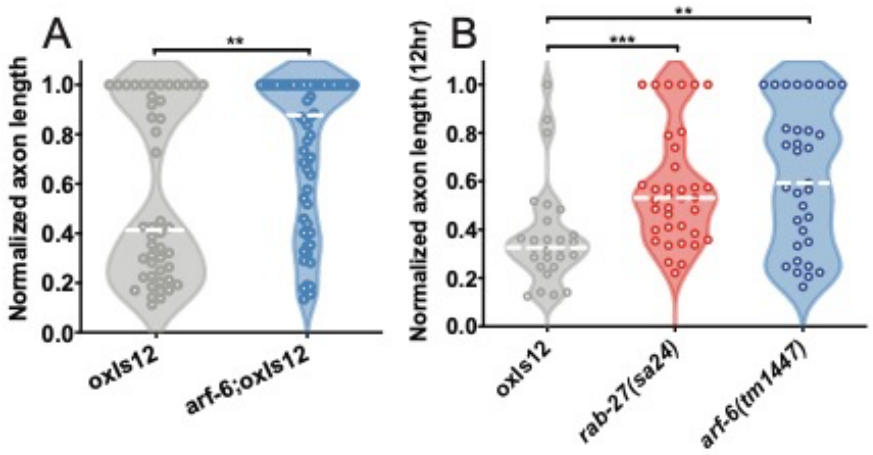

Figure 4. Regeneration of GABA neurons in *arf-6(tm1447)* mutants. A) Normalized regenerating axon length in control (*oxIs12*) and *arf-6(tm1447)* mutant backgrounds after 24 hours of recovery. Number of axons cut per genotype, L to R: 46, 64. Kolmogorov-Smirnov test was used. ns, not significant, * $p < 0.05$, ** $p < 0.005$. B) Normalized regenerating axon length in control (*oxIs12*), *rab-27(sa24)* and *arf-6(tm1447)* mutant backgrounds after 12 hours of recovery. Number of axons cut per genotype, L to R: 27, 36, 33. Kolmogorov-Smirnov test was used. ns, not significant, * $p < 0.05$, ** $p < 0.005$, *** $p < 0.0005$.

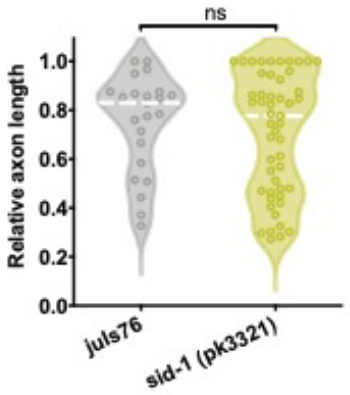

Figure 5. Axon regeneration in *sid-1(pk3321)* mutants. Normalized regenerating axon length in control (*juIs76*) and *sid-1(pk3321)* mutant backgrounds. Number of axons cut per genotype, L to R:23, 51. Kolmogorov-Smirnov test was used. ns, not significant.

Conclusions and future directions

My dissertation work covered the identification and characterization of the small GTPase RAB-27 as a novel, conserved inhibitor of axon regeneration, as well as the identification of the *C. elegans* intestine as a new and important tissue in the negative regulation of regeneration. I have found that loss of *rab-27* leads to significant enhancement of regeneration in the *C. elegans* DD/VD GABAergic neurons. RAB-27 functions in part in the GABA neurons themselves to inhibit regeneration, as GABA neuron-specific re-expression of RAB-27 is partially able rescue normal regeneration levels. RAB-27's neuronal inhibition of regeneration functions independently of its well-known role in synaptic vesicle tethering and synaptic transmission, as coregulators of this process, including the similar RAB-3, do not inhibit regeneration, and are indeed required to permit the high regeneration phenotype seen in *rab-27* mutants.

In contrast to our early findings, which pointed to RAB-27 as a wholly cell-intrinsic regeneration regulator, neuronal RAB-27 is not fully responsible for regeneration inhibition. While neuron-specific RAB-27 re-expression does partially restore normal regeneration, we have found that it is not sufficient to fully rescue the mutant *rab-27* phenotype. This discrepancy is likely attributable to transgene leakage via the *unc-54* 3'UTR, a noncoding sequence commonly used in the *C. elegans* field to stabilize artificially-expressed constructs. The *unc-54* 3'UTR sequence contains the cis-regulatory and early coding sequence of *aex-5*, an intestinally expressed gene that indeed functions in a shared pathway with

rab-27 to regulate defecation and axon regeneration. Use of the *unc-54* 3'UTR leads to substantial off-target expression of transgenes in the posterior intestine. Replacement of this UTR with a neuronal-specific *rab-3* 3'UTR led to improvements in expression specificity, and a subsequent decrease in the ability of neuronally-expressed RAB-27 to inhibit regeneration, results that we believe more accurately reflect the role of neuronal RAB-27 in regeneration inhibition.

Instead, we show that RAB-27's principal site of regeneration inhibition is the intestine, a tissue not previously implicated in axon regeneration regulation. Re-expression of RAB-27 in the intestine is sufficient to fully restore normal axon regeneration success, and unlike synaptic transmission, RAB-27's functions in the intestine cannot be recapitulated by RAB-3, pointing to a unique role for RAB-27 in regeneration regulation separate from its synaptic vesicle tethering cofactors. Instead, RAB-27 inhibits regeneration from the intestine through the regulation of a gut-to-neuron signaling pathway, one which overlaps significantly with the defecation motor program (DMP), and which relies on the formation and secretion of the neuropeptide NLP-40 in dense core vesicles. Disruption of multiple steps in this intestinal pathway, including dense core vesicle maturation, neuropeptide precursor cleavage, and vesicle fusion at the plasma membrane lead to significant improvements in axon regeneration epistatic to *rab-27* itself. Together, these findings point to novel functions for RAB-27 and the *C. elegans* intestine as key negative regulators of axon regeneration after injury.

The identification of the intestine, and of an intestinal neuropeptide secretory pathway, as regeneration inhibitors has important implications for the field of axon regeneration. Most studies on regeneration regulators, particularly those in *C. elegans*, focus on intrinsic regulatory mechanisms, as *C. elegans* provides an excellent model for the study of intracellular neuronal processes in living animals. Most extrinsic regeneration regulators identified in worms are found in the immediate extracellular environment of the regenerating axon, and play roles in axon stabilization. Our results point to a major new source of regulatory signals for regeneration, particularly for powerful regeneration inhibitors, coming from distant tissues and relying on exocrine signaling pathways. As important regulators of diverse neuronal processes, it is not surprising that neuropeptides may play important roles in the regulation of axon regeneration. Similarly, discoveries in *C. elegans* and beyond increasingly identify the gut as an essential source of regulatory signals for many body systems, including in the nervous system, and the intestine may yet play more key regulatory roles in neurobiological processes such as regeneration.

Several essential questions remain to completely describe this novel inhibitory pathway, and to determine how conserved this mechanism of regeneration inhibition is across species. While extrinsically-secreted signals clearly play an important role in regeneration inhibition in *C. elegans*, whether this function is conserved across species is not known. High-throughput, *in vitro* screening approaches, relying on isolated populations of neurons, are limited in

their ability to identify extrinsic regulators of regeneration. Instead, limited screening approaches of target gene classes may present a more effective strategy for identifying extrinsic regulatory mechanisms of axon regeneration. Rab GTPases are indeed an ideal example of this strategy, as analysis of individual global Rab mutants can provide insight into unexpected tissues or trafficking processes regulating regeneration. Similarly, a careful analysis of neuropeptides, their processing machinery, and their neuronally-expressed G-protein coupled receptors could greatly enhance our understanding of long-distance signaling mechanisms regulating regeneration, both for NLP-40 itself, and for potential novel regulatory signals that target regenerating axons. A combinatorial genetic and cell-biological approach targeting specific gene classes and functions regardless of expression could greatly enhance our understanding of how axon regeneration is regulated.